

1-1-1978

# Macromolecular diffusion in polymer melts.

Paul T. Gilmore

*University of Massachusetts Amherst*

Follow this and additional works at: [https://scholarworks.umass.edu/dissertations\\_1](https://scholarworks.umass.edu/dissertations_1)

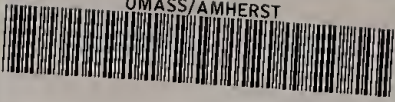
---

## Recommended Citation

Gilmore, Paul T., "Macromolecular diffusion in polymer melts." (1978). *Doctoral Dissertations 1896 - February 2014*. 629.  
[https://scholarworks.umass.edu/dissertations\\_1/629](https://scholarworks.umass.edu/dissertations_1/629)

This Open Access Dissertation is brought to you for free and open access by ScholarWorks@UMass Amherst. It has been accepted for inclusion in Doctoral Dissertations 1896 - February 2014 by an authorized administrator of ScholarWorks@UMass Amherst. For more information, please contact [scholarworks@library.umass.edu](mailto:scholarworks@library.umass.edu).

UMASS/AMHERST



312066 0024 5973 4

MACROMOLECULAR DIFFUSION IN POLYMER MELTS

A Dissertation Presented

By

PAUL T. GILMORE

Submitted to the Graduate School of the  
University of Massachusetts in partial fulfillment  
of the requirements for the degree of

DOCTOR OF PHILOSOPHY

September 1978

Polymer Science and Engineering

© Paul T. Gilmore 1978  
All Rights Reserved

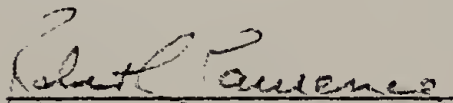
MACROMOLECULAR DIFFUSION IN POLYMER MELTS

A Dissertation Presented

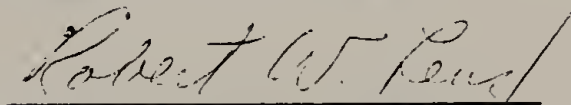
By

PAUL T. GILMORE

Approved as to style and content by:



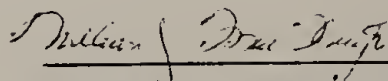
Robert L. Laurence  
Committee Chairperson



Robert W. Lenz, Member



Frank E. Karasz, Member



William J. MacKnight, Member  
Department Chair  
Polymer Science and Engineering

To Rosanna,  
for her love and friendship.

## ACKNOWLEDGMENTS

I must first acknowledge the influence of Professor Fraser P. Price, who initially suggested this research and whose friendship and attitude toward scientific inquiry provides a continuing example for all who knew him.

My thanks go particularly to Professor Robert L. Laurence, advisor and friend, who has helped me very much; to Professor Frank E. Karasz, for his inspiring questions and insight; to Professor William J. MacKnight, for many stimulating discussions; and to Professor Robert W. Lenz, for his knowledgeable comments and suggestions.

I would also like to thank Professor R.S. Porter and Professor E.L. Thomas for their advice and assistance and Rosanna Falabella for developing the computer program for data analysis.

I wish to express my appreciation to all members of the Polymer Science and Engineering Department, whose collective attitude creates an atmosphere conducive to research.

## ABSTRACT

Macromolecular Diffusion in Polymer Melts

(September 1978)

Paul T. Gilmore

B.S.Ch.E., Michigan Technological University  
M.S., University of Massachusetts  
Ph.D., University of Massachusetts

Directed by: Professor Robert L. Laurence

This dissertation reports on efforts to develop a technique to measure macromolecular diffusion in miscible binary polymer systems. Determination of a diffusion coefficient for such systems has applications in lamination of polymer films, polymer welding, and coextrusion of several polymers. Knowledge of the diffusional behavior will allow predictions of the effects of mixing, during and after processing, on the physical properties of the materials.

Several pairs of polymers have been found to be miscible throughout the entire concentration range. One system to which much attention has been paid is poly(vinyl chloride)/poly( $\epsilon$ -caprolactone) [PVC/PCL]; it has been shown to be compatible on the molecular level, making it viable as a system in which to study interdiffusion of polymeric materials.

The experimental technique is a novel application of



scanning electron microscopy (SEM) and energy dispersive analysis of x-ray fluorescence (EDS). Films of PVC and PCL placed in contact with each other were allowed to diffuse for a period of about a month at elevated temperature. The sample was then fractured so as to expose the interface and examined in the SEM. By measuring the chlorine concentration by EDS as a function of position, a concentration profile was developed for the interdiffused sample. Many such profiles were measured and evaluated by a solution to the diffusion equation. All such curves were plotted on a normalized master curve from which a diffusion coefficient was calculated.

The diffusion coefficient for the PVC/PCL system was on the order  $10^{-12}$  to  $10^{-13}$   $\text{cm}^2/\text{sec}$ . That for another system, polystyrene/poly(o-chlorostyrene), was even lower,  $\sim 10^{-14}$   $\text{cm}^2/\text{sec}$ . The effect of molecular weight on the diffusion coefficient was examined for PVC/PCL. It was observed that  $D \propto M^{-1}$ , a result not predicted by any of the few theories extant in the literature dealing with polymeric diffusion in the melt state. Measuring diffusion rates at several temperatures resulted in determination of the activation energy for diffusion of 11.7 kcal/mol, a value comparable to others in the literature.

Experimental values for the mutual diffusion coefficient of a miscible binary polymer have been determined and

the effects of molecular weight and temperature calculated. Although no theoretical model for diffusion in the melt has been proposed, the data provide further insight into the diffusional behavior of polymers and a firmer base on which to formulate such a theoretical treatment. The experimental technique holds promise as a means of measuring diffusion in polymer/plasticizer systems as well as in polymer/polymer systems.

## TABLE OF CONTENTS

	Page
ACKNOWLEDGMENTS . . . . .	v
ABSTRACT . . . . .	vi
LIST OF TABLES . . . . .	xi
LIST OF FIGURES . . . . .	xii
Chapter	
I. INTRODUCTION . . . . .	1
II. BACKGROUND . . . . .	4
II.1 Diffusion . . . . .	4
II.2 Diffusion in Polymer Melts . . . . .	5
II.3 Importance of Scale . . . . .	11
II.4 Mathematical Analysis of Diffusion . . . . .	16
II.5 An Experiment . . . . .	26
III. EXPERIMENTAL . . . . .	28
III.1 Scanning Electron Microscopy . . . . .	31
III.2 Energy Dispersive Analysis of X-Ray Fluorescence . . . . .	35
III.3 Polymer Samples . . . . .	49
III.4 Experimental Technique . . . . .	58
III.5 Data Analysis . . . . .	79
IV. RESULTS . . . . .	105
IV.1 Diffusion in the PVC/PCL System . . . . .	105
IV.2 Diffusion in the PS/PoCS System . . . . .	122
V. DISCUSSION . . . . .	126
VI. RECOMMENDATIONS FOR FUTURE WORK . . . . .	134
VII. CONCLUSION . . . . .	139

REFERENCES . . . . .	Page 141
Appendix	
A. REGRESSION ANALYSIS . . . . .	146
B. PROPAGATION OF ERROR . . . . .	152

LIST OF TABLES

Table	Page
1. Comparison of D, x, and t for several diffusion systems . . . . .	14
2. Experimental materials--PVC and PCL . . . . .	57
3. Cl x-ray counts vs. stage angle for pure PVC . . .	68
4. Raw Data--Line vs. x-ray counts of typical concentration profile . . . . .	74

## LIST OF FIGURES

Figure	Page
1. Polymer chain constrained by fixed obstacles . . .	7
2. Density vs. wt% PCL for PVC/PCL system . . . . .	21
3. Phenomena resulting from electron beam bombardment . . . . .	30
4. Schematic diagram of characteristic x-ray generation . . . . .	34
5. Semiconductor type x-ray detector . . . . .	39
6. Schematic diagram of x-ray detection . . . . .	42
7. X-ray spectrum showing chlorine $K_{\alpha}$ and $K_{\beta}$ peaks .	44
8. Representation of relative positions of interface, electron beam, and x-ray generation volume . . .	48
9. The effect on $T_m$ and $T_g$ of weight fraction PCL ( $x_2$ ) . . . . .	52
10. Crystallinity of PVC-6/PCL-4 blend as a function of weight fraction PCL-4 ( $x_2$ ) . . . . .	55
11. Interdiffused sample of PVC/PCL with interface exposed as seen in SEM . . . . .	63
12. Photomicrograph of interface of PVC/PCL films . .	65
13. Electron beam penetration in relation to orientation of interface . . . . .	70
14. Example photomicrograph showing photographically recorded positions of concentration measurement . . . . .	76
15. Concentration profile, distance vs. number of chlorine x-rays counted in 20 seconds . . . . .	78
16. Master curve for PCL-1/PVC-6 . . . . .	83
17. Master curve for PCL-2/PVC-6 . . . . .	85
18. Master curve for PCL-3/PVC-6 . . . . .	87
19. Master curve for PCL-4/PVC-6 . . . . .	89
20. Master curve for PVC-1/PCL-4 . . . . .	91
21. Master curve for PVC-2/PCL-4 . . . . .	93
22. Master curve for PVC-3/PCL-4 . . . . .	95
23. Master curve for PVC-4/PCL-4 . . . . .	97
24. Master curve for PVC-5/PCL-4 . . . . .	99
25. Master curve for PVC-6/PCL-4 at 90°C . . . . .	101
26. Master curve for PVC-6/PCL-4 at 110°C . . . . .	103
27. Master curve for PS/PoCS . . . . .	108
28. D vs. M for PCL (with PVC-6) . . . . .	111
29. D vs. 1/M for PCL (with PVC-6) . . . . .	113
30. D vs. M for PVC (with PCL-4) . . . . .	116
31. D vs. 1/M for PVC (with PCL-4), PVC-1 not included . . . . .	118

Figure	Page
32. Log D vs. $1/T$ for PVC/PCL ( $T = 70^{\circ}\text{C}, 90^{\circ}\text{C}, 110^{\circ}\text{C}$ ) . . . . .	121
33. Wide angle (bottom) and small angle (top) x-ray scattering from PVC-1 film . . . . .	124
34. Flow chart of non-linear regression analysis . . . . .	151

## C H A P T E R I

### INTRODUCTION

The physical and processing characteristics of polymer blends depend greatly on diffusional phenomena, yet little data pertaining to macromolecular diffusion in polymeric systems exist in the literature. Commercially available polymer blends are produced by physical mixing and coextrusion, a procedure which does not provide complete mixing on the molecular level. One would expect that after processing, polymer molecules continue to diffuse, resulting in transitory effects on the properties of such blends. Knowledge of a diffusion coefficient for a pair of polymers would be of considerable importance to the understanding of the lamination, or of similar processing, of the two materials. As well, the analysis of coextrusion of two miscible polymers would be facilitated by greater knowledge of the mixing characteristics of the components.

A recent review in the literature (Pearson, 1976) attempted to link times required for processing to the relative times of relaxation and diffusion of the polymer molecules. A more detailed treatment of the problem has been given by Duda et al. (1976). These relationships have only been estimated in the past partially because of the lack of diffusion



data; this work provides definitive information on diffusion of macromolecules. Accurate determination of the magnitude of the diffusion coefficient also will have great applicability in the field of adhesion, particularly when the recent discussions in the literature are considered. Voyutskii (1963, 1971) has consistently put forth the thesis that bonding of high polymers can be interpreted from the standpoint of macromolecular diffusion. The antithesis is put forth by Wake (1969) and Anand (1969, 1973) that autohesion and adhesion are more attributable to surface phenomena than to diffusional effects. The results of this study will not resolve the controversy; they will probably only enhance it. At least three will be added basis for future discussion. On a less immediately practical level, the knowledge of the diffusion coefficient for a binary polymer system can provide the information required to test the few theoretical treatments of the polymeric melt state and the diffusion of macromolecules.

A polymer molecule in the solid or melt state is known to undergo several types of motion, each on a different molecular level. There are vibrational and rotational motions of single atoms and the articulated motion of short chain segments within the polymer molecules. A combination of motions results in the translational motion of the entire molecule, i.e., the diffusion of the polymer molecule. The most important factors determining the time required for macro-

molecular diffusion in polymer blends are the miscibility of the components and the diffusion rate. The rate of diffusion may be determined by measuring the mutual diffusion coefficient for the system. The goal of this research has been to study diffusion in compatible polymer/polymer systems. Due to the peculiar physical properties of macromolecules as contrasted with small molecules, the experimental procedures normally employed to measure the diffusion of small molecules (often optical techniques) cannot be applied to the study of the motion of macromolecules.

Diffusion in polymer systems is a very slow process; to attain appreciable interpenetration of the diffusion materials, the time scale of a diffusion experiment must be large. As well, the depth of interpenetration of the polymer components is small, requiring greater resolution than is found in standard experimental methods. This work has developed a novel technique for the study of polymer/polymer diffusion, employing a scanning electron microscope and energy dispersive analysis of x-ray fluorescence to directly observe the interface and measure the concentration profile of the interdiffused polymeric materials.

## C H A P T E R   I I

### BACKGROUND

#### II.1 Diffusion

Diffusion is the process consisting of random motions by which matter is transported from one spatial position within a system to another. If it were possible to observe a single particle in a diffusing system, it would be noted that its motion would be completely random and could be described by the familiar "random walk" model. Theoretical analysis of the diffusion mechanism has been provided by Frenkel (1926) and Wagner and Schottky (1931). Although the mean square distance traveled in a given period of time can be calculated, it is not possible to say in which direction a molecule will move at any instance. This must be reconciled with the fact that diffusion, or transfer of material from a position of higher concentration to a position of lower concentration, occurs. It must be concluded that, on the average, a fraction of the molecules in a volume element of higher concentration will be transferred to a position in a volume element of lower concentration, and vice versa, in a given period of time. Simply because there are more particles of one type in the first volume element than in the

second, a net transfer will occur.

## II.2 Diffusion in Polymer Melts

II.2.1 Theory. The mechanism for diffusion of polymer molecules has been discussed infrequently in theoretical terms, particularly when dealing with the interaction of chain molecules. P.G. de Gennes (1971) has put forth the concept of reptation, as follows. By constraining the polymer molecule to move in a thin pipe (Figure 1) defined by the fixed segments in a cross-linked polymeric gel, the motion of the trapped molecule is restricted to two types: motion of small "defects" along the chain and motion of the chain as a whole (essentially changing the configuration of the confining tube). The result is a dependence of the diffusion coefficient,  $D$ , on  $M^{-2}$ , where  $M$  is the molecular weight. The description of the diffusing system is, of necessity, simplified. The extension of de Gennes' results for the system of one chain in a fixed gel to that of many more mobile chains is extremely difficult.

Edwards (1973) limits the motion of an individual chain by using frozen obstacles as hindrances (Figure 1). These obstacles define a "pipe" in which the molecule moves; as well, the pipe may move. Since, in actuality, the network is not frozen, Edwards treats these effects as cooperative and calls the motion cooperative diffusion. He also treats the system using topological invariants, constraining

Figure 1. Polymer chain constrained by fixed obstacles.



the system by its topology. Again, many simplifications must be made to accommodate the analytical description of the system. The result differs from that of de Gennes in that the diffusivity,  $D$ , depends upon  $M^{-3}$ . Interestingly, both Edwards and de Gennes conclude that the mean square displacement of a polymer chain will demonstrate a  $1/4$  power dependence on time for strongly entangled polymers in the melt state.

Bueche (1952) developed a theoretical description of macromolecular diffusion using a much simpler assumption, that of a frictional force acting on a segment due to its contact with other molecules. This method is an extension of the concept developed for the "free-draining" or "zero distortion" approximation used for calculating the viscosity of a polymer in a low molecular weight solvent (Debye, 1946). Instead of determining the frictional losses due to a segment sliding past solvent molecules, each segment is in contact with another polymer segment. In addition, the molecules may be intertwined and in order to move, one molecule may have to drag others with it. Using Debye's "free draining" calculation of the viscosity,  $\eta$ , and the classical Einstein relation for the diffusion coefficient,  $D$ , Bueche's result is:

$$D\eta = (A\rho kT/36) (R^2/M) \quad (1)$$

where  $A$  is Avogadro's number,  $\rho$  is the density of the poly-



mer,  $R^2$  is the mean square end-to-end chain distance, and  $M$  is the molecular weight. Since  $R^2/M$  is essentially a constant for a bulk polymer, the right hand side of Equation 1 can be considered a constant, thus allowing a prediction of  $D$  if  $\eta$  is known.

The utility of any of these theoretical treatments can only be decided by comparison with experimental evidence. Unfortunately, the lack of adequate experimental data matches the lack of adequate theoretical descriptions of macromolecular diffusion.

II.2.2 Experimental. To accompany Bueche's theoretical work, Bueche, Cashin and Debye (1952) published some data they obtained for self-diffusion of poly(n-butylacrylate). The experimental technique involves the use of  $C^{14}$  tagged polymer. The tagged polymer is applied as a thin film to a block of untagged polymer and measurement of the decrease of the intensity of emitted radiation is used to determine the diffusion rate. The work was a pioneering effort but many difficulties were encountered. The thickness of radioactive polymer was 5-25  $\mu\text{m}$ ; as will be noted later, this is on the order of the thickness of the interpenetration distance. Simply for this reason the data must be substantially smeared since the measurements were made assuming that the layer of radioactive material occupied a specific position with respect to the interface. Deconvolution tech-



niques cannot remove this effect entirely. When the technique was extended to polystyrene, no appreciable diffusion was noted in several weeks; in effect, the resolution of the experimental apparatus was exceeded when trying to measure diffusion of polystyrene. The results presented later for a modified polystyrene system will shed some light on the difficulty encountered by Bueche and coworkers.

Klein and Briscoe (1975, 1977) have developed a technique based on infrared microdensitometry to measure the diffusion of large molecules in polymers. The current resolution of the technique limits the procedure to systems with diffusion coefficients greater than  $10^{-10}$  cm<sup>2</sup>/sec, but certainly is applicable to polymer-plasticizer systems.

More recently, Sillescu (1977) has used NMR free induction decay to determine the diffusion of polystyrene in perdeuterated polystyrene. He was not able to determine the diffusion coefficient exactly, but estimated it as  $10^{-13}$  cm<sup>2</sup>/sec. His procedure requires monodisperse polymers, but he asserts that the resolution is such that diffusivities as low as  $10^{-16}$  cm<sup>2</sup>/sec may be measured.

An electron microscopic technique was applied to the interdiffusion of polymers by Voyutskii et al. (1965, 1966). In this study, two polymers were placed in contact with one another and heated by a stream of hot air for a given period of time (on the order of one hour). Because of the need for thin specimens for observation in the transmission electron

microscope, thermoplastic materials were used, thus facilitating microtoming at room temperature. The glassy materials were microtomed normal to the interfacial plane, and the sample was examined in the electron microscope. (The difference in electron densities of the two polymers provided a measure of the interdiffusion.) There are difficulties inherent to this technique. The materials used have not been shown to be compatible (Krause, 1972). The method of heating allowed no measure of the diffusion temperature or time, making calculations of the diffusion coefficient impossible. Vyutskii therefore has used his measurements of interdiffusion simply to indicate that it does indeed occur. His examination of the diffused species by electron microscopy is certainly valid; when modified as described in this work, the measurement of a diffusion coefficient becomes a real possibility.

### II.3 Importance of Scale in Choice of Experimental Technique

For any diffusion experiment, one must necessarily devise an experimental apparatus such that the extent of mixing of the system's components is achieved in a reasonable time and can be accurately detected. For diffusing gases, the standard apparatus consists of a tube of one meter in length (Jost, 1952). The concentration profile can be measured by chemical analysis and the diffusion coefficient is

on the order of  $10^{-1}$   $\text{cm}^2/\text{sec}$ . The diffusion coefficient for low molecular weight liquids is smaller than for gases, around  $10^{-5}$   $\text{cm}^2/\text{sec}$ . The experimental apparatus are of various configurations and have been described by Jost (1952), Johnson and Babb (1956), and recently by Ertl, Ghai, and Dullien (1973). In general, optical techniques are used. One can easily assume that polymers will interdiffuse even slower than low molecular weight liquids, suggesting a microscopic technique. This suggestion can be confirmed by realizing that the concentration distribution for a diffusing sample is a function of  $x^2/Dt$ , where  $x$  is the distance of interpenetration,  $D$  the diffusion coefficient, and  $t$  the diffusion time. In most experiments, this quantity, which will be designated the "Fick" number ( $F_i$ ), is on the order of one (1). Table 1 gives a comparison of the various time scales required for a diffusion experiment, given an approximate value for  $D$  and  $x$ . Note that for gases and liquids the times required are relatively short, while for diffusion of metals in metals the times are substantially longer.

The physics of diffusion in polymers is exceedingly complicated; the variables include the chemical nature of the polymer, its molecular weight and molecular weight distribution, the glass transition temperature, and the interaction between the diffusing species. The current status of diffusion of small molecules in polymers is described by Crank and Park (1968) and Machin and Rogers (1972). Table 1 il-

Table 1. Comparison of  $D$ ,  $x$ , and  $t$  for several diffusing systems.

SYSTEM	D (cm <sup>2</sup> /sec)	x (cm)	t (sec)	Fi
GASES	1	10	10 <sup>2</sup>	1
LIQUIDS	10 <sup>-5</sup>	1	10 <sup>5</sup>	1
METALS	10 <sup>-12</sup>	10 <sup>-2</sup>	10 <sup>8</sup>	1
GASES IN POLYMERS	10 <sup>-6</sup>	10 <sup>-1</sup>	10 <sup>4</sup>	1
LIQUIDS IN POLYMERS	10 <sup>-8</sup>	10 <sup>-1</sup>	10 <sup>6</sup>	1
BULK POLYMERS	10 <sup>-12</sup>	10 <sup>-2</sup>	10 <sup>8</sup>	1

strates the scale of the experiments when dealing with low molecular weight diffusants in polymers. The techniques employed generally involve microscopic measurement of the diffusion rate because of the small interpenetration distances and small diffusion coefficients ( $\sim 10^{-8}$  cm<sup>2</sup>/sec) for these systems.

In polymer/polymer systems, the diffusion rate is even slower because of the peculiar nature of macromolecules. An individual molecule may be considered to be made up of many segments which are, in turn, made up of atoms. The motion of the entire molecule results only from the combination of the motions of the segments. One must expect a very small diffusion coefficient, and take this into account when designing the diffusion experiment. Table 1 uses the value  $10^{-12}$  cm<sup>2</sup>/sec, as reported by Bueche et al. (1952). If one assumes an interpenetration distance of  $10^{-2}$  cm (100  $\mu$ m), a rather large distance in this case, the time scale of the experiment is on the order of  $10^8$  seconds, or months. Clearly, a technique must be used that will allow accurate determination of the concentration profile across a distance of no more than 100  $\mu$ m to assure a diffusion time within reasonable range.\* Certainly, optical microscopic techniques can resolve a 100  $\mu$ m distance; but the technique must have much better resolution than that because the concentration profile

---

\*One would hope to have the experimental time be less than the lifetime of the graduate student.



must be resolved within a field of 100  $\mu\text{m}$  breadth. The use of electron microscopy quickly suggests itself since its resolution is typically 100  $\text{\AA}$ .

Given that electron microscopy can provide the resolution required, the problem of measuring the concentration profile still remains. In this work, energy dispersive analysis of x-ray fluorescence (EDS) has been used; the details are given in the chapter dealing with experimental technique. Thus, we have proposed a method to solve the problem which has presented itself: the need of a novel technique to adequately measure diffusion rates in polymers in the melt state. The experimental procedure has consisted of measuring the interdiffusion of two compatible polymers, films of which were placed in contact and allowed to diffuse for a known period of time. The thickness of the individual films was much greater than the depth of interpenetration. Therefore, the films have been considered to be of infinite thickness with respect to the distance of interpenetration. The next requirement is an adequate mathematical description of the diffusing system so that a diffusion coefficient can be determined.

#### II.4 Mathematical Analysis of Diffusion

In 1855, Fick first developed an equation describing diffusion by relating the mass flux to the concentration gradient of an interpenetrating system. Since that time,

Many authors have modified the equation and imposed various initial and boundary conditions applying to specific circumstances, resulting in a plethora of analytical results to the diffusion equation. Boltzmann (1894) first provided a solution allowing for concentration dependence of the diffusion coefficient. Many reviews of the literature have been written over the years, including those by Jost (1952), Johnson and Babb (1956), and Crank (1975). All provide many solutions to the diffusion equation for different experimental conditions.

4.1 Development of a diffusion equation. There is no theoretical justification for the attempt to describe diffusion in polymers by use of Fick's law. In fact, justification is only available for low molecular weight materials through the kinetic theory of gases, most assuredly inapplicable in this case. However, describing the diffusion process in the traditional manner does provide ready analysis of the data and a useful diffusion coefficient.

Diffusion is relative motion. Therefore, the flux of diffusing material is defined with respect to a certain coordinate system in such a way as to allow a simple description of the diffusion process. In this discussion, the mass flux of one diffusing species will be referred to the volume average velocity of the sample. The notation of Bird, Stewart, and Lightfoot (1960) will be followed throughout



and will be applied only to diffusion in a binary system.

Given the two components of the system are A and B, the flux is defined by:

$$j_A^{\blacksquare} = \rho_A (v_A - v^{\blacksquare}) \quad (2)$$

where  $j_A^{\blacksquare}$  is the mass flux of component A with regard to the volume average velocity,  $v_A$  is the velocity of A with regard to a fixed coordinate system,  $v^{\blacksquare}$  is the volume average velocity, and  $\rho_A$  is the mass of A per unit volume of material. The volume average velocity is defined by:

$$v^{\blacksquare} = \rho_A v_A \tilde{V}_A + \rho_B v_B \tilde{V}_B \quad (3)$$

where  $\tilde{V}_A$  and  $\tilde{V}_B$  are the partial mass volumes of the two components. Since  $\rho_A \tilde{V}_A + \rho_B \tilde{V}_B = 1$ , Equation 1 becomes:

$$j_A^{\blacksquare} = \rho_A \rho_B \tilde{V}_B (v_B - v_A) \quad (4)$$

The mass flux based on the volume average velocity can be related to the mass flux based on the mass average velocity,  $j_A$ .

$$j_A = \rho_A (v_A - v) \quad (5)$$

where  $v$  is the mass average velocity.

$$v = \frac{1}{\rho} (\rho_A v_A + \rho_B v_B) \quad (6)$$

Therefore,

$$j_A = \frac{\rho_A \rho_B}{\rho} (v_A - v_B) \quad (7)$$

Substituting Equation 7 into Equation 4,

$$j_A^{\square} = \tilde{V}_B \rho j_A \quad (8)$$

Now,  $j_A$  is defined as (Bird, 1960):

$$j_A = -\rho D \nabla \omega_A \quad (9)$$

where  $\omega_A = \rho_A / \rho$  (the mass fraction of A) and  $\rho_A + \rho_B = \rho$ . We assume that the partial mass volumes of the two components are constant. This can be demonstrated in Figure 2, where it is shown that the density is nearly a linear function of mass fraction (Russell, 1978). Therefore:

$$\tilde{V}_A \nabla \rho_A + \tilde{V}_B \nabla \rho_B = 0 \quad (10)$$

and

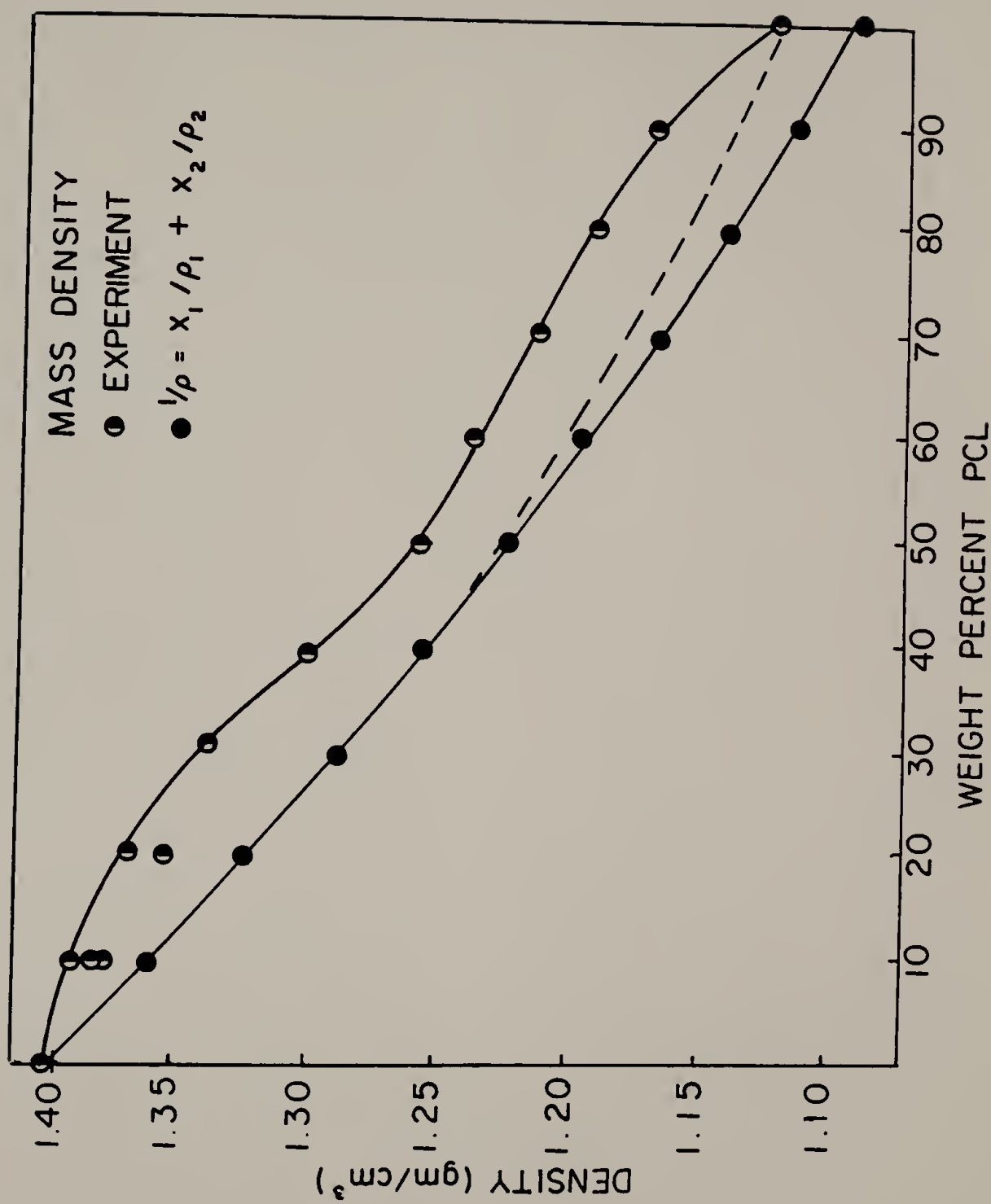
$$\nabla \rho = \left( \frac{\tilde{V}_B - \tilde{V}_A}{\tilde{V}_B} \right) \nabla \rho_A \quad (11)$$

It is now simple to show that

$$j_A = \frac{-D \nabla \rho_A}{\rho \tilde{V}_B} \quad (12)$$

and thus

Figure 2. Density versus wt% PCL for PVC/PCL system.  
Lower curve represents volume additivity.



$$j_A^{\blacksquare} = -D \nabla \rho_A \quad (13)$$

i.e., the mass flux of component A based on a volume average velocity is equal to the negative of the diffusion coefficient multiplied by the gradient of the mass density of A.

A short comment must be made about the nature of the diffusion coefficient,  $D$ . A mass flux can be defined for each of the diffusing species:

$$j_A^{\blacksquare} = -D_A \nabla \rho_A \quad (14)$$

and

$$j_B^{\blacksquare} = -D_B \nabla \rho_B \quad (15)$$

From our definition of  $j_A^{\blacksquare}$ , Equation 2, and of  $v^{\blacksquare}$ , Equation 3, it can be shown that

$$j_A^{\blacksquare} \tilde{V}_A + j_B^{\blacksquare} \tilde{V}_B = 0 \quad (16)$$

So

$$D_B \nabla (\rho_B \tilde{V}_B) = -D_A \nabla (\rho_A \tilde{V}_A) \quad (17)$$

From Equation 10, it follows that:

$$D_A = D_B \quad (18)$$

Therefore, the diffusion coefficient given in Equation 13 and used in all subsequent calculations may be considered to

a mutual diffusion coefficient for the binary system.

The mass balance for the system is given by:

$$\frac{\partial \rho_A}{\partial t} + \nabla \cdot (\rho_A \mathbf{v}_A) = R_A \quad (19)$$

is the rate of production of component A within a volume element of the diffusing system. In cases where there are no chemical reactions,  $R_A = 0$ . Substituting Equation 2 into Equation 19,

$$\frac{\partial \rho_A}{\partial t} + \nabla \cdot (\rho_A \mathbf{v}^{\square}) + \nabla \cdot (\mathbf{j}_A^{\square}) = 0 \quad (20)$$

assuming that the volume average velocity,  $\mathbf{v}^{\square}$ , equals zero,

$$\frac{\partial \rho_A}{\partial t} = -\nabla \cdot \mathbf{j}_A^{\square} \quad (21)$$

Many investigators have solved various diffusion equations for binary systems with a concentration dependent diffusion coefficient (Boltzmann, 1894; Matano, 1933; Stokes, 1952; Wilkins, 1952; Lee, 1971). There are a number of systems where  $D$  varies little with concentration or is constant (Jost, 1967). With a constant diffusion coefficient, Equation 21 and Equation 13 become:

$$\frac{\partial \rho_A}{\partial t} = D \nabla^2 \rho_A \quad (22)$$

Implicit in the assumption of  $\mathbf{v}^{\square} = 0$  is the fact that  $\tilde{\mathbf{V}}_A$  and

$\tilde{V}_B$  are constant.

II.4.2 Solution to the diffusion equation. A reasonable experiment would be to layer two polymer films such that the thickness of each film is much greater than the interpenetration distance. In such a case, the diffusion may be construed to be one-dimensional, i.e., in the x direction only. Hence,

$$\frac{\partial \rho_A}{\partial t} = D \frac{\partial^2 \rho_A}{\partial x^2} \quad (23)$$

The boundary conditions are as follows:

$$\text{At } t = 0, \rho_A(x) = \rho_0 \text{ at } x \leq 0$$

$$\text{and } \rho_A(x) = \rho_1 \text{ at } x > 0$$

$$\text{At } t > 0, \rho_A(x) = \rho_0 \text{ at } x = -\infty$$

$$\text{and } \rho_A(x) = \rho_1 \text{ at } x = +\infty$$

Defining

$$y = \frac{\rho_A(x) - \rho_0}{\rho_1 - \rho_0}$$

and

$$\eta = \frac{x - x_0}{\sqrt{4Dt}}$$

where  $x_0$  is the position of the interface, Equation 23 becomes:

$$-2\eta \frac{\partial y}{\partial \eta} = \frac{\partial^2 y}{\partial \eta^2} \quad (24)$$

The solution to this equation, using the dummy variable  $q$  and boundary conditions, is:

$$y(x) = \frac{1}{\sqrt{\pi}} \int_{-\infty}^{\eta} e^{-q^2} dq \quad (25)$$

Using the definition of the error function,  $\text{erf}(\eta)$ :

$$y(x) = \frac{1}{2} [1 + \text{erf } \eta] \quad (26)$$

$$\frac{\rho_A(x) - \rho_0}{\rho_1 - \rho_0} = \frac{1}{2} \left[ 1 + \text{erf} \left( \frac{x - x_0}{\sqrt{4Dt}} \right) \right] \quad (27)$$

The last equation will be used to analyze the experimental data by fitting the data to the equation by numerical analysis (Appendix A) to determine a value for the diffusion coefficient. The necessary data, then, are a measure of the density of one of the components,  $\rho_A$ , as a function of distance relative to the interface,  $x - x_0$ , and the diffusion time,  $t$ . In the following equations and discussion the symbol used for mass density is changed from  $\rho_A$  to  $c$ . This



change is simply for consistency with the literature. The symbols  $\rho$  and  $c$  represent identical quantities, mass density (or mass concentration).

### II.5 An Experiment

In order to make use of the mathematical description arrived at in the previous section, the data must provide a measure of the concentration profile as a function of time. Assuming that the technique which will be employed is effective for collecting the necessary information, the possible variables must be described.

The variation of the diffusion coefficient with molecular weight of one of the components can be related to studies done on the variation of the bulk viscosity with molecular weight (Graessley, 1973; Porter, 1969). These data can also be used to determine the validity of Bueche's theory (1952) relating the bulk viscosity to the diffusion coefficient. Above a certain molecular weight (a critical molecular weight) where many physical properties begin to show a small dependence on molecular weight, it has been shown experimentally that  $\eta \propto M^{3.4}$  (Graessley, 1973). Bueche's theory states that since  $D\eta$  is approximately constant, one would expect to see that  $D \propto M^{-3.4}$ . This work will provide an opportunity to experimentally evaluate this relationship.

The diffusion coefficient can be expressed as:

$$D = D_0 \exp(-Q/RT) \quad (28)$$

where  $Q$  is the energy of activation for diffusion (Jost, 1952). The activation energy for diffusion can be determined by conducting several experiments at various temperatures. The result will be compared to that found by Bueche et al. (1952) for poly(n-butylacrylate) ( $Q = 13.2$  kcal/mol).

Of primary importance is the need for developing an experimental technique which will provide accurate, reproducible data. To a certain extent, trial and error plays a role in this development. An extensive discussion of the techniques which were used is included in the following section.

The primary system studies was poly(vinylchloride)/poly( $\epsilon$ -caprolactone). Various molecular weights of the compounds were used. To further demonstrate the applicability of the technique, diffusion was observed in the system polystyrene/poly(o-chlorostyrene).

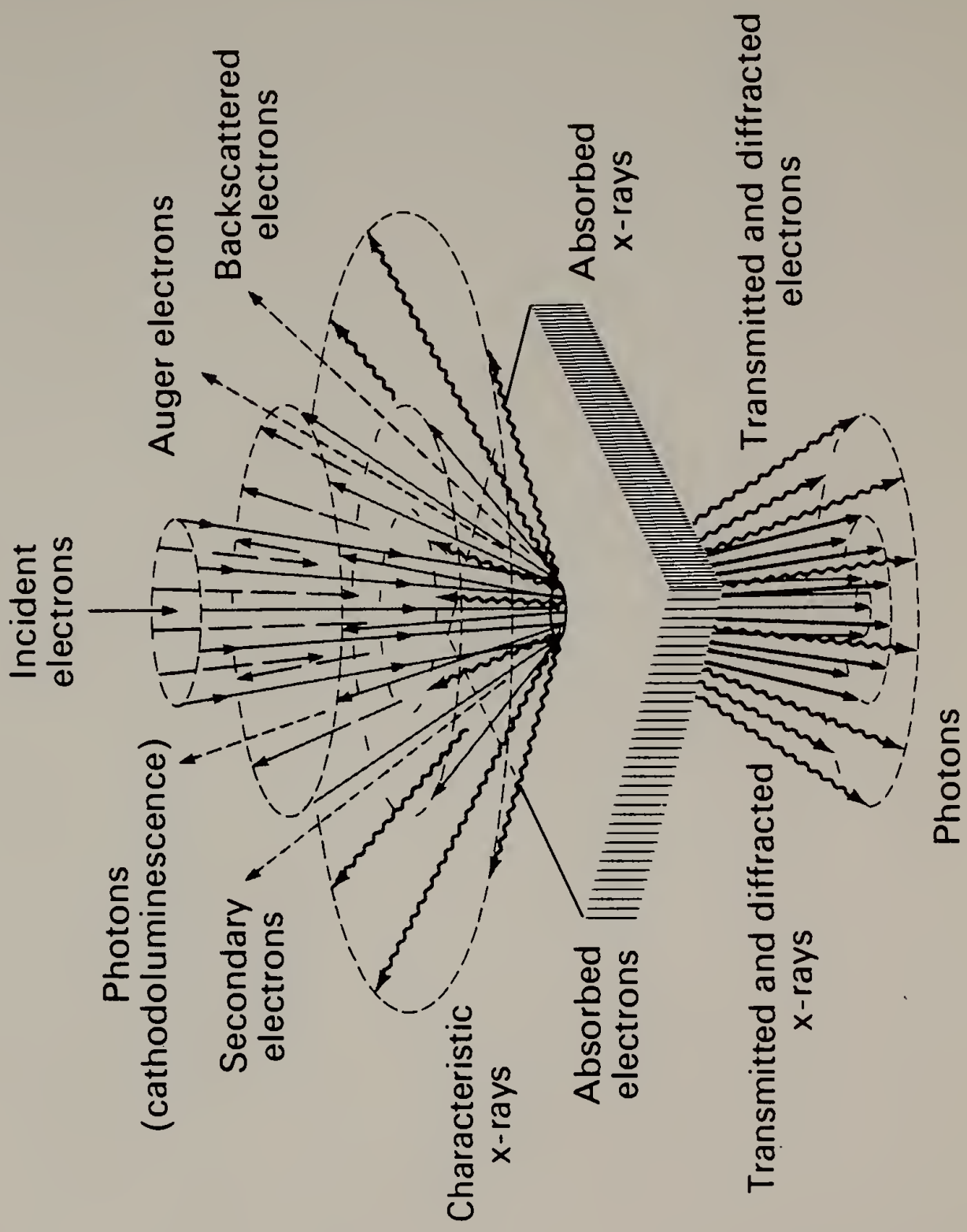
## CHAPTER III

### EXPERIMENTAL TECHNIQUE

An experimental method is needed which will allow observation of a concentration profile which is less than 100  $\mu\text{m}$  in depth. Further, not only must the interface be detectable but the concentration gradient must be resolvable. The optical microscope has found application as a technique for diffusion experiments involving small molecules (diluent) in polymers (Crank and Park, 1968; Paul, 1970) but the interpenetration distance for this type of experiment is substantially larger than for the interdiffusion of two polymers. An electron microscopic technique has already been suggested; specifically, a scanning electron microscope (ETEC Autoscan U-1) was used for the purpose of observing the interface. The resolution of the scanning electron microscope (SEM), 100  $\text{\AA}$ , is sufficient to observe the interface and resolve much smaller distances than the distance covered by the majority of the concentration gradient ( $\sim 10 \mu\text{m}$ ).

Once the interface can be observed, a method for detecting the concentration of one or both of the components is necessary. When an electron beam impinges on a sample surface, many types of radiation are emitted, including what are known as characteristic x-rays (Figure 3). Each element

Figure 3. Phenomena resulting from electron beam bombardment.



emits x-rays with specific energies. Therefore, if the energy of the x-rays emitted can be detected and the element from which they emanated is unique to one of the polymeric components, then the possibility of measuring a concentration exists if one can count the number of x-ray events. This technique of detecting the energy of emitted x-rays is called energy dispersive analysis of x-ray fluorescence (EDS) and, in conjunction with SEM, is the technique which has been used to observe the concentration profiles necessary for calculating a diffusion coefficient for the system.

### III.1 Scanning Electron Microscopy

The scanning electron microscope was first described by Knoll (1935) but was not commercially developed until the work by Stewart and Snelling (1965) was announced. The instrument works by irradiating the specimen with a finely focused electron beam. This results in secondary electrons, back scattered electrons, characteristic x-rays, and several other types of radiation (Figure 3). The intensity of these signals will depend in some way on the shape and chemical composition of the irradiated volume. To produce a picture of the surface, the beam is scanned in a raster pattern. (The electron beam is moved discretely from one point on the surface to another. The secondary electrons which emanate from each position are collected and transformed into a picture on a CRT by coordinating the position of the electron



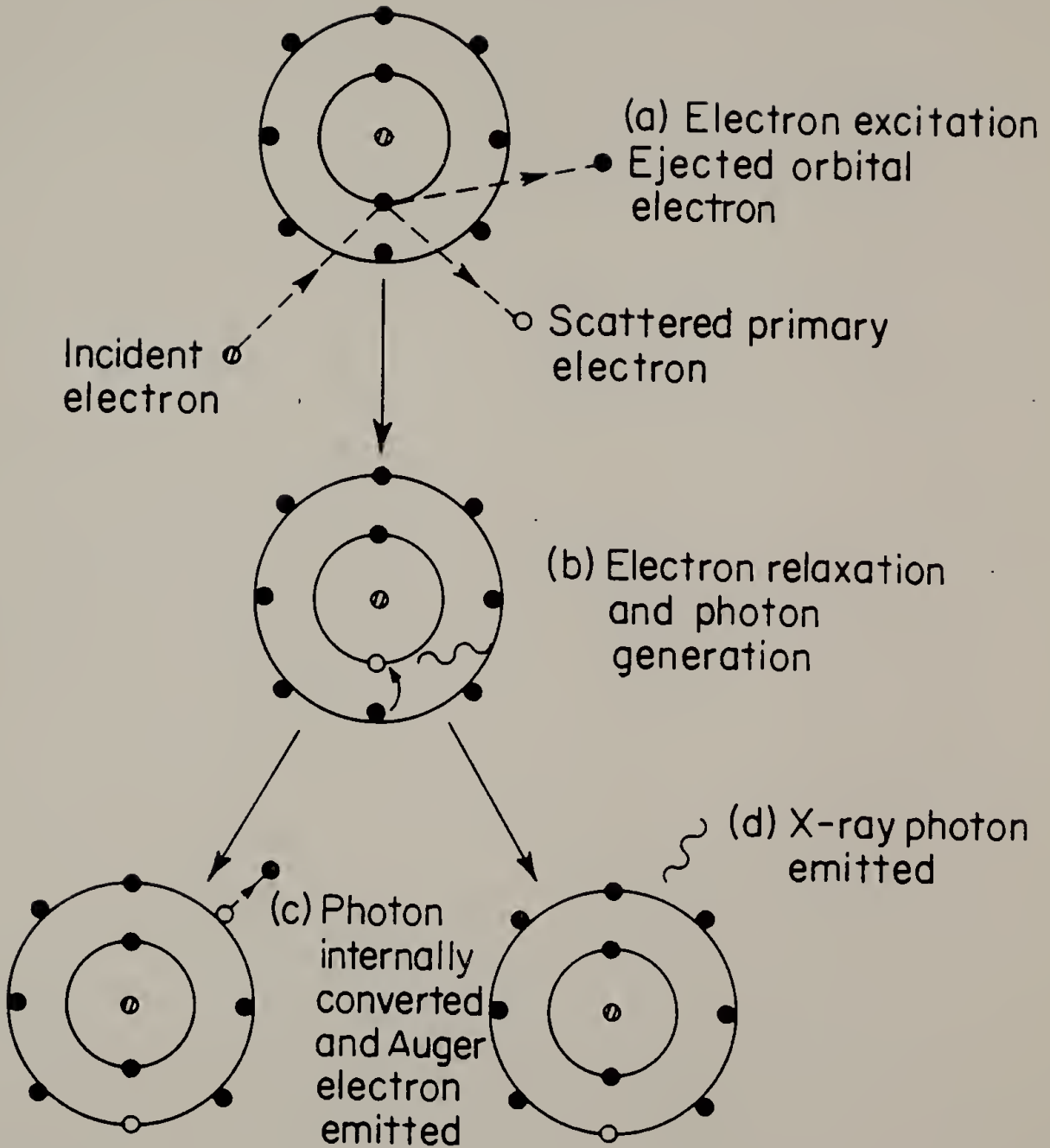
beam on the sample to the position of the electron beam within the CRT, the intensity of which is proportional to the secondary electron signal at each position on the sample surface.) To obtain an x-ray analysis of a given position on a specimen, the beam remains stationary at the specified position. Details of the construction and operation of the SEM are readily available (Wells, 1974; Holt et al., 1974).

The small diffusion rates which were expected for interdiffusing polymers would result in a small distance of interpenetration and require that the experimental apparatus be capable of resolving much smaller distances than the  $10^{-25}$   $\mu\text{m}$  across which the majority of the concentration gradient would lie. The practical choices were thus narrowed to transmission or scanning electron microscopy. The SEM was used because it had the necessary resolution ( $100 \text{ \AA}$ ) and it did not require thin specimens, an experimental difficulty encountered by Voyutskii et al. (1965, 1966).

The quality of the image obtained using SEM depends upon the phenomena which occur as a result of electron beam bombardment of the surface. Secondary electrons, electrons ejected from the sample surface (or immediately below it) having a low energy, less than 50 eV, provide an image of the surface (Wells, 1974) and were used in this study for observing the surface topography of the interdiffused samples. This topography was recorded using a high resolution CRT affixed to the SEM specifically for the purpose of photographi-

Figure 4. Schematic diagram of characteristic x-ray generation.





cally recording SEM images. However, merely viewing the interface is not sufficient. The method used for measuring the concentration will now be described.

### III.2 Energy Dispersive Analysis of X-ray Fluorescence

When an atom is struck by high velocity electrons, some of the energy may be transferred to bound electrons of the atom, exciting them to higher energy levels and creating vacancies in the atomic structure. Each vacancy is almost immediately filled by another electron from a higher energy level, the energy difference being emitted as an x-ray photon (Figure 4). The difference in energy levels is characteristic for a given element. Therefore, if the energy of the emitted x-ray photon can be measured, the element from which it originated can be identified. The number of x-ray events of a given energy can be recorded using a multichannel analyzer, the result being a spectrum of the number of x-ray events versus x-ray energy for the specimen being irradiated (Russ, 1971; Woldseth, 1973).

In determining the concentration profile by energy dispersive spectroscopy (EDS), the phenomena of x-ray generation and detection must be taken into account. Details of the technique are presented in the following sections.

III.2.1 X-ray signal. The main feature of the x-ray micro-analysis technique is that the number of x-ray counts occur-

ring at a given energy is proportional to the number of atoms in the irradiated volume from which those x-rays originated (Maurice et al., 1965). The detected count rate,  $N$ , of the  $K_\alpha$  x-rays will be given by a product of the electron flux,  $J$  (electrons/cm<sup>2</sup>/sec), the number of atoms of the specific element per unit volume,  $n$  (atom/cm<sup>3</sup>), the ionization cross section for K shell excitation,  $Q_k$  (cm<sup>2</sup>), the fluorescence yield of K shell x-rays,  $\omega_k$ , the ratio of the yield of  $K_\alpha$  x-rays to the total K shell yield,  $K_\alpha + K_\beta$ , and finally the detector efficiency,  $T$  (solid angle and quantum detection efficiency of  $K_\alpha$  x-rays) (Joy and Maher, 1977).

$$N = JnQ_k\omega_k\left(\frac{K_\alpha}{K_\alpha + K_\beta}\right) T \quad (29)$$

Sample self-absorption of x-rays also must be taken into account. Normally for thick samples one employs suitable standards to calibrate the system because the ionization cross section depends on the electron energy, making x-ray yield depth dependent and the absorption effects difficult to calculate analytically. Fortunately the system under study has built in standards: concentrations of the pure materials can be measured far from the interface. The concentration profile can thus be determined by integrating the particular  $K_\alpha$  peak for a constant total electron dose for a constant total electron dose for a given irradiated position. Background counts from sample Bremsstrahlung and

system background are measured at the  $K_\alpha$  peak far from the interface. We define the concentration profile as:

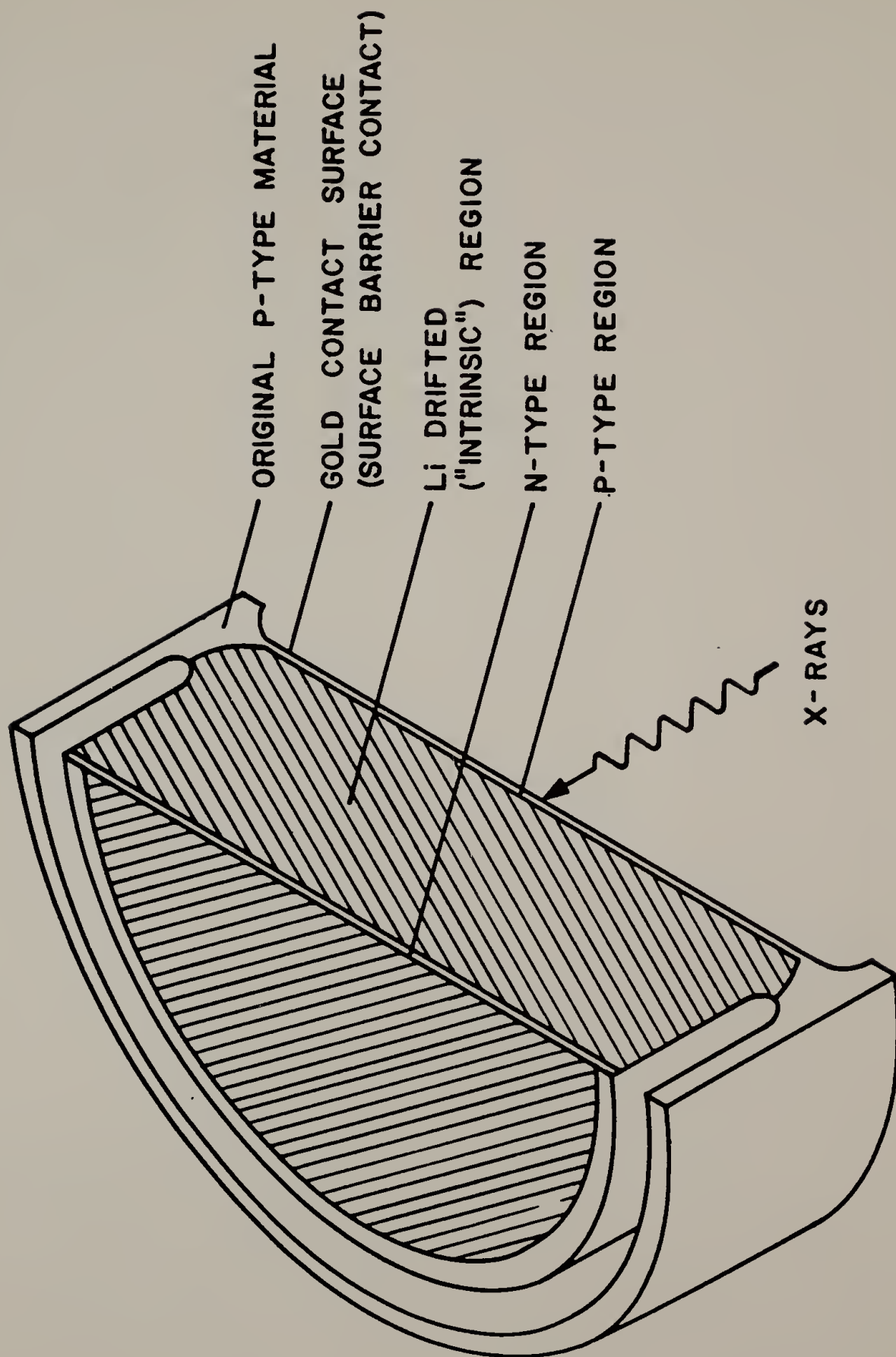
$$\frac{c(x) - c_0}{c_1 - c_0} = \frac{\frac{\int_{FWHM} N(\epsilon, x) d\epsilon}{K_\alpha} - \frac{\int_{FWHM} N(\epsilon, \infty) d\epsilon}{K_\alpha}}{\frac{\int_{FWHM} N(\epsilon, -\infty) d\epsilon}{K_\alpha} - \frac{\int_{FWHM} N(\epsilon, \infty) d\epsilon}{K_\alpha}} \quad (30)$$

where the integrals at full width half maximum (FWHM) are 160 eV wide. The positions  $x = \infty$  and  $x = -\infty$  represent the two pure components. The result is the reduced concentration required for the equation.

III.2.2 EDS detection system. The detector used for x-ray energy discrimination is a semiconductor of lithium drifted silicon, Si(Li). Its use rests on the absorption of the impinging radiation (x-ray photons) and the effective ionization of the material. The semiconductor crystal has an electric potential applied across it; when the crystal becomes ionized by the incident x-ray, the charge is carried through the detector by the applied potential as a charge pulse. The key to energy spectroscopy is the proportionality between charge and energy deposited by the impinging radiation.

Figure 5 is a diagram of a typical EDS detector and its development is discussed in detail by Woldseth (1973). The detection system used in this work was produced by EDAX. It included a Si(Li) detector and a multichannel analyzer for

Figure 5. Semiconductor type x-ray detector.





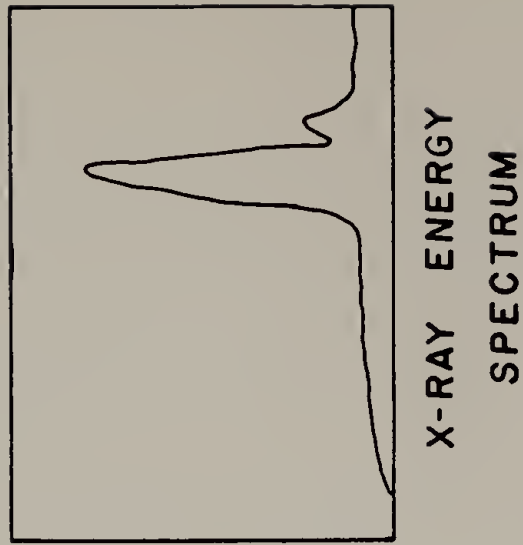
storing the spectrum. The detector is maintained at liquid nitrogen temperature to preserve the semiconductor nature of the detector (at room temperature the Li is too mobile). Also, the detector is maintained in vacuum. This requires that the detector be completely enclosed. To allow the x-rays to reach the detector, the face of the detector is covered with a thin beryllium "window." Since Be will absorb some of the low energy x-rays emanating from the sample, there is an immediate limitation placed on the detection system. However, some sacrifice of detectability must be made to make x-ray detection economically practical. There exists a class of detectors which are called "windowless" detectors, i.e., exposed directly to the vacuum of the system in which the sample is being irradiated. These detectors require much higher vacuum than that normally found in the SEM.

The detector used is capable of resolving 160 ev at full-width-half-maximum (FWHM). Thus, any two elements which emit x-rays at energies closer than this will not be clearly resolvable. This can lead to difficulties when looking at an unknown sample, but in the system under study only one fluorescing specie, chlorine, was being observed. The specific transition was that ascribed to the  $K_{\alpha}$  of chlorine, centered at 2.6 Kev. No elements which fluoresce near this value of x-ray energy were contained in the sample.

A simple description of the process by which an x-ray spectrum is developed is shown in Figure 6. Figure 7 is a

Figure 6. Schematic diagram of x-ray detection.





MULTI-  
CHANNEL  
ANALYZER

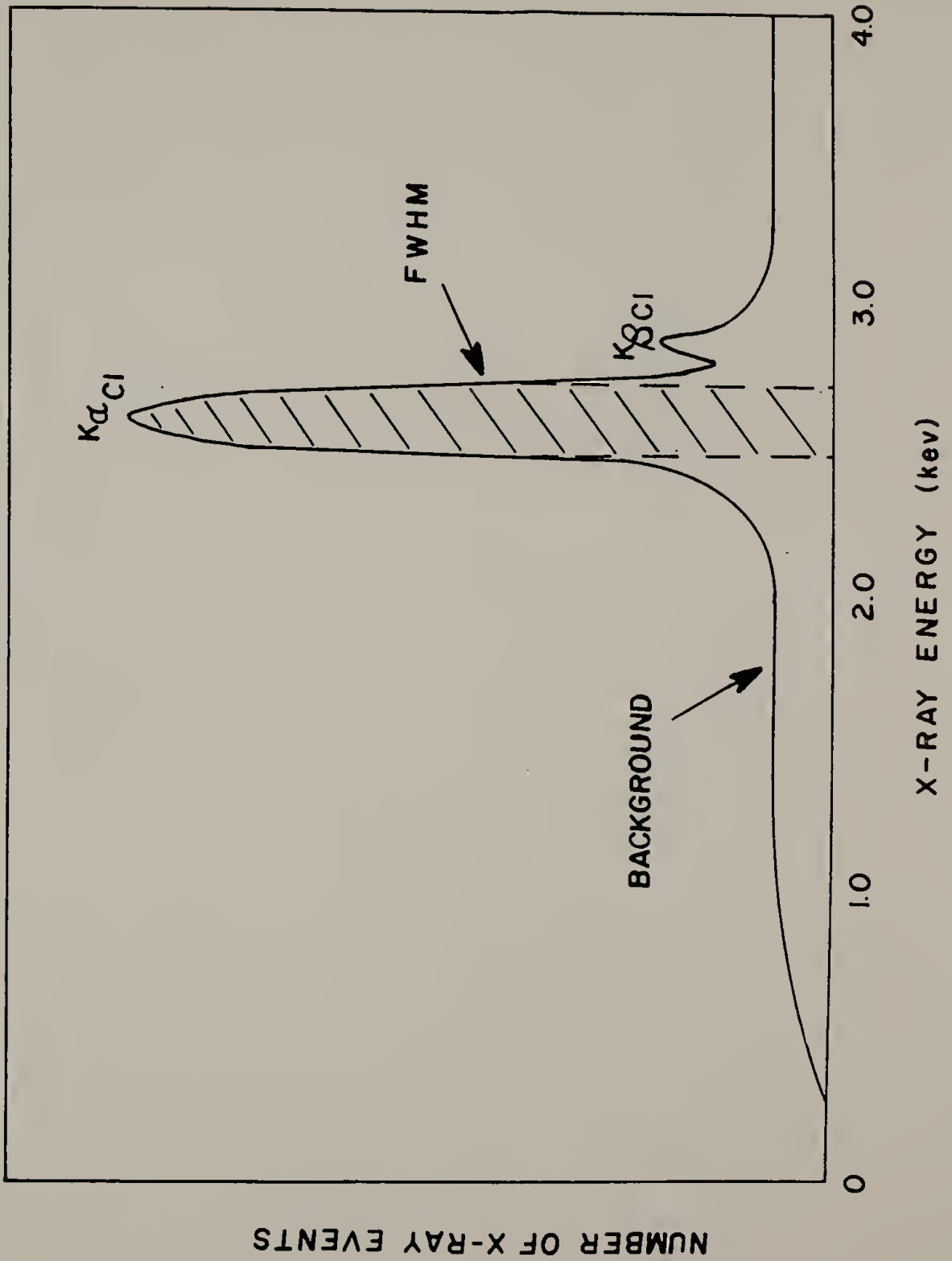


DETECTOR

X-RAY 

The text 'X-RAY' is positioned to the left of a solid black arrow pointing upwards, indicating the input to the Detector.

Figure 7. X-ray spectrum showing chlorine  $K_{\alpha}$  and  $K_{\beta}$  peaks.  
Hashed area used to count x-ray events.



more detailed example of the x-ray spectrum for a sample containing chlorine. Note that there are two transitions associated with chlorine,  $K_{\alpha}$  and  $K_{\beta}$ ; only the  $K_{\alpha}$  was used to determine concentrations of chlorine in the sample.

### III.2.3 Experimental determination of the concentration pro-

file. There are two ways to measure the concentration profile. The first is to direct the electron beam in a line perpendicular to the interface of the interdiffused materials. (This was attempted but did not give consistent, quantitative results.) The rate of x-ray generation for the  $Cl K_{\alpha}$  peak can be plotted as a function of position of the beam on the sample. The major drawback to this method is the need for a very slow scan in order to pick up the weak chlorine fluorescence signal. The resulting high electron dose in the scanned region causes a rapid loss of chlorine signal due to radiation damage (Delgado, 1976) and a heavy contamination layer buildup on the sample surface due to electron beam induced polymerization of microscope system contaminants. Alternatively, one may scan the beam parallel to the polymer/polymer interface and collect the signal (at a given distance) from a much larger sample region, thus minimizing radiation damage and contamination errors. The only precaution is to ensure that the beam is scanned exactly parallel to the interface. Of course one must also orient the sample such that the incident beam direction is parallel

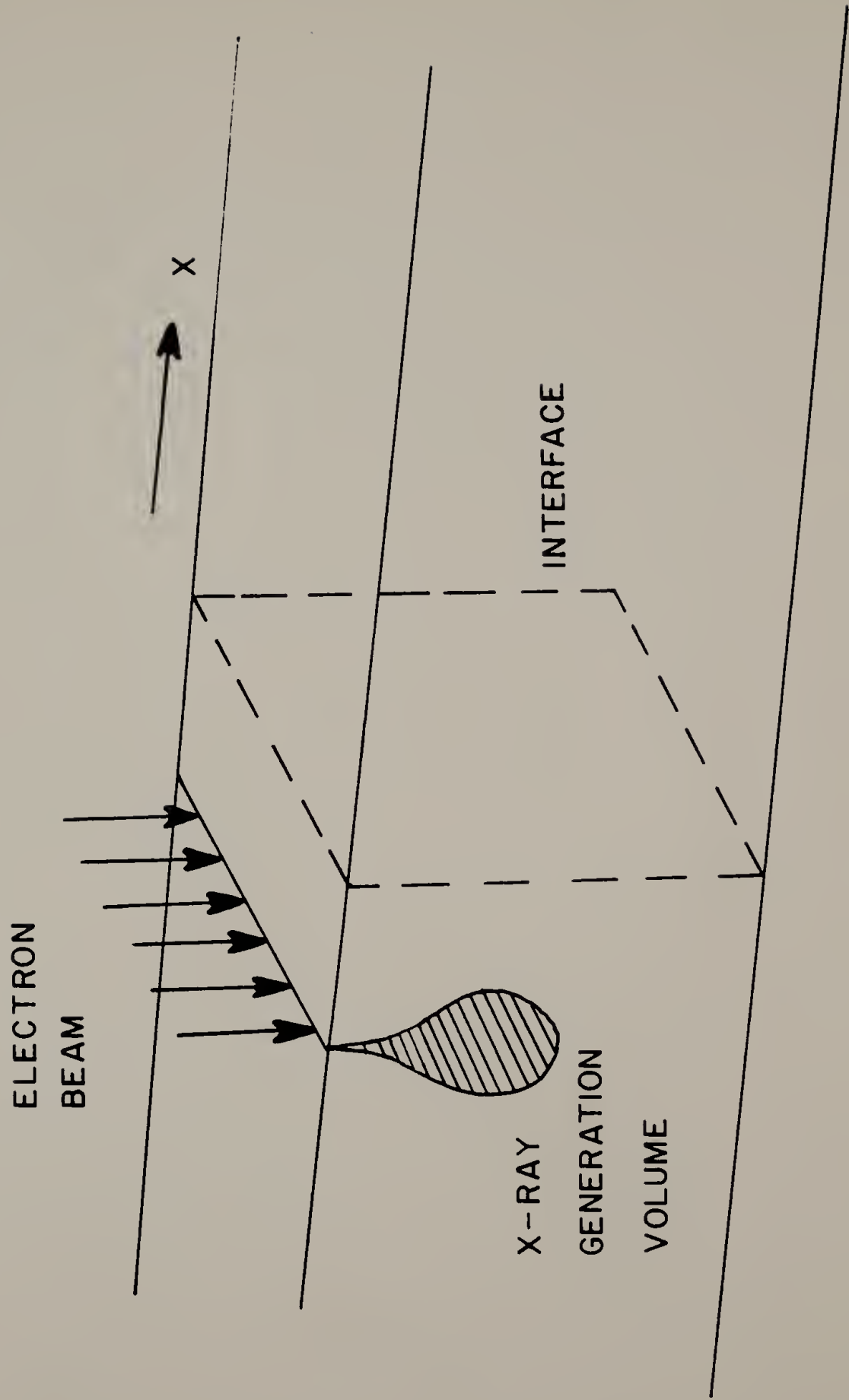
to the plane of contact of the two diffusing species (Figure 8).

As is the case in measuring a spectral curve using a slit detector, the observed concentration profile is the convolution of the actual concentration profile,  $c(x)$ , and the probe width,  $p(x)$  (diameter of x-ray generation volume, Figure 8). The quantity  $p(x)$  acts as a spread function so that the observed concentration profile will be somewhat more diffuse than the actual profile, e.g.,

$$c(x)_{\text{obs}} = c(x)_{\text{true}} * p(x) \equiv \int c(X)_{\text{true}} p(x-X) dX \quad (31)$$

One would like to simply decrease  $p(x)$  to a delta function and thus arrive at the true concentration profile but the physics of the electron-sample interaction causes the incident beam to scatter into a tear drop shape (Lifshin et al., 1969). This is illustrated in Figure 8. For thick (greater than electron penetration depth) specimens of hydrocarbon polymers, the lateral spread of the beam will be on the order of 1 micron (and hence the x-ray generation volume will be  $\sim 1 \mu\text{m}$  diameter) for 20 KV electrons (Reed, 1969). This spreading effect is therefore obviously most serious for sharply varying concentration profiles. Generally one should wait sufficiently long during the diffusion time so that concentration gradients are small with respect to the scale of  $p(x)$  and the observed concentration profile is an accurate representation of the true concentration profile. Also,

Figure 8. Representation of relative positions of interface, electron beam and x-ray generation volume.



positions at which concentration measurements are made should be sufficiently separated so that no overlap of x-ray generation volumes will occur. Most of the x-ray generation occurs at or immediately below the position at which the electrons hit the sample surface (Wells, 1974). Measuring the concentration at separation distances markedly greater than the diameter of the x-ray generation volume will reduce the smearing effect and give a more exact concentration profile.

### III.3 Polymer Samples

The specific materials to which most attention has been paid is the compatible system poly(vinylchloride)/poly( $\epsilon$ -caprolactone). Koleske and Lundberg (1969) found that PVC/PCL blends were compatible over the entire concentration range. Their conclusion was based on the observation of only one  $T_g$  for any blend composition. They also found that the  $T_g$  for the blend could be described by the Fox copolymer equation (Fox, 1956):

$$(1/T_{g12}) = (X_1/T_{g1}) + (X_2/T_{g2}) \quad (32)$$

where  $T_{g12}$  is the glass transition temperature of the blend,  $T_{g1}$  and  $T_{g2}$  are the glass transitions for the homopolymers, and  $X_1$  and  $X_2$  are weight fractions (See Figure 2).

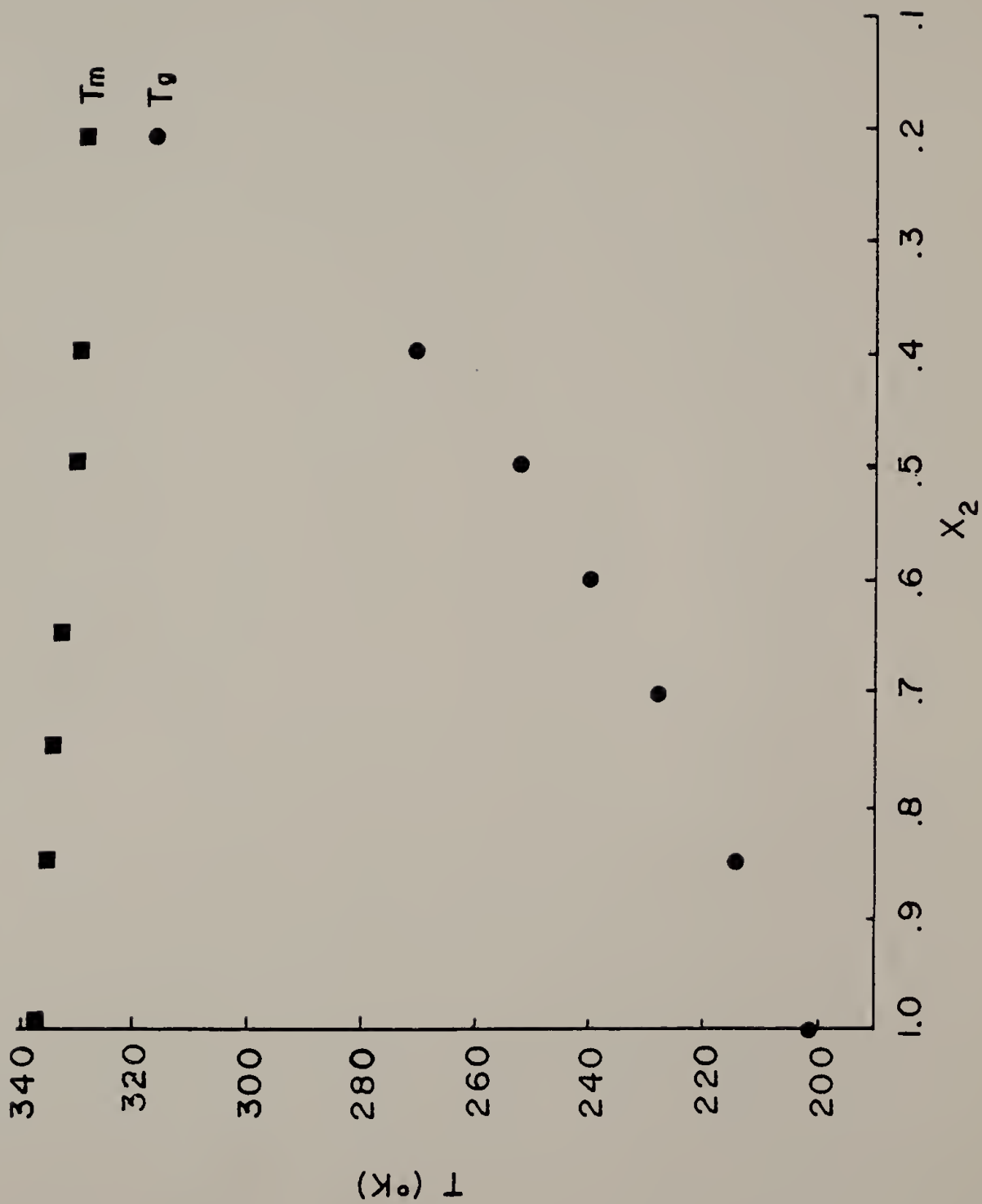
Ong (1973) studied other aspects of the PVC/PCL system, including crystallinity and dynamic mechanical proper-



ties, as a function of blend composition. Figure 2 (Russell, 1978) demonstrates the density of a solution cast blend of PCV/PCL as a function of blend composition for the samples designated as PVC-6 and PCL-4 in Table 2. The change in density as a function of composition is seen to be about 30%. However, more importantly it is noted that the density is an approximately linear function of concentration, showing the validity of the assumption of constant partial mass density. The variation which is observed will have some effect on the accuracy of the calculated diffusion coefficient (Duda and Vrentas, 1966). In fact, the effect of the density variation is not large when compared to the inaccuracy of the measurement of concentration; this last factor overshadows all others.

Figure 9 (Ong, 1973) shows the effect of blend composition on  $T_g$ , the glass transition temperature. It was this method, i.e., blending with PVC, by which Koleske and Lundberg (1969) initially determined the  $T_g$  of pure PCL. Due to the large amount of crystallinity, detection of the glass transition temperature of pure PCL is not possible using normal techniques. Producing a blend with PVC allows measurement of the  $T_g$  values as a function of composition and, using such relationships as the Fox equation mentioned earlier, the value of  $T_g$  of the pure polymer can be calculated. The figure shown here is an example of the behavior of a compatible polymer blend. Only one  $T_g$  is observed, an

Figure 9. The effect on  $T_m$  and  $T_g$  of weight fraction PCL ( $x_2$ ).



indication that the material is homogeneous and not phase separated. Ong's results indicated that although the two materials were compatible in the melt state, below the melting temperature of the PCL ( $\sim 65^{\circ}\text{C}$ ), the PVC molecules were excluded from the PCL lamellae and restricted to the inter-lamellar regions. The PCL is highly crystalline at room temperature and crystallinity is observed in the blends up to a composition of 70% PVC (Figure 10). Further, small angle x-ray scattering (SAXS) studies by Russell and Stein (1978) indicate that in the melt state the PVC/PCL system is compatible on the molecular level. This conclusion is reached because the scattering invariant disappears, implying a complete lack of phase separation (Alexander, 1970).

The various samples of PVC and PCL are shown in Table 2. All are commercially available materials and were used as received. All samples were obtained from Union Carbide Corp. with the assistance of Dr. R.D. Lundberg, except for PVC-1 and PVC-4, which were obtained from Dr. J. Tkacik at Hooker Chemical Corp. The polystyrene used was that produced by Waters Associates with a molecular weight of 20,000 and polydispersity of 1.06. The poly(o-chlorostyrene) was prepared by P. Alexandrovich and has a weight average molecular weight of 160,000 and a polydispersity of 2.1. All molecular weights were determined by gel permeation chromatography using the Q method of molecular weight determination. The Q values used were 23 for PCL (from Cellomer Associates),

Figure 10. Crystallinity of PVC-6/PCL-4 blend as a function of weight fraction PCL-4 ( $x_2$ ).

- BY HEAT OF FUSION
- ▲ BY DENSITY
- BY X-RAY



Table 2. Experimental Materials--PVC and PCL.

SAMPLE	$M_n$	$M_w$	$M_w / M_n$
PVC - 1	1,700	4,000	2.3
PVC - 2	18,500	46,500	2.5
PVC - 3	33,200	73,700	2.2
PVC - 4	33,600	86,400	2.6
PVC - 5	40,300	97,800	2.4
PVC - 6	40,600	102,000	2.5
PCL - 1	1,200	1,800	1.5
PCL - 2	1,400	2,600	1.8
PCL - 3	5,400	9,400	1.7
PCL - 4	19,200	37,200	1.9



25 for PVC (Alliet and Pacco, 1968), and 41 for PS (Waters Associates).

The materials were all used as received. Thus, it was assumed that there was some thermal stabilizer present in the PVC samples; this would be on the level of 0.01% by weight and was assumed to have no effect on the diffusion rates. No other additives were expected to be present.

### III.4 Experimental Technique

III.4.1 Preparation of PVC films. PVC films were prepared by dissolving the polymer in tetrahydrofuran (THF) at a concentration of 0.5% by weight and then casting the solutions on glass at room temperature. The flat glass dishes used for this were made by welding a ring of Pyrex<sub>TM</sub> glass (diametric slice cut from a long tube) to a flat piece of Pyrex<sub>TM</sub> glass sheet. The bottom surfaces of these dishes (100 mm in diameter) were found to be much flatter than a Petrie dish and provided more uniform films. The films were cast at room temperature and allowed to dry for several days. After air drying, the optically clear films, about 100  $\mu\text{m}$  thick, were placed in a vacuum oven for several weeks, again at ambient temperature, to ensure removal of THF. Films were prepared by this method for all PVC samples.

III.4.2 Interfacial contact between diffusants. PCL is a highly crystalline material with a melting point of  $\sim 65^{\circ}\text{C}$ .

Therefore, all diffusion experiments were carried out at temperatures above 65°C to ensure that both components of the pair were in an amorphous state.

A film of PVC was placed in a vacuum oven (produced by Blue M Comp.) maintained at the selected diffusion temperature. The temperature used during the studies of the effect of molecular weight on the diffusion coefficient was 70°C. PCL, in the pellet or flake form in which it was received, was placed on top of the PVC film. The sample, PVC film covered with solid PCL, was enclosed in the vacuum oven and the chamber evacuated using a mechanical vacuum pump. The vacuum helped reduce oxidative degradation observed in unstabilized PVC at elevated temperature (Hawkins, 1973). Temperature was maintained with an accuracy of  $\pm 1^\circ\text{C}$ .

The sample gradually heated to the temperature of the oven. Upon melting, the PCL flowed easily and provided excellent interfacial contact. This was easily verified by electron microscopic examination. The PCL remained viscous enough to remain on top of the PVC sheet even at the higher temperatures.

The times for a diffusion experiment varied between  $5 \times 10^5$  sec and  $10^7$  sec (7 days to three months). Observations of the concentration profile were made at approximately one week intervals, resulting in profiles at several diffusion times. At the time a measurement of the concentration profile was to be made, the sample was removed from the

vacuum oven and cooled to room temperature. A small section was cut from the sample with a scalpel and the main portion returned to the vacuum oven. This process took about 30 minutes, interrupting the diffusion process for a negligible period of time. The excised section was cooled in liquid nitrogen and fractured perpendicular to the plane of contact between the PVC and PCL, exposing the interface. The fractured segment was mounted on edge on a SEM sample stub with the cross-section facing up; this placed the interface in a position directly below the electron beam in the SEM, the plane of contact being parallel to the electron beam. The material used to mount the sample on the SEM stub was a colloidal suspension of graphite in isopropanol, trade named DAG. The sample was coated with a thin layer of chromium,  $\sim 200 \text{ \AA}$  thick, using a Denton DV-502 vacuum evaporator with a rotary attachment made by E.F. Fullam. This coating helped reduce the effects of sample charging and electron beam heating but, due to its x-ray fluorescence at 5.4 Kev ( $\text{Cr K}_{\alpha}$ ), did not adversely affect the fluorescence of chlorine.

The procedures for the PS/PoCS system were similar except that the PoCS was hot pressed at  $135^{\circ}\text{C}$ , forming a film  $\sim 100 \text{ \mu m}$  thick. The film was covered with particulate PS and maintained at a diffusion temperature of  $150^{\circ}\text{C}$ .

III.4.3 Observation in the SEM. The sample, with interface exposed, is placed in the SEM. At low magnification the sample appears as in Figure 11. This is an edge-on view of the interdiffused sheets, the PVC on top and the PCL below. The position of the interface can be seen in Figure 12, the same sample as in the previous figure but at higher magnification. The excellent interfacial contact is readily seen. The change in morphology is obvious and facilitates location of the interface. This microstructural change is due to the crystallinity of the PCL at room temperature. Crystallization effectively "freezes" the diffusion process. It has little effect on the concentration profile because, although Warner et al. (1977) noted that crystallization of PCL in a PVC/PCL blend segregated the PVC to the interlamellar spaces of the PCL crystallites, the size of PCL crystallites and interlamellar spaces are on the order of  $100 \text{ \AA}$  and this is several orders of magnitude less than the size of the x-ray generation volume and the magnitude of the spacings between concentration measurements. Since concentration measurements will be made by an electron beam crossing many lamellae, the effect of segregation is negligible.

III.4.4 Development of the concentration profile. Once the interface was located, the magnification was increased to between 2000 and 5000. Within this range the majority of the interfacial thickness could be viewed on the screen of the

Figure 11. Interdiffused sample of PVC/PCL with interface exposed as seen in SEM.



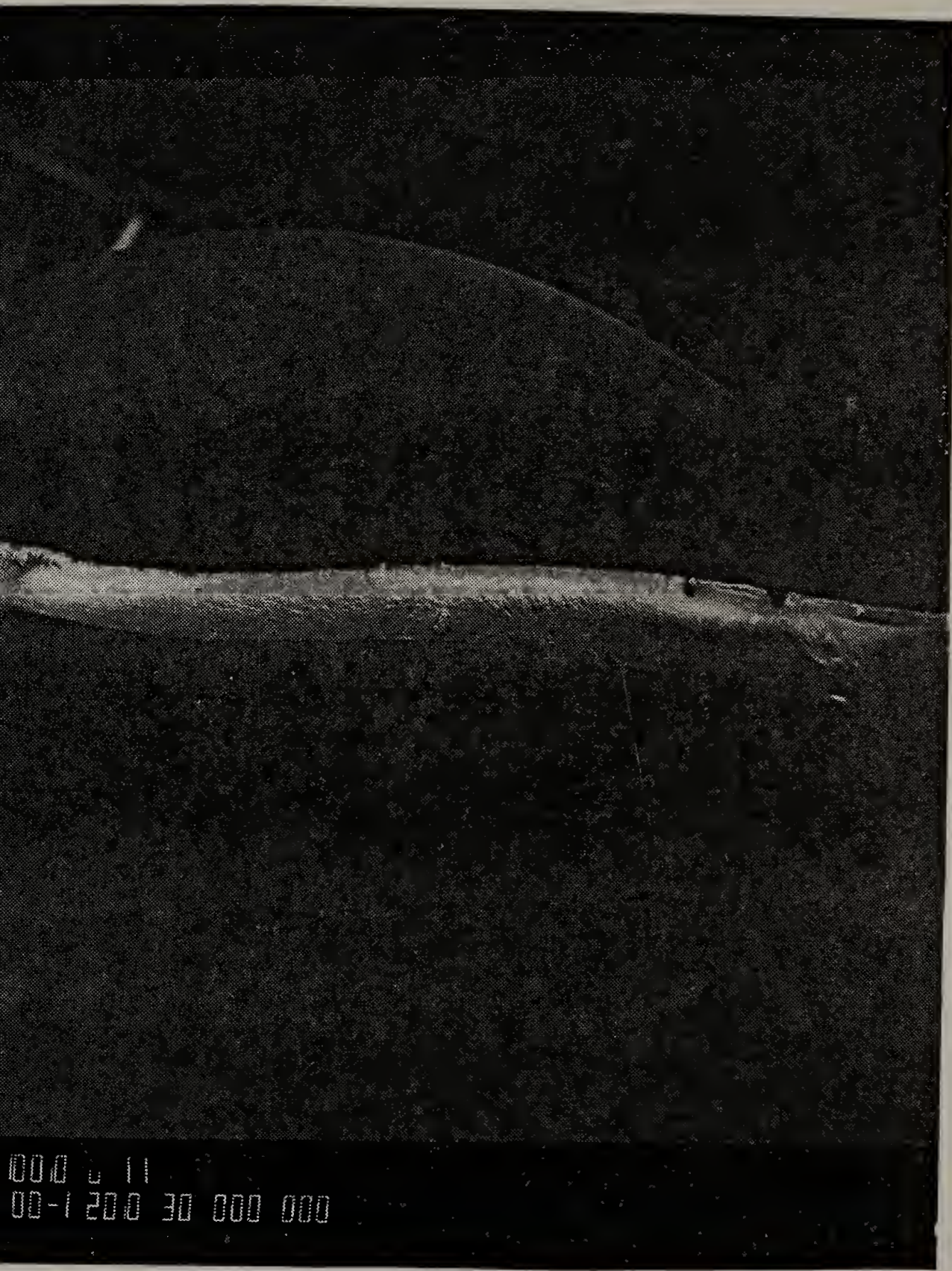


Figure 12. Photomicrograph of interface of PVC/PCL films. PCL at bottom.





000 J H  
03-2 200 25 000 000



SEM. Obviously the magnification used was dependent on the temperature and diffusion time, both of which would influence the depth of interpenetration.

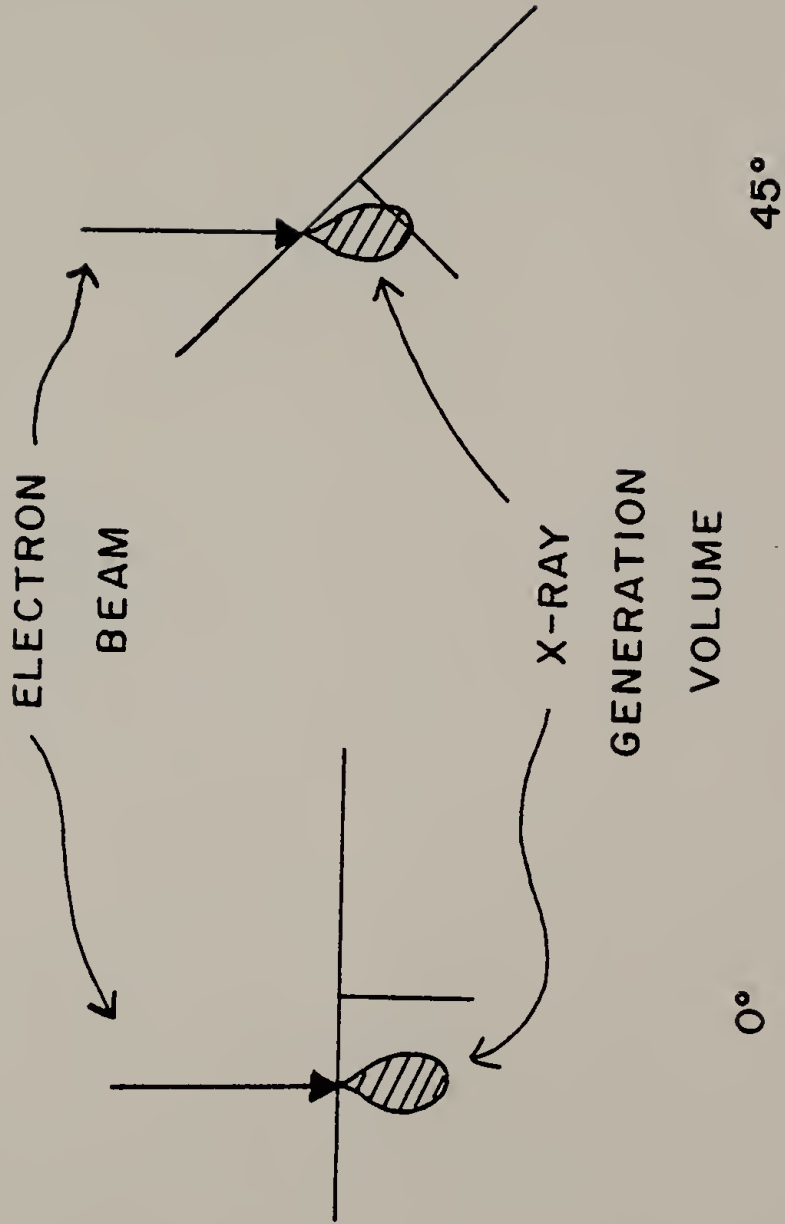
Prior to concentration measurement, several precautions had to be taken. The first was to ensure that the surface of the sample facing the electron beam was flat. Although no change in x-ray count rate was observed as a function of angle for a PVC sheet between the angles of  $0^\circ$  and  $30^\circ$  (Table 3), this precaution is not unreasonable. It was also necessary to make sure that the plane of interfacial contact was perpendicular to the SEM stub (parallel to the electron beam). Then the electron beam would penetrate the sample parallel to the interfacial plane; penetration at an angle would smear the concentration measurement (Figure 13). The alignment of the interfacial plane was accomplished in two steps. The sample was mounted perpendicular to the sample stub surface; thus the interfacial plane was quite close to being perpendicular. Further examination in the SEM revealed the position at which the exposed plane of the PVC film was parallel to the electron beam. Since the PVC films were of uniform thickness, translating the sample the distance necessary to observe the interface resulted in the other side of the PVC film, i.e., the interfacial plane, also being parallel to the electron beam.

With the interface positioned in a horizontal fashion (as viewed on the SEM screen), a photomicrograph was taken.

Table 3. Cl x-ray counts vs. stage angle for pure PVC.

ANGLE	COUNTS
0	10768
5	11112
10	11065
15	11257
20	11473
25	11390
30	11279

Figure 13. Electron beam penetration in relation to orientation of interface.



The photomicrographic unit places on the micrograph a bar indicating the length of a standard unit (e.g., one micron). The electron beam was then changed from a raster scan to a line scan. The line viewed on the SEM screen was then moved to the bottom of the screen. At this point analysis of the chlorine concentration was begun.

The EDS system used (EDAX 707B) has an internal timer which allows the operator to count the number of x-rays generated during a specific period of time. The time used in this study was 20 seconds; the next lower time, 10 seconds, resulted in too few counts and the next higher time, 40 seconds, showed degradation of PVC (Delgado, 1976). The number of chlorine x-rays generated in 20 seconds at the position of the electron beam was totalled for the Cl  $K_{\alpha}$  peak at FWHM (160 ev wide). This was used for all concentration measurements throughout this study. When the twenty seconds had elapsed, counting was automatically terminated and the total number of x-ray events occurring with the appropriate energies was displayed on the EDS screen. This was recorded along with the relative position of the line and the actual position of the line was recorded photographically on the surface picture mentioned earlier. Then the position of the line was moved "up" on the screen the equivalent of  $\sim 5 \mu\text{m}$  and the counting of x-ray events begun. This procedure, moving the line, counting x-ray events for 20 seconds, photographing the position of the line, was repeated until

the entire area shown on the SEM screen had been traversed. Examples of the recorded data and photomicrograph are shown in Table 4 and Figure 14. Measurements such as these were made at several positions along the interface. After each set of x-ray counts was taken, the area of view was moved far from the interface by translating the position of the sample, the magnification being kept constant. This translation was done while using a raster scan. The beam was again changed to a line scan and several measurements of the number of x-rays generated in 20 seconds were made. This procedure was carried out on both sides of the interface at distances which were essentially infinitely far from the interfacial position, i.e., near the edge of the sample. No chlorine peaks were observed in the PCL. These measurements provided values for  $c_0$  and  $c_1$  necessary to normalize the concentration in Equation 27, values which were effectively those for pure PCL and pure PVC.

The concentration profile, x-ray counts versus distance, was developed from the photomicrograph by measuring the micron bar equivalent using a vernier caliper, and then measuring the distances between the lines on the micrograph and summing these distances. Figure 15 is an example of such a profile. Several such profiles were developed for each sample at each diffusion time.

It was noted earlier that there would be some smearing of the concentration profile due to a finite x-ray

Table 4. Raw Data--Line vs. x-ray counts of typical concentration profile.



LINE	COUNT
1	488
2	606
3	666
4	767
5	990
6	1547
7	1854
8	2023
9	2183
10	2346
11	2412
12	2438

Figure 14. Example photomicrograph showing photographically recorded positions of concentration measurement.

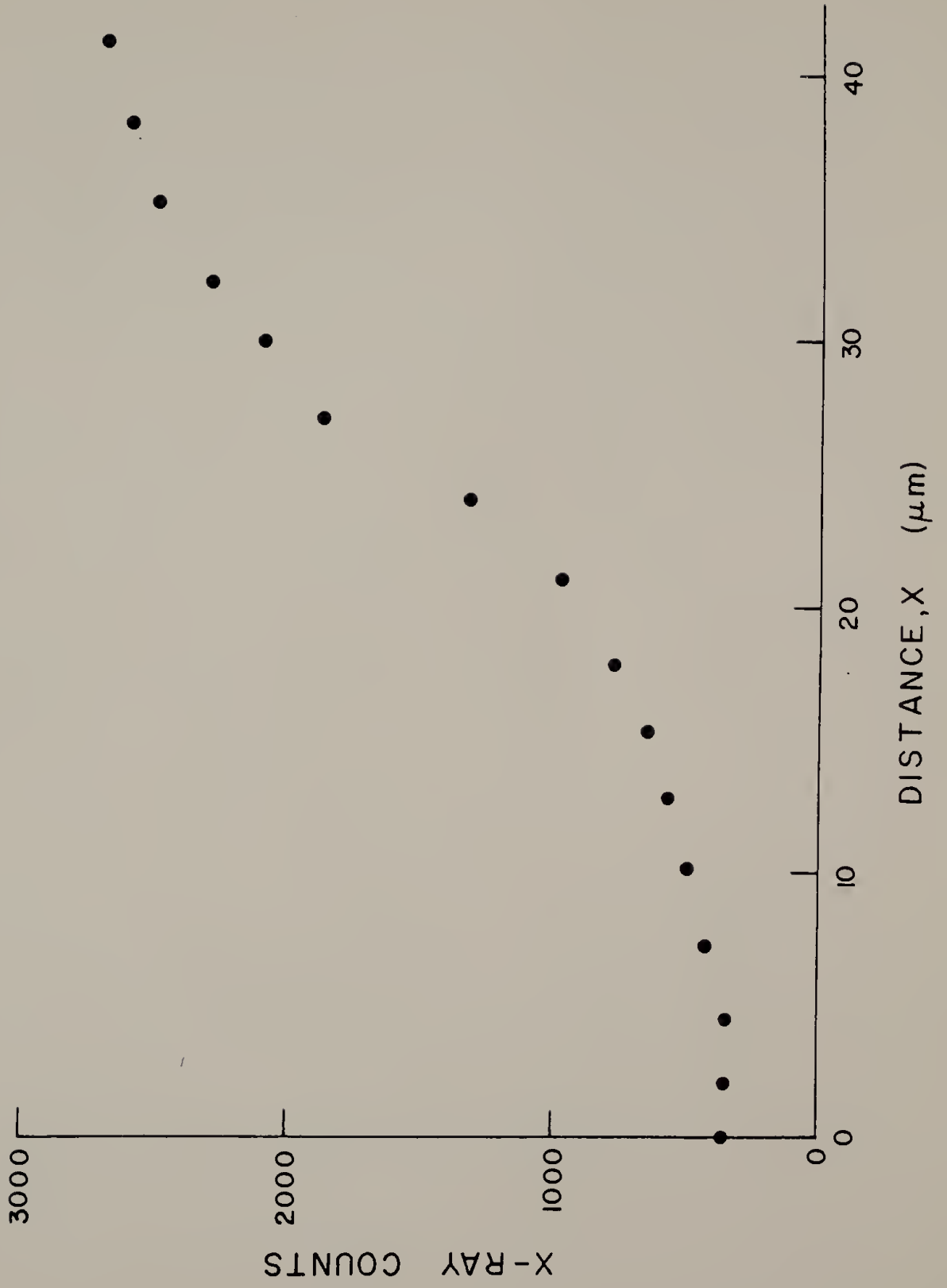




0010 0 H  
02-3 200 25 000 000



Figure 15. Concentration profile, distance versus number of chlorine x-rays counted in 20 seconds.



generation volume. An attempt was made to measure a "zero time" concentration profile to determine the actual smearing function,  $p(x)$  (Equation 31). The PVC and PCL were placed in contact for a very short time (less than 1 hr) and handled as described previously. Although interfacial contact appeared quite good, the observed concentration profile was effectively infinitely sharp. There appeared to be no diffusion, thus allowing us to assume that by maintaining adequate distances between concentration measurements, the smearing function,  $p(x)$ , was approximately a delta function.

### III.5 Data Analysis

III.5.1 Determination of reduced concentration. The concentration profile as shown in Figure 15 must first be normalized with respect to the concentration of chlorine measured far from the interface, resulting in reduced concentrations ranging between 0 and 1. This is done by taking the number of x-ray counts at a given position and subtracting the background counts (pure PCL, no chlorine), and then dividing by the maximum change in the number of x-ray counts (pure PVC - pure PCL):

$$\text{Reduced concentration} = \frac{c(x) - c_0}{c_1 - c_0} \quad (33)$$

The value of the reduced concentration is then used for the left side of Equation 27. It is also necessary to

know the exact position of the interface in order to determine the diffusion coefficient.

III.5.2 Calculation of interfacial position,  $x_0$ . In Equation 27 the position of the interface relative to the positions of concentration measurement (as in Figure 15) is needed. This can be done by fitting the experimental data to the solution of the diffusion equation. One can define the interface by stating that its position corresponds to the value of  $x$  where the reduced concentration equals  $1/2$  (Jost, 1952). The data are then fit to the right side of Equation 27, using a non-linear regression analysis based on the Gauss-Jordan-Rutashauser matrix inversion technique (Appendix A). The variables are the diffusion coefficient and the position of the interface,  $D$  and  $x_0$ , consecutive iterations being made until the error is minimized. The results for an individual data set are values of  $D$  and  $x_0$ .

The data, however, are amenable to reduction to the point where all data for an individual polymer pair can be represented by one curve. Reduced concentrations can be determined for each data set. The solution to the diffusion equation includes the diffusion time; thus, each set of data is reduced by its own diffusion time. Using the regression analysis, a value of  $x_0$  may be determined for each data set. Therefore, a graph of reduced concentration vs.  $(x-x_0)/\sqrt{t}$  could be constructed and all data taken for a given polymer

pair or diffusion temperature could be represented by one best fit line, the only variable being the diffusion coefficient for the system. After each individual set of data has been analyzed and values of  $x_0$  and  $D$  returned, all sets of data are again analyzed by the regression routine. This time, however, the input data are reduced concentration and  $(x-x_0)/\sqrt{t}$ . As is noted in Appendix A, all data points are treated collectively and fit to Equation 27, the only variable being the diffusion coefficient for the system.

This procedure, i.e., fitting the individual data sets to Equation 27 to determine individual values of  $x_0$  then fitting all data sets to the same equation to determine one value of  $D$  for the system, was carried out for each system examined, whether the variable was molecular weight, temperature, or polymer pair. A master curve, representing all data for a particular system, was constructed for each system.

The master curves for all PVC/PCL systems at 70°C are represented in Figures 16-26. The units for  $(x-x_0)/\sqrt{t}$  are  $\mu\text{m}/\text{sec}^{1/2}$ . The line running through the data is the best fit line for Equation 27 using the calculated diffusion coefficient. Although it appears that there is a great deal of error when comparing the experimental points to the calculated line, the large amount of data reduces the standard error to 10% according to the error analysis within the computer program. A calculation of the error by standard propagation of error techniques, however, results in an error



Figure 16. Master curve for PCL-1/PVC-6.

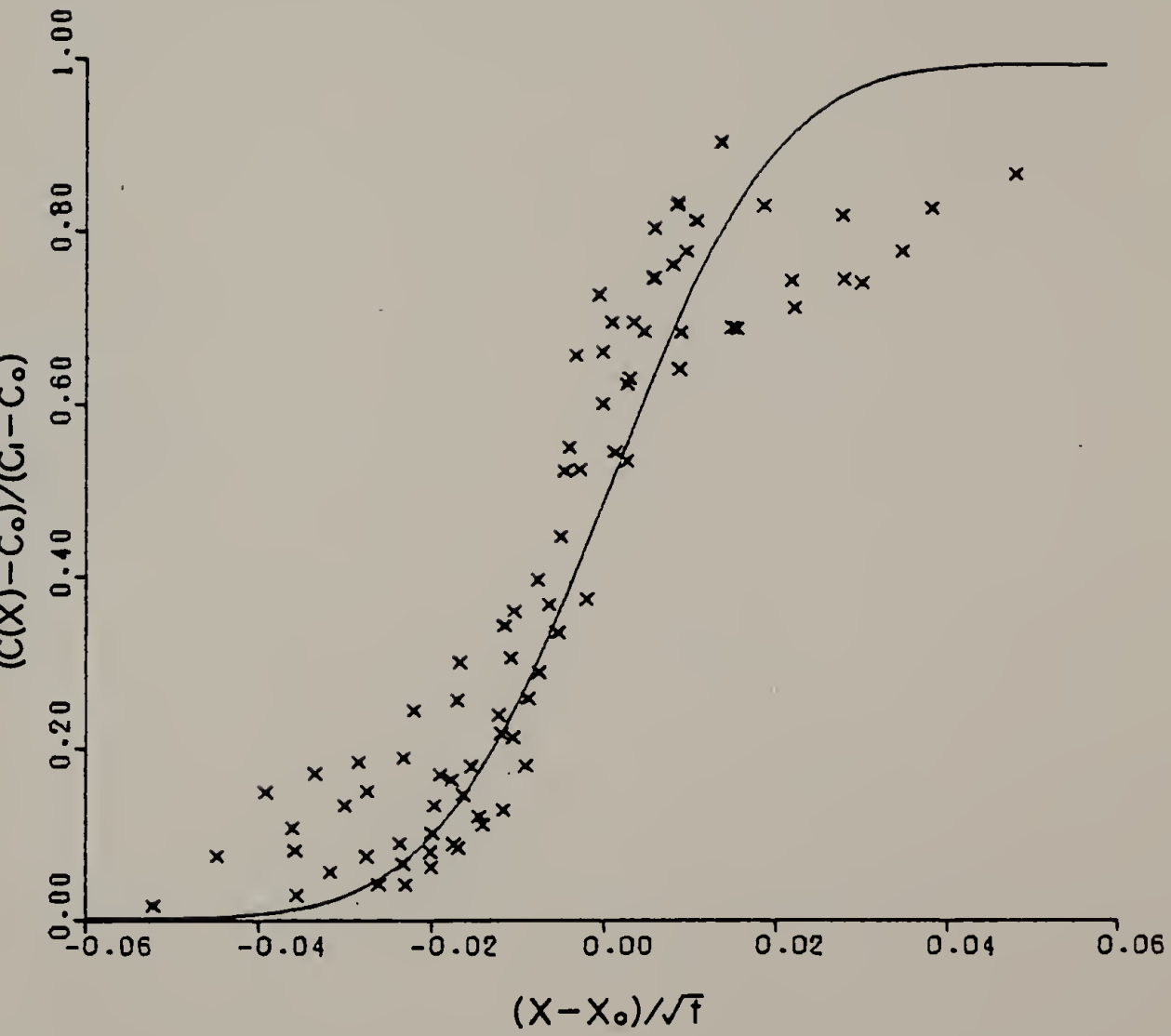


Figure 17. Master curve for PCL-2/PVC-6.

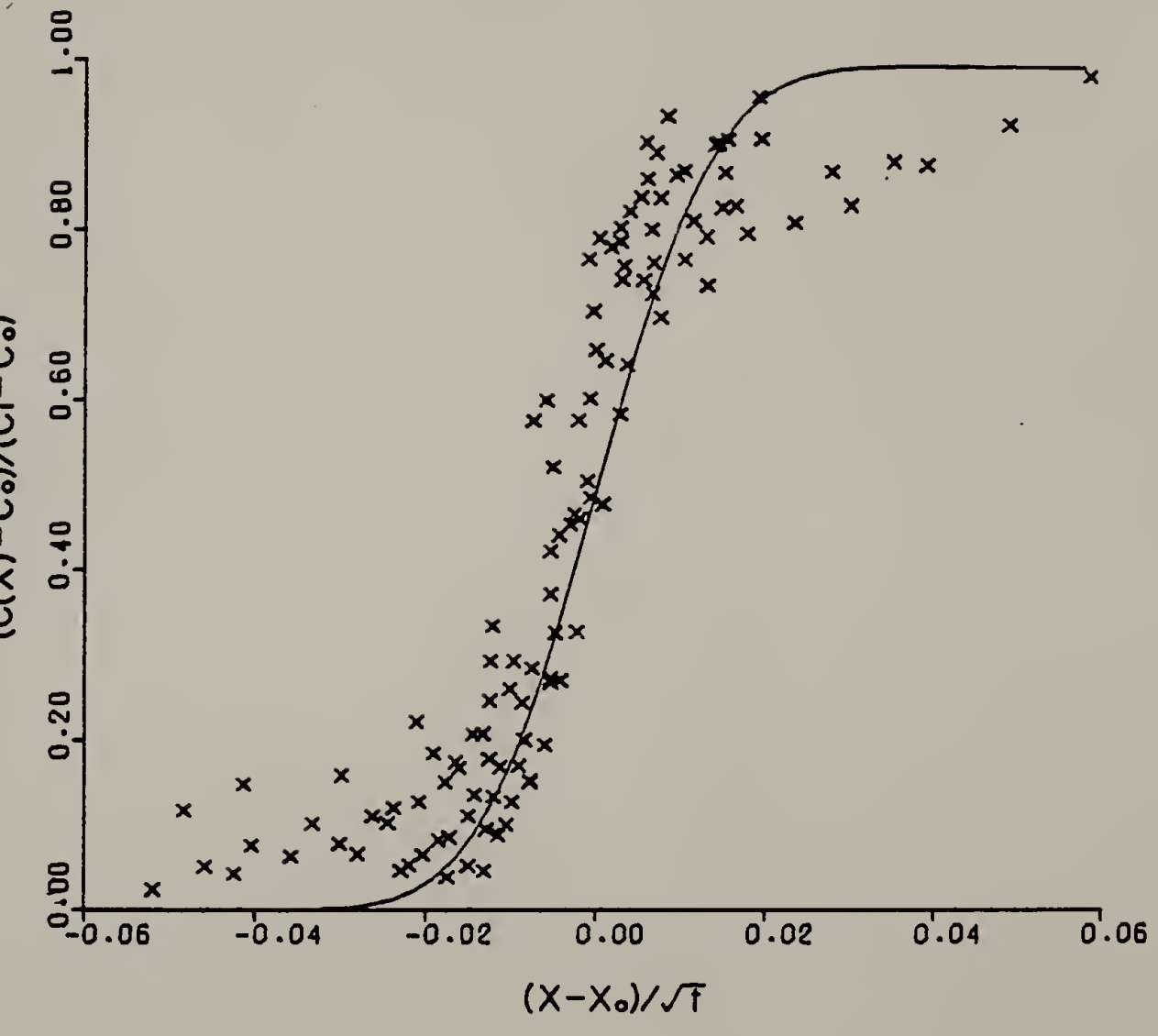


Figure 18. Master curve for PCL-3/PVC-6.

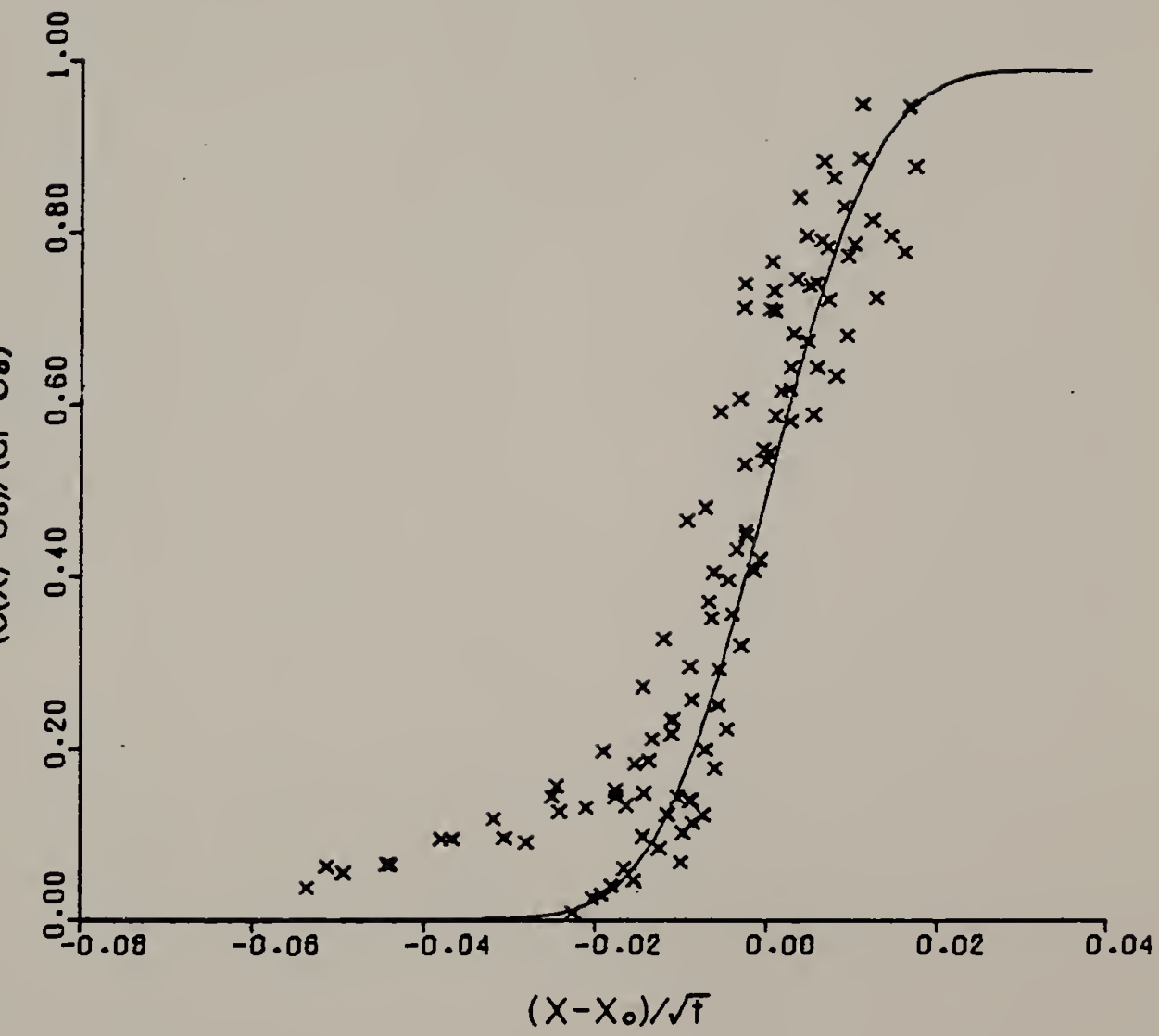


Figure 19. Master curve for PCL-4/PVC-6.

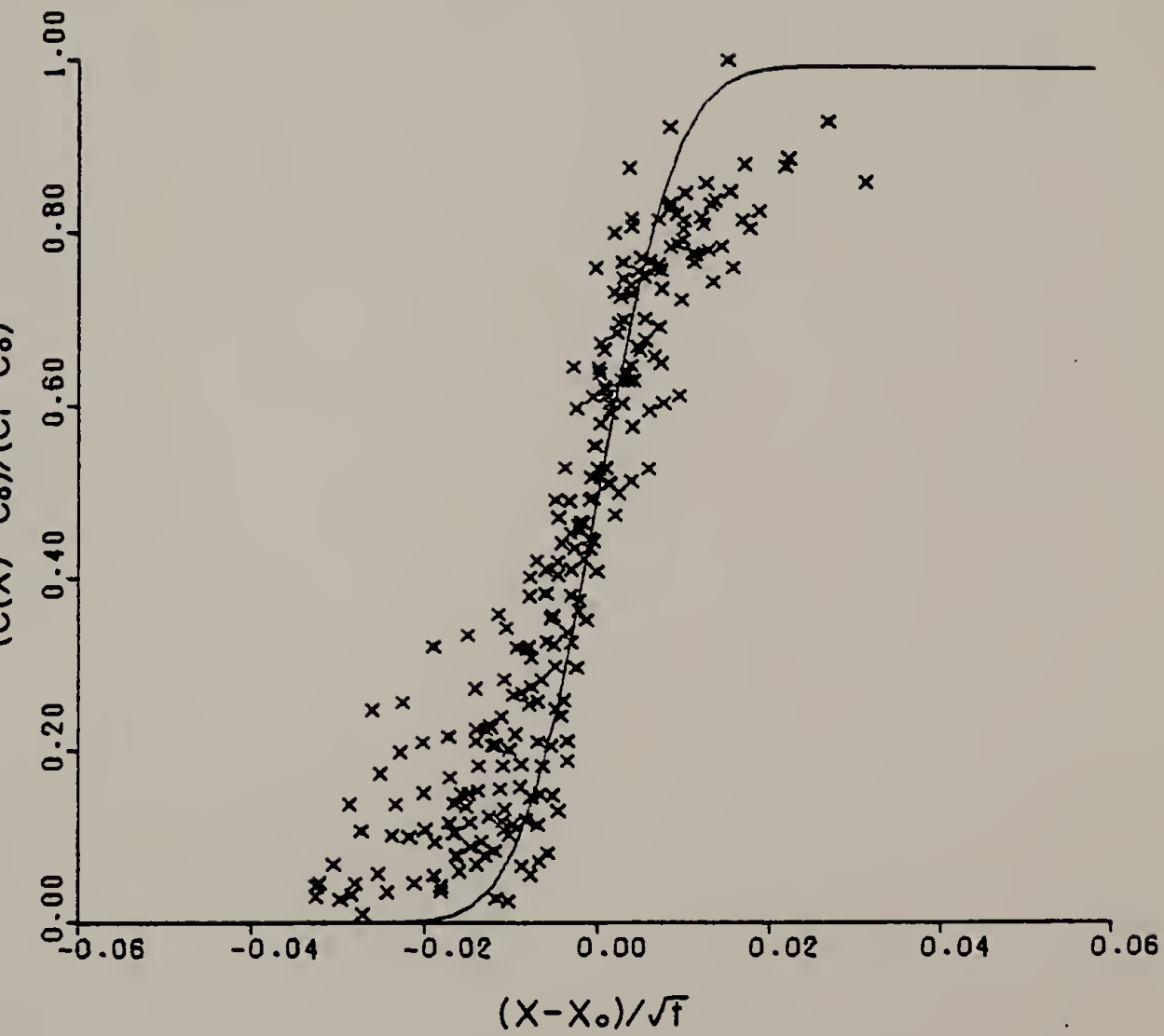




Figure 20. Master curve for PVC-1/PCL-4.

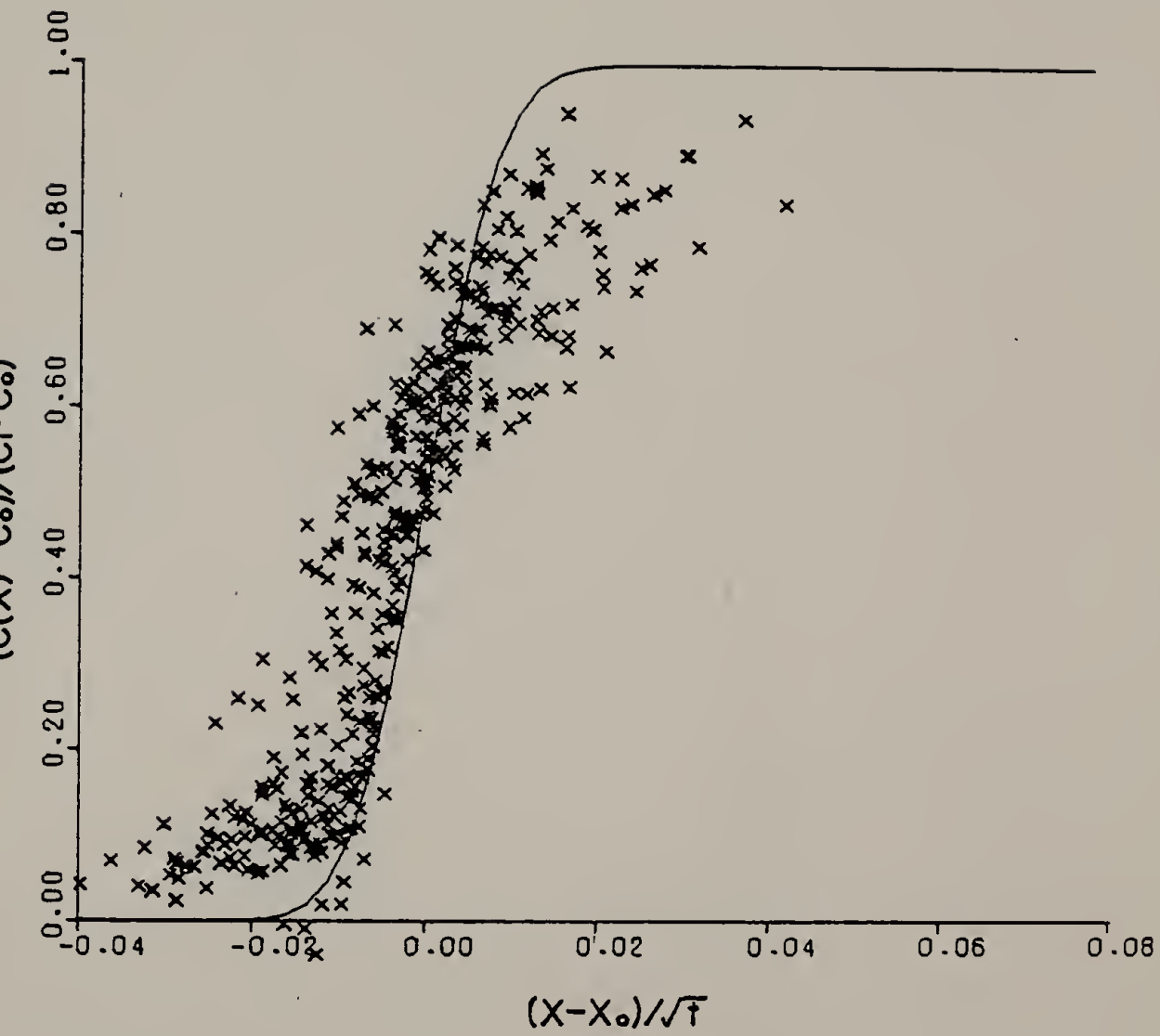


Figure 21. Master curve for PVC-2/PCL-4.

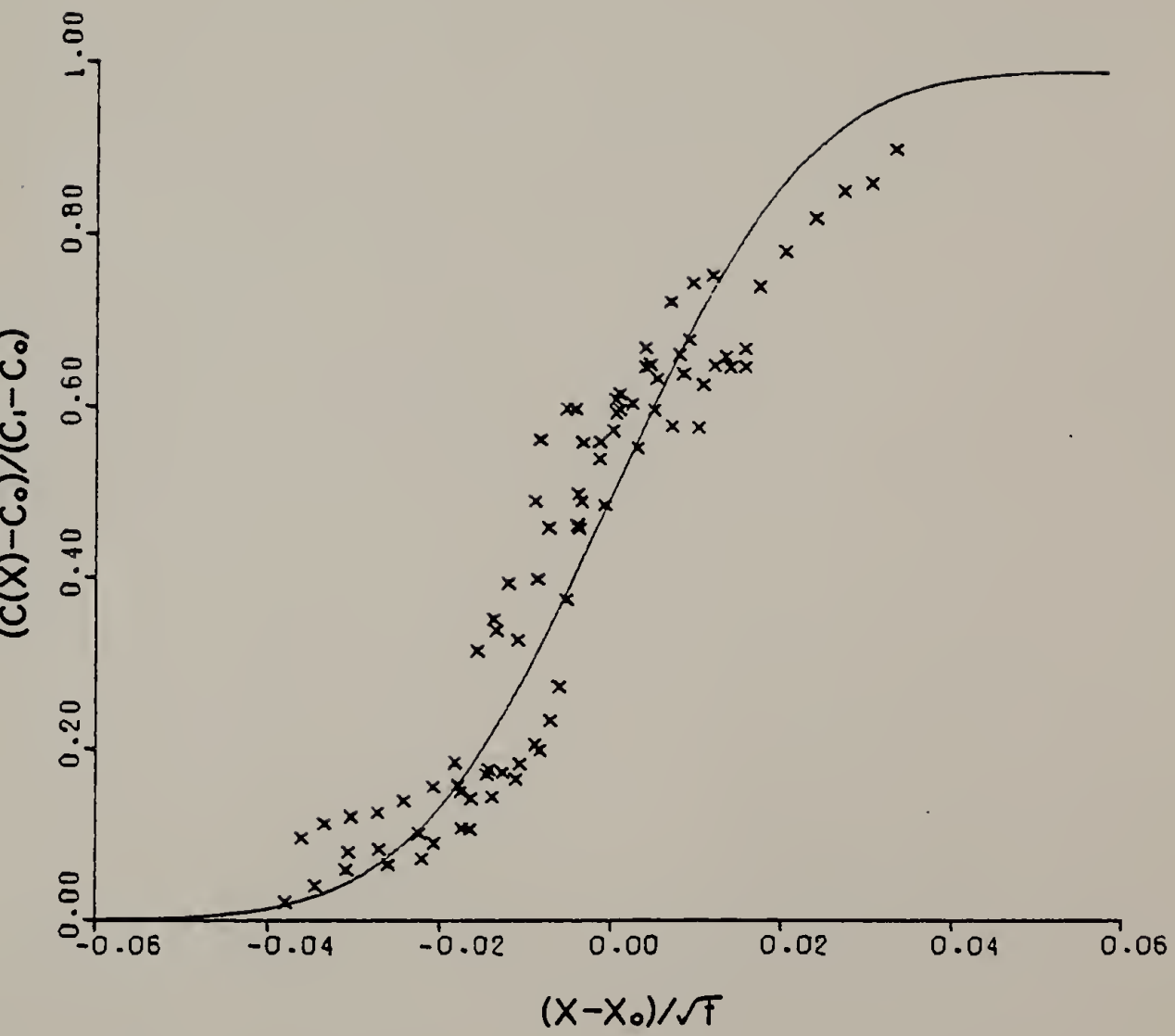


Figure 22. Master curve for PVC-3/PCL-4.

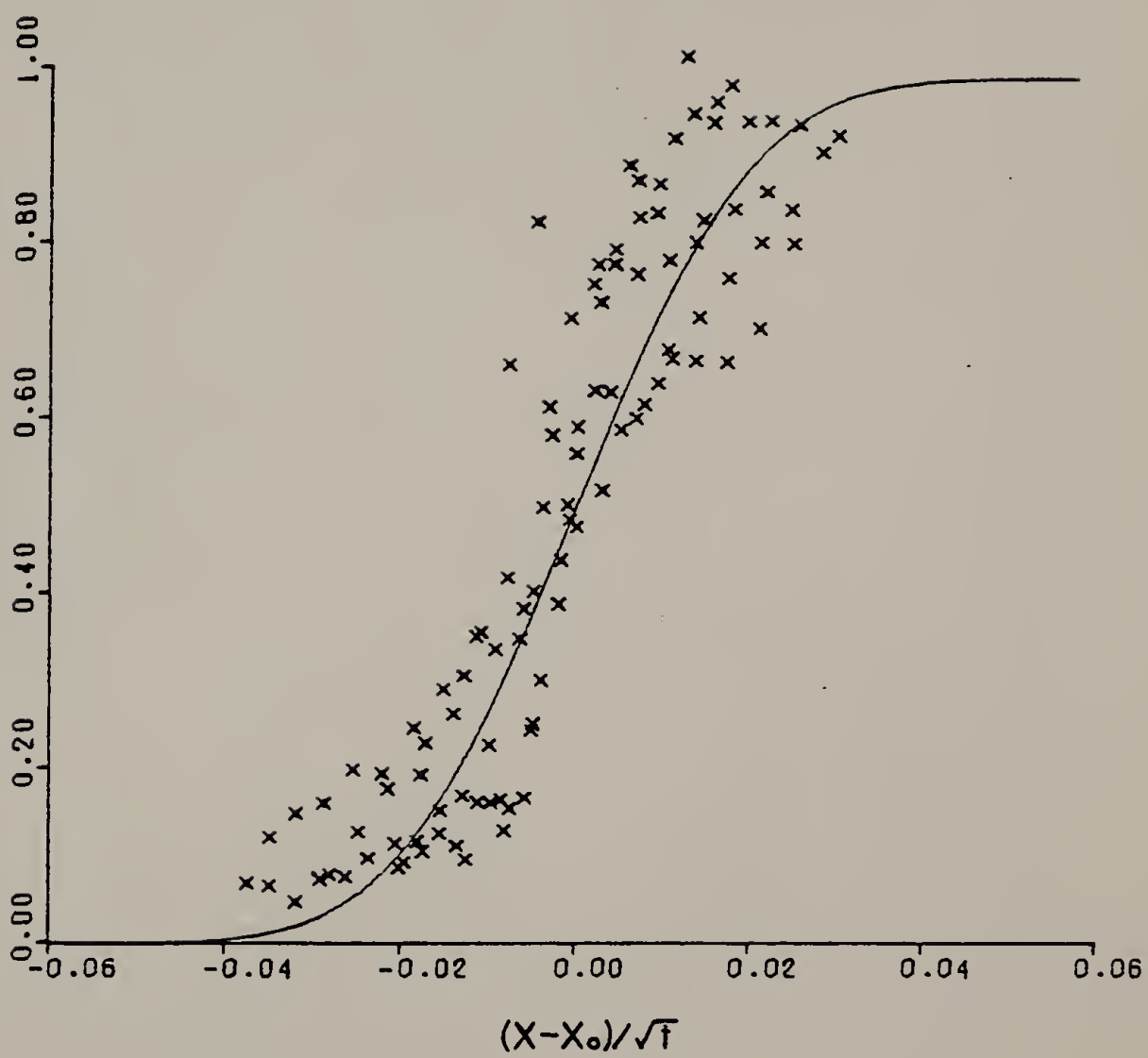


Figure 23. Master curve for PVC-4/PCL-4.



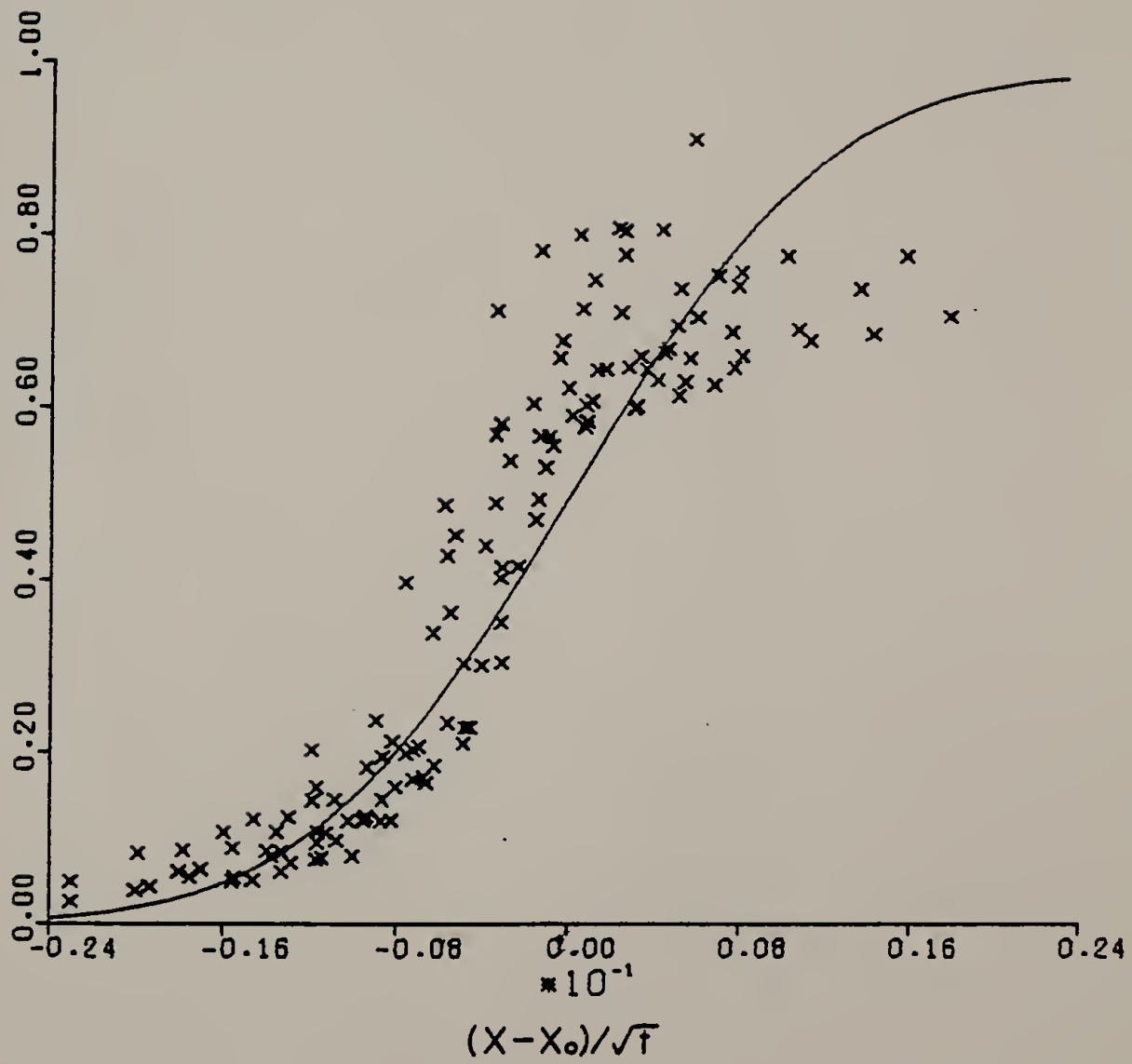


Figure 24. Master curve for PVC-5/PCL-4.

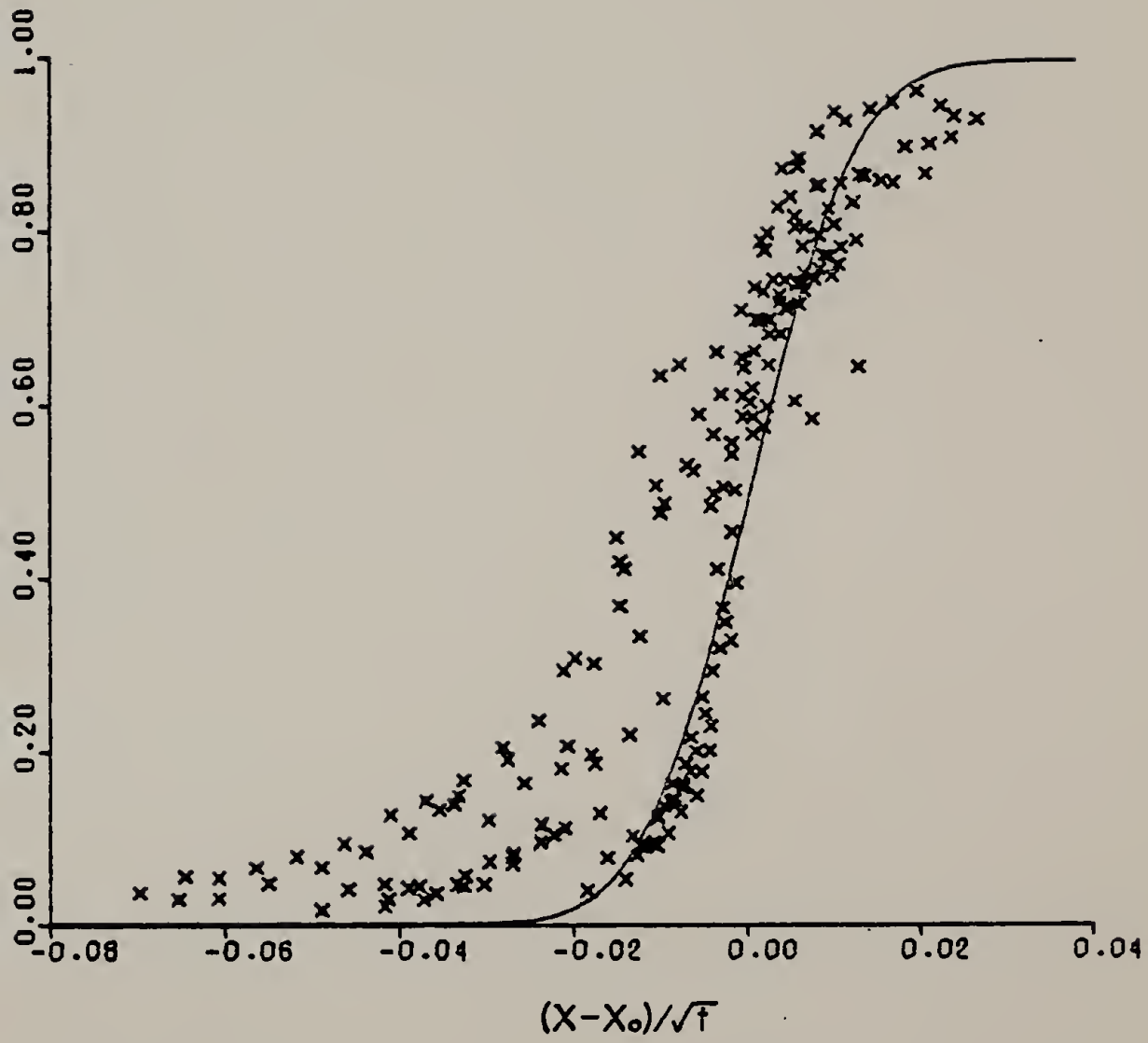


Figure 25. Master curve for PVC-6/PCL-4 at 90°C.

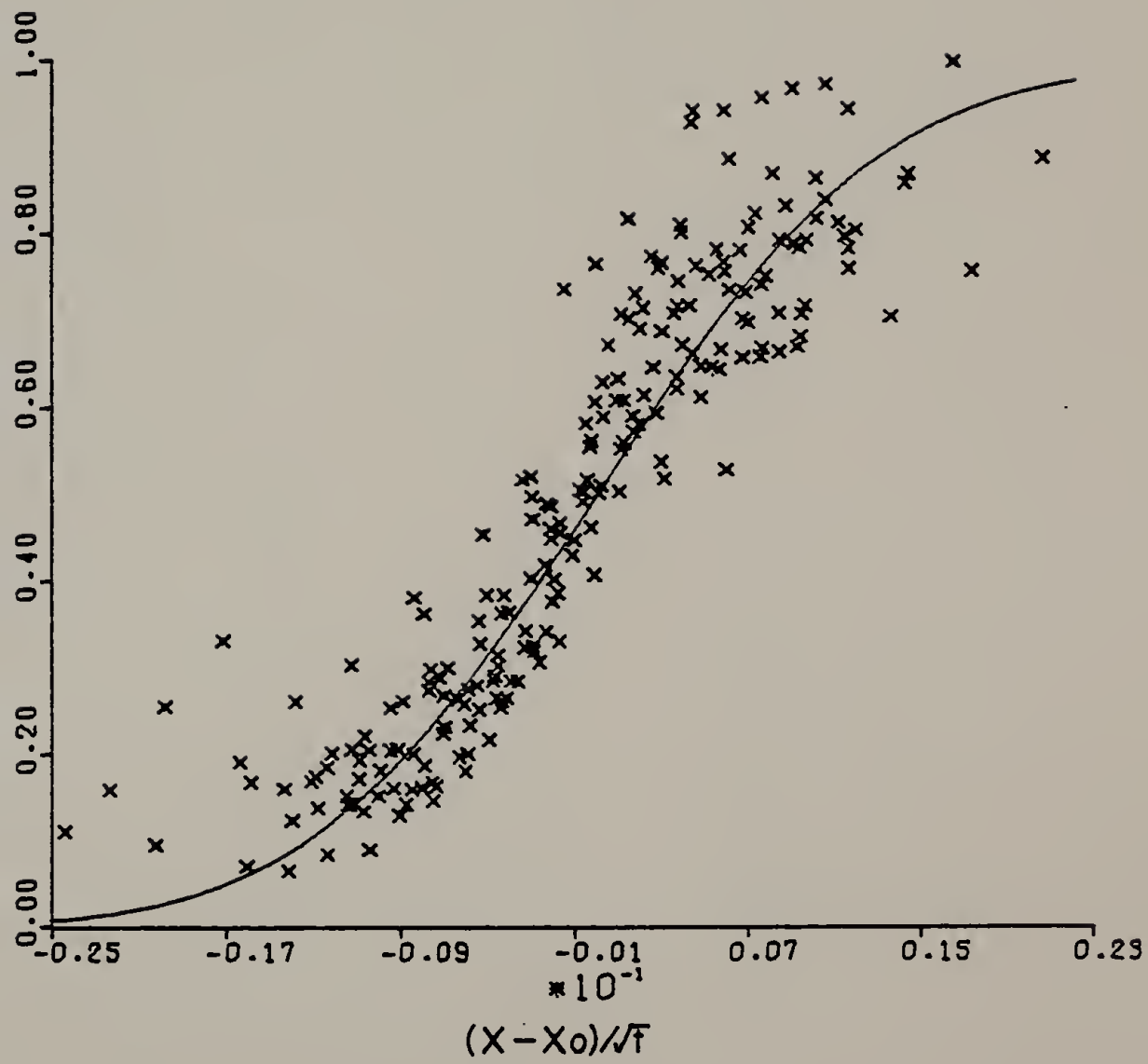
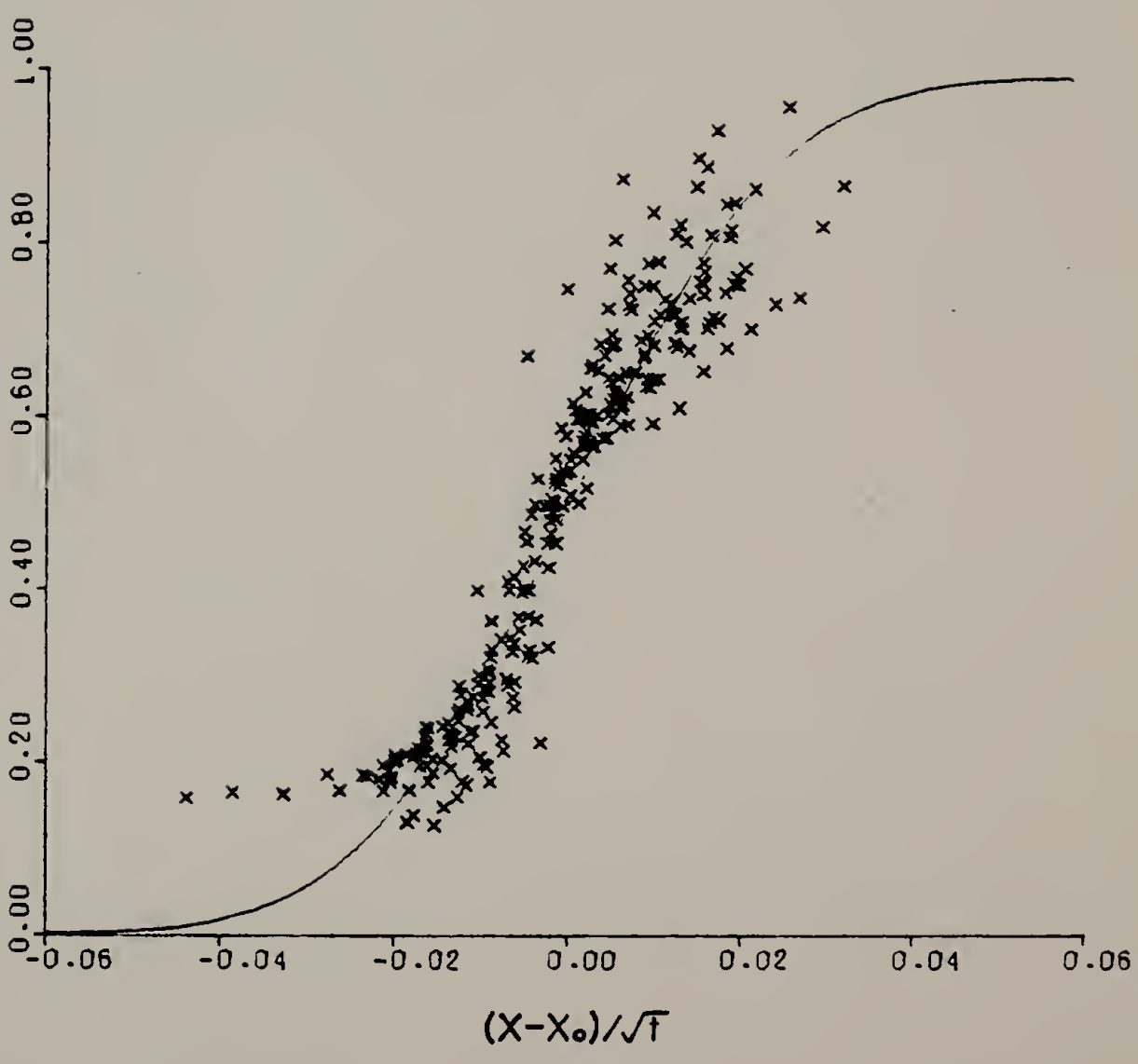


Figure 26. Master curve for PVC-6/PCL-4 at 110°C.





of about  $\pm 25\%$  for the diffusion coefficient (Appendix B). This error is almost solely due to the error in concentration measurement. The accuracy of an individual concentration measurement is 10%. When this is translated into reduced concentration, the error in  $(c-c_0)/(c_1-c_0)$  is 25%, the major source of inaccuracy in the diffusion coefficient.

Given that the diffusion coefficients could be calculated for the systems observed, the next task was to look at the results of the effects of the variables under consideration within this study.

## C H A P T E R I V

### RESULTS

#### IV.1 Diffusion in the PVC/PCL System

The primary system under investigation was that of poly(vinylchloride)/poly( $\epsilon$ -caprolactone). This polymer pair has been extensively studied (Koleske and Lundberg, 1969; Ong, 1973; Warner et al., 1976) and found to be compatible throughout the concentration range. Recently Russell (1978) performed some small angle x-ray scattering experiments with this system and found that the scattering invariant disappeared, indicating compatibility on the molecular level between the two materials. Certainly inter-diffusion will occur between two partially compatible polymers, but this may affect the concentration profile and necessitate a change in the equation used to describe the diffusion process.

IV.1.1 Effect of molecular weight. The effect of molecular weight on the diffusion coefficient might be expected to be similar to the effect seen on the bulk viscosity. Graessley (1973) provides an extensive review of the experimental and theoretical results. Essentially, it is found that above some minimum molecular weight, which is frequently called the critical molecular weight,  $M_c$ , many physical characteristics

of polymeric materials no longer change with further increases in molecular weight. Above this critical molecular weight the bulk viscosity,  $\eta$ , has been shown experimentally to vary with  $M^{3.4}$  for a wide variety of polymers. Theoretical treatments predict the exponent of  $M$  to be 3.3-3.5; each theory claims good agreement with experiment.

Bueche (1952) developed the proposition that:

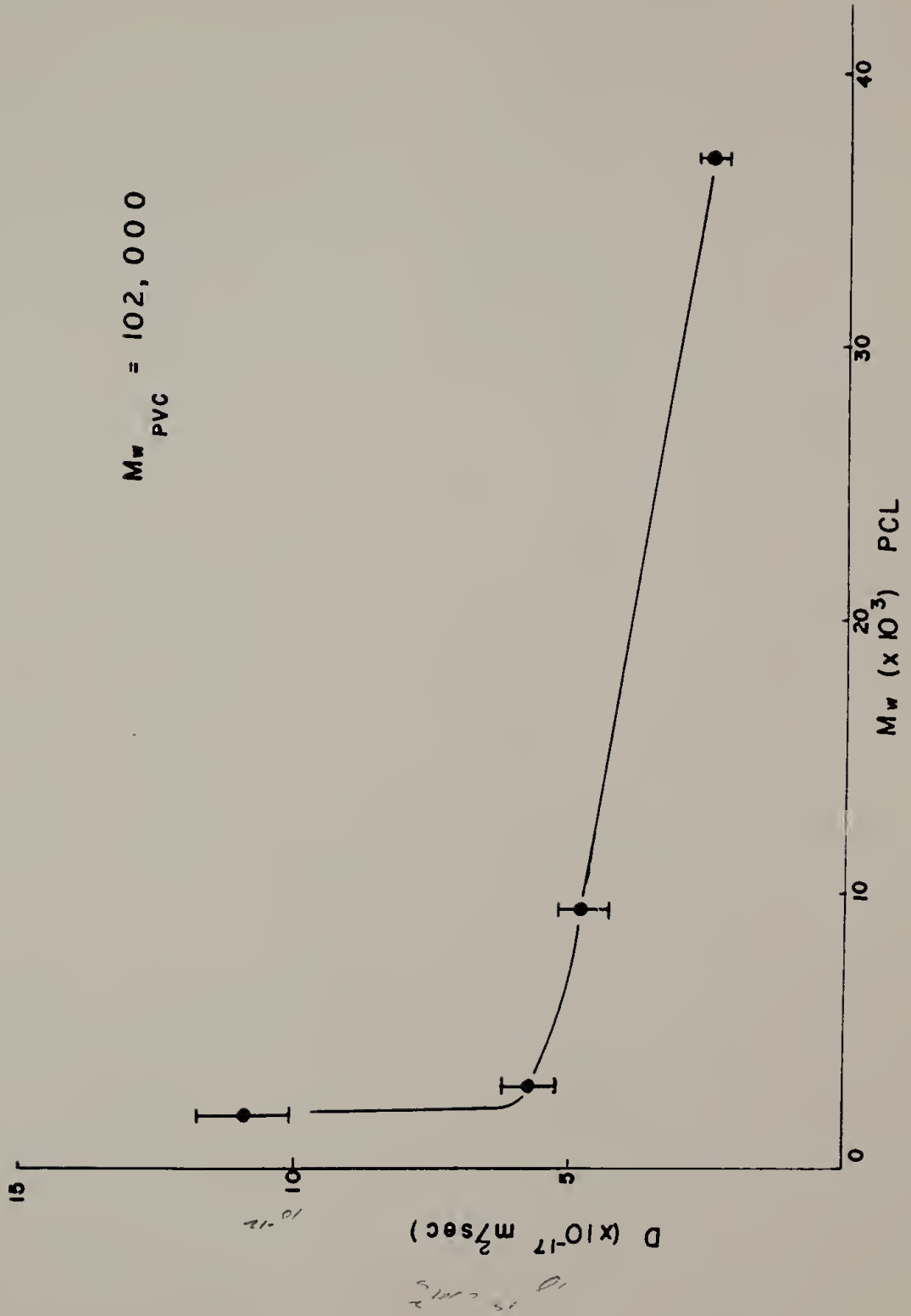
$$D = (A\rho kT/36) (R^2/M) \quad (34)$$

where  $R^2$  is the mean square end-to-end distance of the chain,  $M$  the molecular weight,  $A$  is Avogadro's number, and  $\rho$  is the density of the polymer. Since  $R^2/M$  is essentially a constant for any bulk polymer and its value readily obtainable from light scattering experiments done in a  $\theta$  solvent for a particular polymer, this theory would allow for a prediction of  $D$  if  $\eta$  is known. Thus, since  $\eta$  varies with  $M^{3.4}$ , it would be expected that  $D \propto M^{-3.4}$  with  $M > M_c$ .

When  $M < M_c$ , it is known that the bulk viscosity varies with  $M^1$  and would indicate that  $D$  is proportional to  $M^{-1}$ .

Figure 27 demonstrates the effect of molecular weight on the diffusion coefficient for PCL. PVC-6 was used for each of the four molecular weights of PCL. It is immediately obvious that the diffusion coefficient is not a function of  $M^{-3.4}$  but rather a linear function of  $M$ . A drastic change in slope occurs at a molecular weight of near 4000. Replot-

Figure 27. D vs. M for PCL (with PVC-6).



ting the data as  $D$  vs.  $1/M$  (Figure 28), it is seen that the data indicate a linear relationship between  $D$  and  $M^{-1}$ .

The critical molecular weight is loosely described as the molecular weight at which entanglements begin to play an important role in the transport processes of a polymer; this can be seen when observing long term relaxation processes in polymers. The indication is that at  $M_c$ , a gradual but drastic change occurs in the translational mobility of the polymer molecules. Below  $M_c$ , the individual molecules move relatively independently. Here the molecular friction factor described by Bueche is the major effect, i.e., the friction between the solvent and solute molecules moving past one another. At higher molecular weights, when  $M > M_c$ , there is an additional contribution to the restriction of motion of the chain. The phenomenon has been called entangling and coupling. Certainly something changes at  $M_c$ . The consequences of this phenomenon have been observed but theoretical descriptions have been inadequate. The data as seen in Figure 28 do not demonstrate this change. Given the values of  $M_c$  for many polymers (Graessley, 1973) it is probable that  $M_c$  for PCL lies within the range of molecular weights used. A preliminary conclusion is, then, that the entanglements which play such a large role in viscous response have less effect when dealing with movements of the entire polymer chain over very long time periods.

Figure 29 shows the variation of  $D$  with  $M$  for PVC;

Figure 28. D vs.  $1/M$  for PCL (with PVC-6).



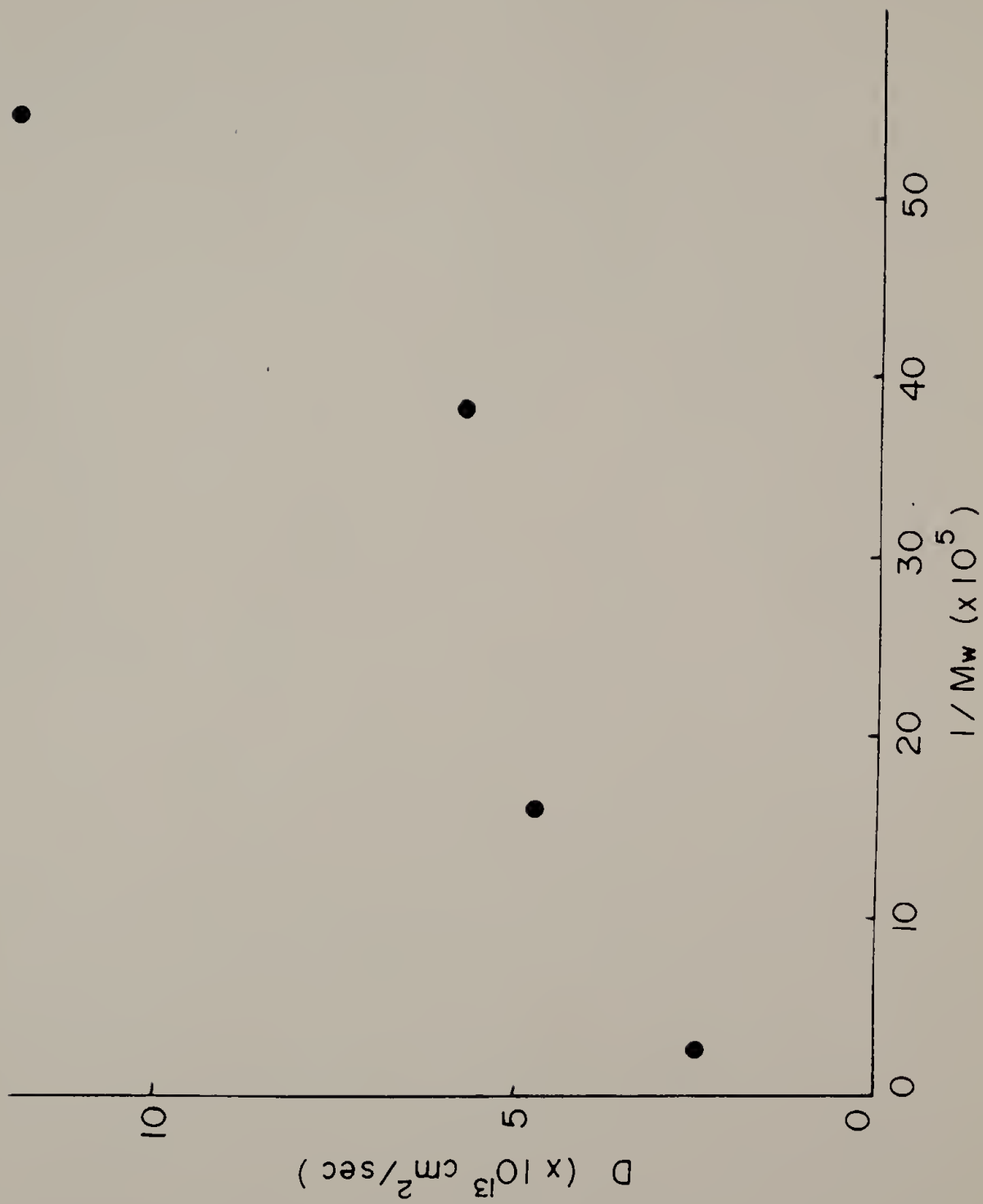
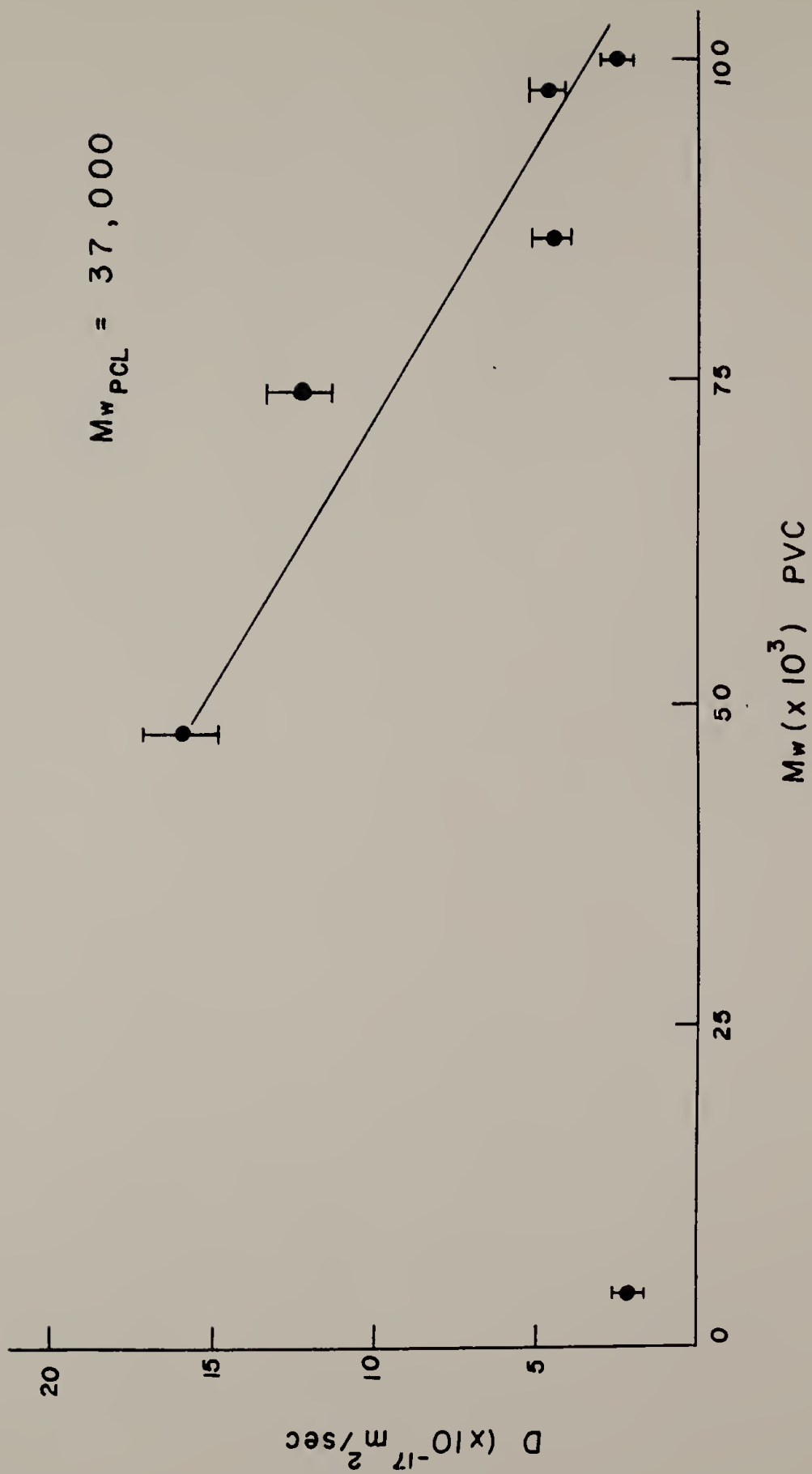


Figure 29. D vs. M for PVC (with PCL-4).



PCL-4 was used in conjunction with all molecular weights of PVC. Again, at higher molecular weights there is a linear relationship between  $D$  and  $M$ . Figure 30 represents  $D$  vs.  $M^{-1}$  for PVC (not including the point at  $M = 5000$ ). The linearity, although not perfect, again indicates that the diffusion coefficient is an inverse function of molecular weight. In this case, though, the low molecular weight material, PVC-1, has a much lower diffusion coefficient than might be expected.

Wide angle x-ray scattering (WAXS) and small angle x-ray scattering (SAXS) were used to see if there was any structure in PVC-1 which might cause the lower than expected diffusion rates which were observed. The scattering patterns (Figure 31) were those of an amorphous film, providing no clues to the reason for this anomalous behavior. The sample PVC-1 is certainly different from the other PVC samples. While they were produced by an emulsion polymerization, it is supposed that PVC-1 was polymerized in suspension. The exact procedure is proprietary information of Hooker Chemical Company. One might suppose, though, that at this low molecular weight end groups would have an effect and may even cause an association of several molecules which would cause an effective molecular weight much greater than that determined by GPC. This phenomenon should be observable by measuring the bulk viscosity of the sample.

In general, the diffusion coefficient depends

Figure 30. D vs.  $1/M$  for PVC (with PCL-4), PVC-1 not included.

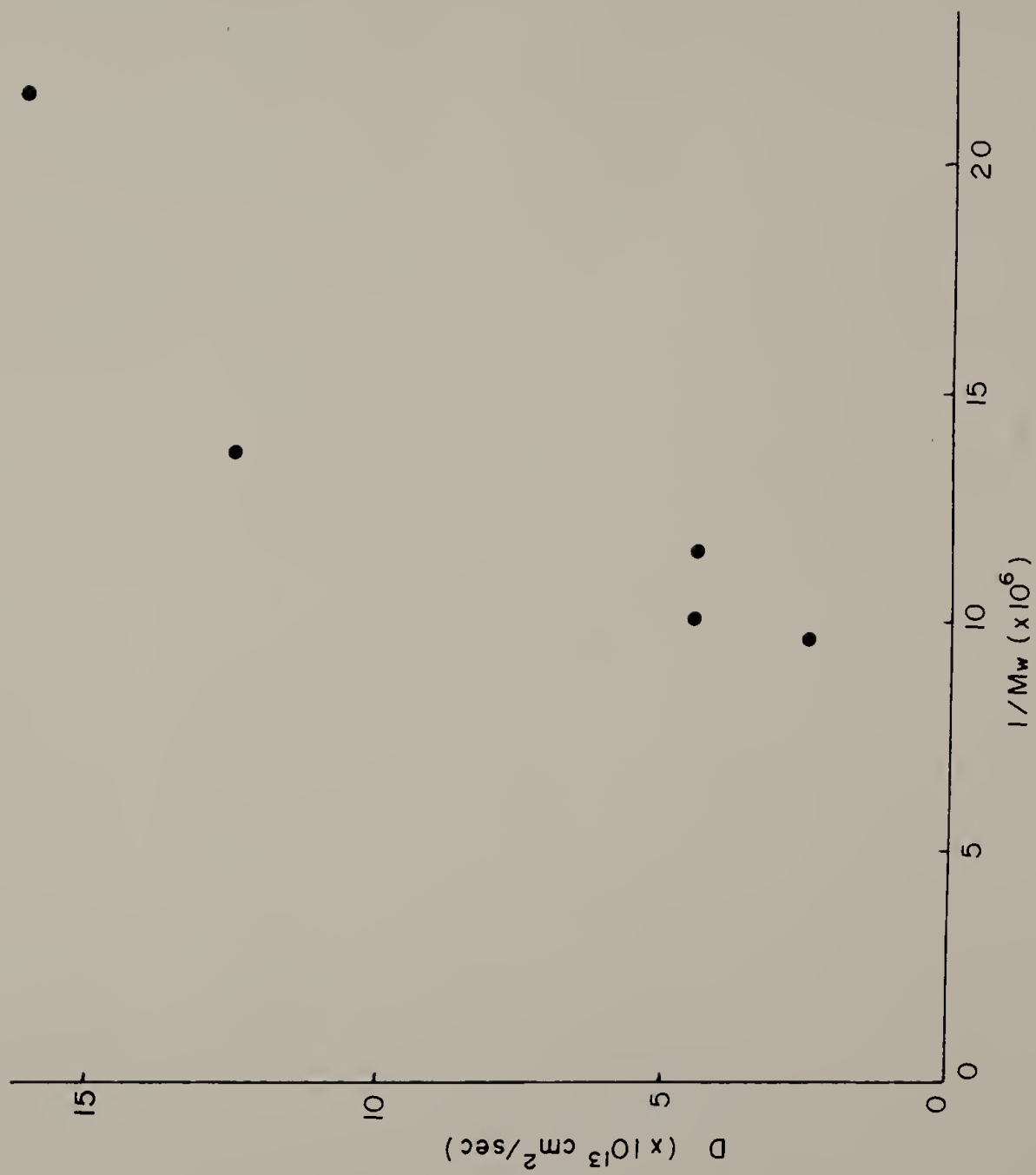
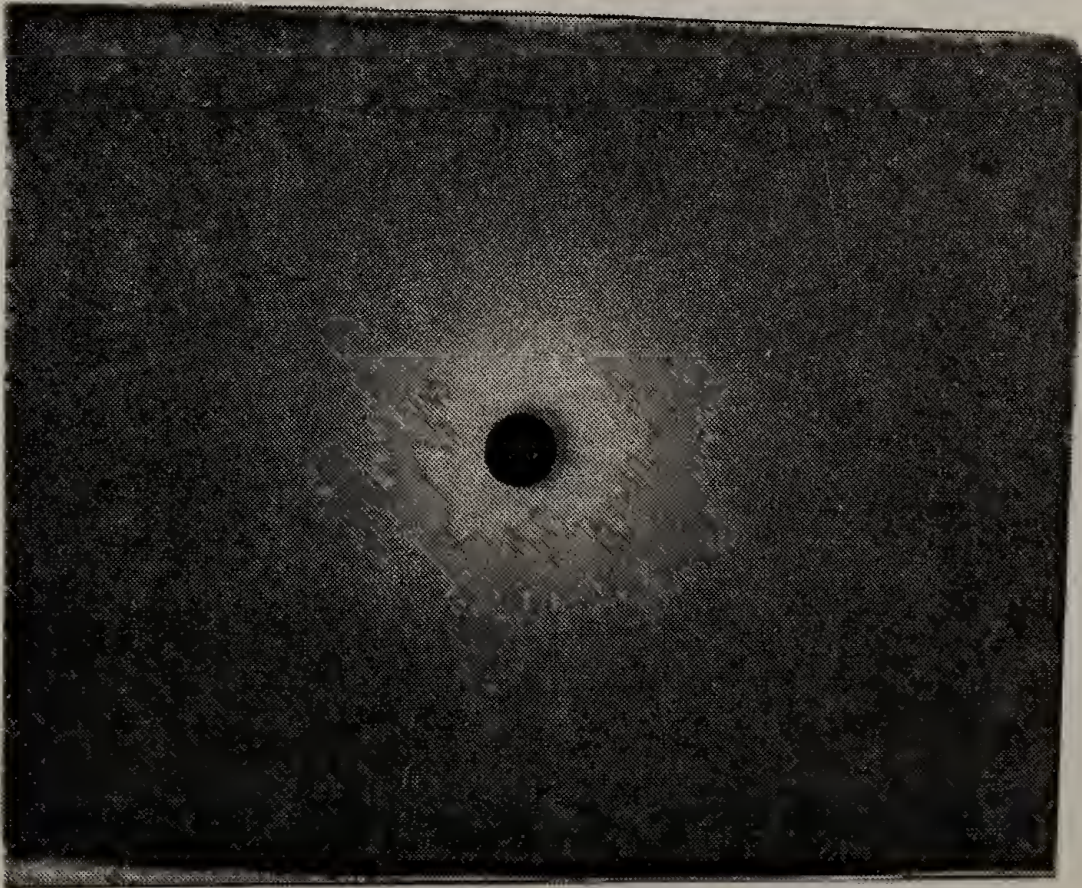
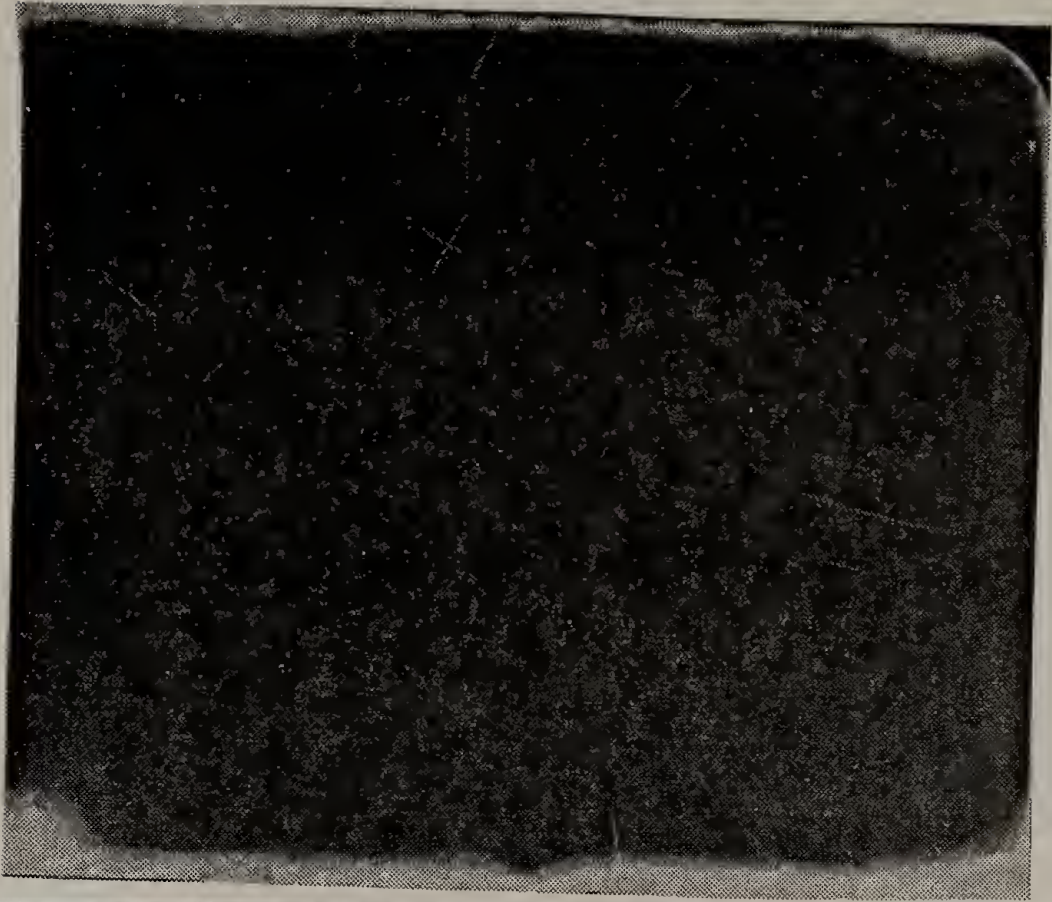


Figure 31. Wide angle (bottom) and small angle (top)  
x-ray scattering from PVC-1 film.



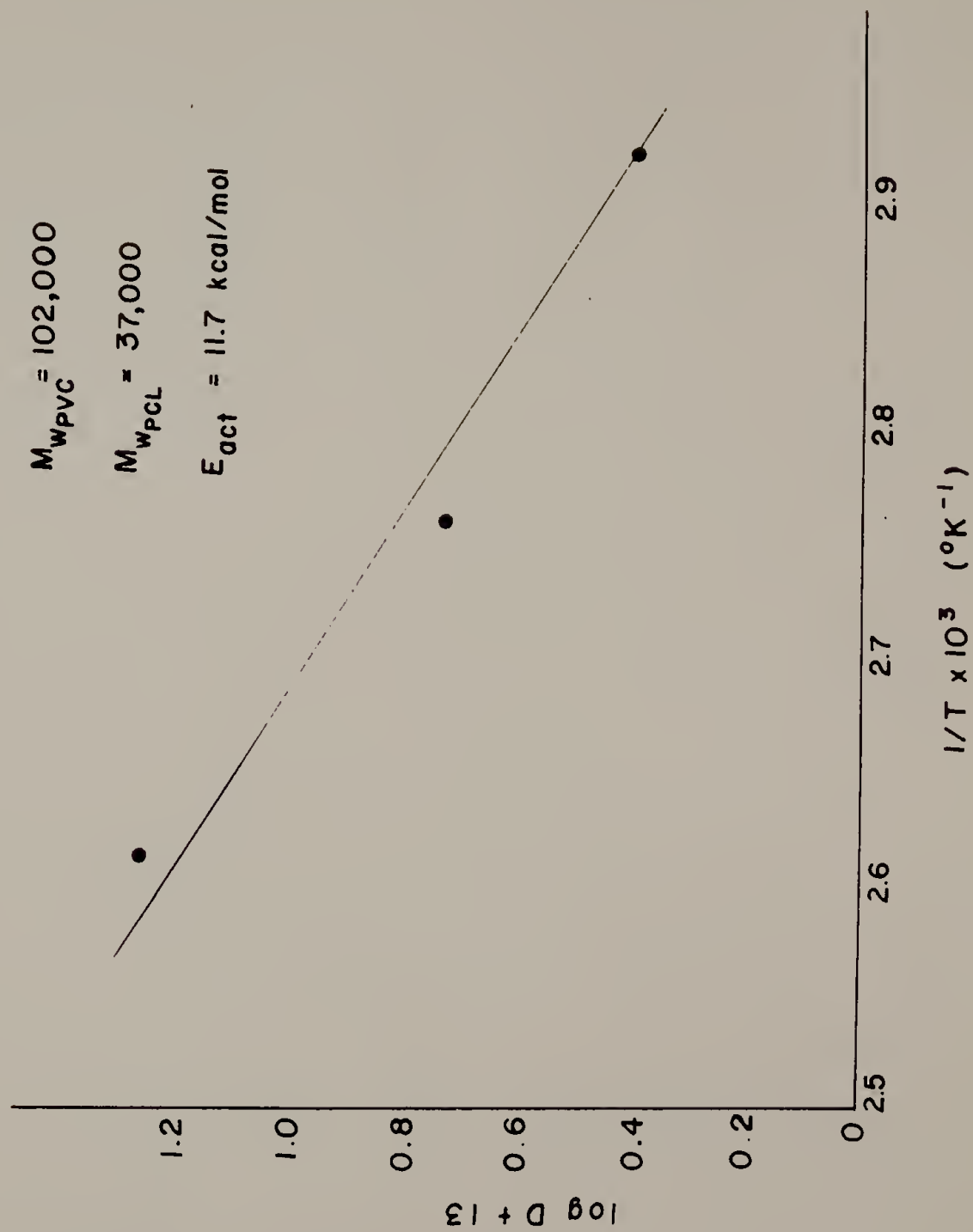


linearly on the inverse of the molecular weight. This is clearly in disagreement with the result predicted by Bueche (1952).

IV.1.2 The effect of temperature. As has been shown, the diffusion coefficient may be described by an Arrhenius type function, having a logarithmic dependence upon the diffusion temperature (Equation 28). Figure 32 demonstrates this dependence. The three points fit well on a straight line, the slope of which gives the activation energy for diffusion. The value of 11.7 Kcal/mol agrees well with that found by Bueche et al. (1952) for poly(n-butylacrylate) of 13.2 Kcal/mol.

The several temperatures used in this study (70°C, 90°C, and 110°C) were selected to provide significant variations of the diffusion coefficient. The precision of the oven used in this study ( $\pm 1^\circ\text{C}$ ) also required reasonable separation of the diffusion temperatures. No temperature higher than 110°C was used because of the degradation of PVC. To eliminate as much oxidative degradation as possible, all diffusing samples were maintained in a vacuum oven. Nonetheless, some degradation inevitably occurred due to thermal dehydrochlorination (Loan and Winslow, 1972). Diffusion at 130°C resulted in rapid, intense color formation, indicative of extensive degradation. Coloration was not nearly as evident at the lower temperatures.

Figure 32. Log D vs.  $1/T$  for PVC/PCL ( $T = 70^{\circ}\text{C}, 90^{\circ}\text{C}, 110^{\circ}\text{C}$ ).





#### IV.2 Diffusion in Polystyrene/ Poly(o-chlorostyrene)

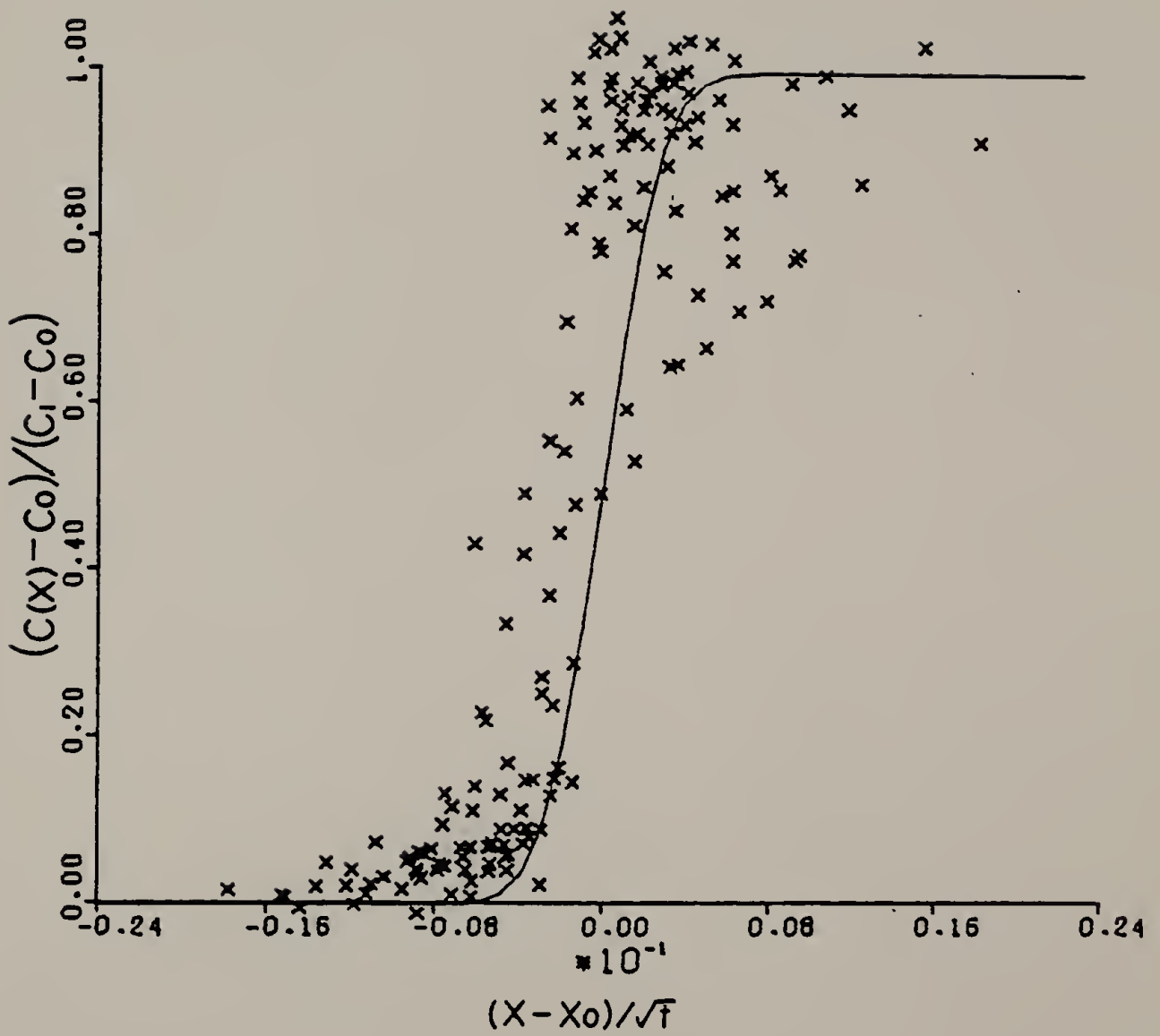
Bueche et al. (1952) initially attempted to measure the self-diffusion of polystyrene but found the diffusion rates too low to be observed by his technique. For the system polystyrene/poly(o-chlorostyrene) (PS/PoCS) one might also expect a lower diffusion coefficient than for the PVC/PCL system simply due to the greater stiffness of the polystyrene chain. Figure 33 is the master curve developed for the PS/PoCS system. The temperature of diffusion was maintained at 150°C. This was a sufficiently high temperature so that both materials were above their respective glass transition temperatures ( $T_g$  of PS  $\approx$  100°C,  $T_g$  of PoCS  $\approx$  125°C). The low molecular weight PS ( $M_w = 20,000$ ) was used because this system can exhibit a lower critical solution temperature, the value of which depends upon the individual molecular weights. The value of the diffusion coefficient for the PS/PoCS system is:

$$D = 2.32 \times 10^{-14} \text{ cm}^2/\text{sec.}$$

This value of  $D$  is an order of magnitude lower than the lowest of those observed for the PVC/PCL system.

By determination of the diffusion coefficients of the various PVC/PCL mixtures and the PS/PoCS system, the validity of the described technique has been established. However, the results will be more useful if they can be

Figure 33. Master curve for PS/PoCS.



related to theoretical treatments of macromolecular diffusion and these, in turn, used as a predictive tool for other systems.



## C H A P T E R V

### DISCUSSION

De Gennes (1971) proposed a model for describing the possible motions of a polymer molecule in a cross-linked gel. Essentially this theoretical treatment went beyond the models of a free polymer chain to include strong entanglements in the system. An individual polymer chain was constrained to move within a "tube" defined by fixed obstacles (Figure 1). The only motion allowed is the migration of defects along the length of the chain, a motion termed reptation. No motion of the chain which required it to cross the obstacles was allowed. The result of thus describing the motion of an independent macromolecule is that the diffusion coefficient (in this case, self-diffusion coefficient) varies as:

$$D \propto M^{-2}$$

as opposed to the result for a free Rouse chain of  $D \propto 1/M$ .

Edwards and Grant (1973) defined similar constraints on a polymer chain. However, in addition to allowing the chain to move within the tube, the tube was also allowed to move, taking into account the fact that the network is not frozen. Edwards called this motion cooperative diffusion. The result varies from that of de Gennes, with

$$D \propto M^{-3}.$$

Edwards' claim was that in packed systems the diameter of the constraining tube is comparable to that of the chain ( $\sim 5 \text{ \AA}$ ) and reptation is effectively suppressed; diffusion of the tube is the dominant mechanism. Interestingly, both Edwards and de Gennes arrived at the result that the mean square displacement of any point on a specific chain is a function of the one fourth power of time.

It has been observed by many experimenters that the bulk viscosity at zero shear rate is a function of  $M^{3.4}$  (Graessley, 1973). Bueche (1952) attempted to relate the diffusion coefficient directly to the bulk viscosity, and said that the product of the two terms was a constant. Then the expected behavior would be

$$D \propto M^{-3.4}$$

at least above the critical molecular weight,  $M_c$ . This is the molecular weight at which a change is observed in the functionality of  $\eta$  on  $M$ . Below this critical molecular weight,  $\eta \propto M^1$ . There have been theories that postulated that  $M_c$  is the minimum molecular weight between entanglements, its absolute value dependent upon the structure of the polymer (Ferry, 1970).

The figures demonstrating the dependence of the diffusion coefficient on molecular weight for the PVC/PCL sys-

tem, Figures 27-30, indicate that the dependence is linear. Plots of  $D$  vs.  $1/M^2$  deviate more from linearity than those of  $D$  vs.  $1/M^1$  but the data cannot be called absolutely definitive on this important point. Stronger conclusions could be drawn if both materials were of the same molecular weight and were monodisperse. Then any diffusing molecule would be surrounded by other molecules of the same molecular weight regardless of its relative position. That fact notwithstanding, the data clearly contradict Bueche (1968) who attempted to measure the diffusion coefficient as a function of molecular weight for polystyrene and noticed no change in the diffusivity as the molecular weight of the matrix material was varied. In his original paper, Bueche et al. (1952) employed the same technique but could not measure a diffusion coefficient for polystyrene. The diffusion coefficient calculated here,  $D = 2.32 \times 10^{-18} \text{ m}^2/\text{sec}$ , for the PS/PoCS system, is vastly different from that reported by Bueche (1968) of  $1.6 \times 10^{-14} \text{ m}^2/\text{sec}$ . It is conjectured that the radioactive tracer technique employed by Bueche is not sufficiently sensitive to adequately measure diffusion in polystyrene. This is based on our measured diffusion coefficient for the similar system, PS/PoCS, and that there is a variation of  $D$  with  $M$ . Bueche (1952) developed a theory relating the diffusion coefficient to the bulk viscosity (Equation 34), which stated that their product,  $D\eta$ , was a constant. This would imply that  $D \propto M^{-3.4}$  when  $M$  was higher than  $M_c$ . This

behavior was not observed for the PVC/PCL system, which showed  $D \propto M^{-1}$ . The difficulty in relating the bulk viscosity to the diffusion coefficient lies in the difference between viscous and diffusive motions. The relaxations involved in viscous dissipation of an applied stress, as in the measurement of zero shear viscosity, are primarily motions of short segments of the macromolecule. Diffusion requires that the entire molecule translate a distance much greater than the molecular size during a time much greater than that used during measurements of viscosity. The data obviously demonstrate a substantially different dependence of  $D$  on  $M$  than would be expected from Bueche's relationship given the observed  $\eta$  vs.  $M$  data (Graessley, 1973; Ferry, 1970). One must conclude that the equation derived by Bueche, although sensible in its attempt to relate  $D$  to  $\eta$ , does not correctly predict the molecular weight dependence of the diffusion coefficient.

It is also immediately obvious that neither de Gennes (1971) nor Edwards and Grant (1973) predict the proper relationship between  $D$  and  $M$ . Both, however, are attempting to describe a somewhat different system than that which most resembles a bulk polymer: a large number of entangled chains. Each attempt to model the motion of one chain in a constrained matrix. The dependence of  $D$  on  $M^{-1}$  is in fact predicted by the Rouse model for a free, non-interacting chain (de Gennes, 1976). It is inherently difficult to envision

interpenetrating polymer coils as having no interactions. It is possible that on the time scale required for diffusion of polymers, the effect of entanglements is small because an individual entanglement is transitory; this would not be true for viscous relaxations. This might partially explain the difference between the observed molecular weight dependencies of diffusivity and viscosity.

The Rouse model has been widely applied to concentrated polymer systems. One of the assumptions of the Rouse model is that the individual monomer (or segment) units do not interact with each other. These interactions, if they occur, would have the effect of influencing the molecular dimensions through the effect of excluded volume. In essence, the Rouse model would have the polymer chain in an unperturbed, or theta, state. If the effect of molecular weight can be shown more carefully to be inversely proportional to the diffusion coefficient, it could be implied that the diffusing molecules have dimensions associated with the theta condition. This possibility is even more interesting in light of Russell's (1978) recent observations of the PVC/PCL system by SAXS, which also indicate that the molecules exist in an unperturbed state.

Recently, de Gennes (1976) has included the effect of hydrodynamic interaction between polymer chains in concentrated polymer solutions. Calling the chain portions between entanglements "blobs" and taking into account ex-



cluded volume, this theory relates the number of entanglements per monomer unit to the concentration of the solution. The predicted dependence of  $\eta \propto M^3$  is not seen by experiment (where  $\eta \propto M^{3.4}$ ) but de Gennes blames this partially on the possibility of segregation of terminal groups, which may explain the low diffusivity of PVC-1. The chain ends would act as aggregates, giving the material an effective molecular weight much higher than that measured in dilute solution. Further experimental work, primarily measurement of bulk viscosity, will provide further insight into this aspect of the study.

One temperature used in this study, 70°C, is below what is normally accepted as the glass transition temperature of PVC ( $T_g \approx 80^\circ\text{C}$ ). The glass transition temperature is known to be a time dependent phenomenon (Roberts and White, 1973; Graessley, 1973). Ferry (1970) has summarized the various treatments of this subject and includes a demonstration of the change of  $T_g$  with time. In fact, it is shown for poly(vinylacetate) that the value of  $T_g$  can change 3 degrees with a change in time scale of a factor of 10. Thus the effective glass transition temperature for PVC over the time scale for diffusion is substantially lower than the usual value.

Duda and Vrentas (1976) touch on this subject during their discussion of a Deborah number for diffusion (here called the Duda number,  $Du$ ). This relates a characteristic

relaxation time,  $\lambda_r$ , to a characteristic diffusion time,  $\theta_d$ ,

$$Du = \lambda_r / \theta_d . \quad (35)$$

At the temperature where the glass transition occurs, the relaxation time becomes effectively infinite--no relaxations occur which require the translation of the entire macromolecule and  $Du$  becomes infinite. This would stop interdiffusion of the polymeric components. The consequence of this would be readily seen in the  $D$  vs.  $1/T$  curve (Figure 34).

The calculated activation energy for diffusion is of the same order as that noted by Bueche et al. (1952). It is generally accepted that this activation energy is that required for segmental motion (Graessley, 1973) rather than for movement of the center of gravity of the macromolecule. Given the value of  $E_a$ , 11.7 kcal/mol, in comparison with that for diffusion of low molecular weight materials (Jost, 1952), this interpretation of the results is a reasonable one.

The conclusion of Graessley (1973) can be drawn here but with even stronger emphasis: present theories which attempt to describe motion of polymer chains in the undiluted state contain serious deficiencies. The attempts to model a system of one chain in a matrix of obstacles are significant contributions but extension to a system of interacting chains has yet to be accomplished. Our understanding of the bulk state is far from complete. The data collected in this study provide a firmer basis for future postulations

of predictive theories of macromolecular motion in the melt.



## C H A P T E R   V I

### RECOMMENDATIONS FOR FUTURE WORK

The technique which was developed here has wide application in the investigation of diffusion in polymer systems. At present, an important limitation can be attributed to the x-ray detector system; i.e., the requirement that one of the components of the diffusing system contain an atom of atomic number greater than 9. Further improvements in windowless detectors may make the use of oxygen and nitrogen containing polymers possible. Until such a time as these improved detectors exist, many other significant aspects of polymer/polymer diffusion can be investigated.

The materials used in this study were all commercially available and had a "most probable" molecular weight distribution (MWD). It can be argued that the lower molecular weight molecules would diffuse more rapidly than the molecules of higher molecular weight in a specific sample. The use of sharp fractions ( $MWD \approx 1$ ) could provide some insight into the effect of molecular weight distribution on diffusivity. Also, if the molecular weights of the two species are not identical, a diffusing molecule will see different molecular weights for its surroundings depending on its position relative to the interface, i.e., a PVC molecule

surrounded by other PVC molecules will not "see" the same surround molecular weight as one embedded in PCL molecules. The best test of the effect of molecular weight on the diffusivity is to use monodisperse materials of identical molecular weight.

Given the theory presented by Bueche (1952), it would be profitable to attempt to correlate the diffusion coefficient with the bulk viscosity of a blend of the materials, particularly with regard to the effect of molecular weight. Several years ago, Prest (1971) did some work examining the bulk viscosity of a blend and the relationships between the observed properties of the blend and those of the individual components. He developed combination rules that can provide a starting point for correlating the bulk viscosity and the diffusion coefficient. The primary difficulty appears to be that while the diffusion coefficient is measured in a sample which covers the entire concentration range, the viscosity is measured for a sample with a specific composition. Through use of adequate combination rules, this difficulty can be resolved and allow correlation between the diffusion coefficient and the zero shear viscosity of the blend.

It is recommended that a study be done similar to the one presented here using two materials, each of which have atoms whose x-ray fluorescence is observable using the equipment available. An example might be a silicon containing polymer diffusing into a chlorine containing polymer. This

investigation would give further proof of the validity of the technique as well as allowing two independent determinations of the diffusion coefficient. This would also provide a method for testing one of the basic assumptions made during the mathematical analysis of the system, i.e., the assumption of constant partial mass volume. Several variations on this theme can also be imagined, e.g., having two traceable atoms on one of the components. Calculation of the diffusion coefficient from the data gathered for each element would allow an interesting comparison to be made.

PVC has been shown to be compatible with a wide range of polyesters (Krause, 1972). Several variations on the polymer poly(pivalolactone) have been produced in this laboratory. Acquisition of one of these variants showing no crystallinity and a low  $T_g$  would allow diffusion experiments to be conducted at room temperature, decreasing the degradation of PVC and perhaps providing a method of determining the  $T_g$  of PVC at long times.

Another important area of research toward which the described experimental method can be turned is the diffusion of plasticizers in polymers. Much attention has been paid to low molecular weight liquids and gases penetrating polymers (Crank and Park, 1968). However, many materials are used as plasticizers which have higher molecular weights and which require a technique with greater resolution than the normally applied methods to measure diffusivities. An exam-

ple might be the diffusion of tricresylphosphate in PVC; this particular system has the added advantage of two traceable atoms, Cl and P. There are many such systems where the partial pressure of the plasticizer is sufficiently low so as to make diffusion rates observable in the low vacuum of the SEM. To facilitate these sorts of studies, a method of lowering the temperature of the sample while in the SEM will be necessary. Adequate equipment for this purpose is commercially available; given the wide use of plasticizers in the polymer industry and, therefore, the applicability of such research, such expenditure as is necessary to implement this research is highly recommended.

The analysis of data has been carried out assuming that deconvolution of the measured concentration profile was unnecessary. The precautions taken to avoid smearing included: (1) discrete measurement of x-ray counts separated by distances substantially larger than the radius of the x-ray generation volume; (2) allowing diffusion to occur over a time period long enough to ensure that the concentration profile covered a large enough distance so that the x-ray generation volume subtended only a small change in concentration. A method of correcting for any smearing would be to measure a concentration profile for a system which had not had sufficient time to diffuse to any great extent. An alternative would be to determine a concentration profile for a binary system which is known to be incompatible and com-



paring the effective diffusion coefficient with that obtained for the miscible systems. This comparison would be an adequate test of the techniques used at present to avoid smearing. Also, deconvolution of the observed concentration profile by determining the smearing function  $p(x)$  might be accomplished by the method just mentioned. Using a known, infinitely sharp concentration profile and measuring the observed concentration profile, a measure of  $p(x)$  could be acquired.

It is recommended that a more comprehensive program studying diffusion in polymers be initiated. The technique developed within this study is applicable to a variety of polymer/polymer systems and, perhaps more importantly, to a large number of polymer/plasticizer systems. A significant advantage of the SEM-EDS technique is that there is no need for specially prepared polymers. The present limitations involve primarily the requirement of a tracer atom of atomic number greater than 9 being attached to one of the components. Several possible improvements in the experimental apparatus include temperature control of the sample within the SEM and automated data acquisition (direct interfacing between the SEM, the x-ray apparatus, and a computer capable of manipulating the data). With the capability of controlling the temperature of the sample in the SEM, the technique can be extended readily to include analysis of diffusion of plasticizers in polymers.

## C H A P T E R   V I I

### CONCLUSION

An experimental technique has been developed for measuring the mutual diffusion coefficient of compatible binary polymer systems. The method involves use of a scanning electron microscope, which has the resolution necessary for these observations, and energy dispersive analysis of x-ray fluorescence; combined, these two techniques allow determination of the concentration profile across the small interpenetration distances typical of the interdiffused polymeric components. The development of this technique, a large portion of the study, has resulted in a useful method of measuring diffusion rates in commercially important polymer systems as well as a means of determining the effects of diffusion in some polymer/plasticizer systems. The ability to characterize diffusion in such systems is important, particularly when considering the phenomena involved in the processing of polymers and the effect of mixing of several components on the physical properties of the blend.

The values of the diffusion coefficient reported here for the poly(vinylchloride)/poly( $\epsilon$ -caprolactone) system ( $\sim 10^{-13}$  cm<sup>2</sup>/sec) are of similar order of magnitude as those reported by earlier investigators. The effects of molecular

weight and temperature on the diffusion coefficient were observed for the PVC/PCL system. The activation energy for diffusion was calculated to be 11.7 kcal/mol which is similar to that calculated from bulk viscosity measurements for other systems. The change in  $D$  with molecular weight was not observed to be that predicted by the few theories which exist that directly address the motion of a macromolecule in the melt state. In fact, there appears to be a linear, inverse proportionality between the diffusion coefficient and the molecular weight, thus questioning the proposed correlation between the diffusion coefficient and the zero shear viscosity. Further work using monodisperse materials, and studies of the bulk viscosity of the PVC/PCL system, will help clarify the relationships between the diffusivity, molecular weight, and viscosity.

The developed technique has also been used to examine the polystyrene/poly(o-chlorostyrene) system. The technique was successful in this case as well, further demonstrating its applicability. It is expected to be a viable method of measuring diffusion in polymer/plasticizer systems. Given suitable materials, i.e., at least one of the diffusing species containing an element observable by EDS, the experimental method of scanning electron microscopy combined with energy dispersive spectroscopy is a useful technique for determining a very important parameter for binary systems--the diffusion coefficient.



## REFERENCES

1. Alexander, A. (1970), "X-Ray Diffraction Methods in Polymer Science," Wiley, New York.
2. Alliet, D.F., and Pacco, J.M. (1968), "Gel Permeation Chromatography," seminar reprints, p. 274.
3. Anand, J.N. (1973), "Re: Contact Theory of Adhesion," J. Adhesion, 5, 265.
4. Anand, J.N., and Karam, H.J. (1969), "Interfacial Contact and Bonding in Autohesion," J. Adhesion, 1, 16.
5. Bird, R.B., Stewart, W.E., and Lightfoot, E.N. (1960), "Transport Phenomena," Wiley, New York.
6. Boltzmann, L. (1894), "Solution of the Diffusion Equation with Concentration Dependent Diffusion Coefficient," Wied. Ann. Phys., 53, 959.
7. Bueche, F. (1952), "Viscosity, Self-Diffusion, and Allied Effects in Solid Polymers," J. Chem. Phys., 20, 1959.
8. Bueche, F., Cashin, W.M., and Debye, P. (1952), "Measurement of Self-Diffusion in Solid Polymers," J. Chem. Phys., 20, 1956.
9. Bueche, F. (1968), "Diffusion of Polystyrene in Polystyrene: Effect of Matrix Molecular Weight," J. Chem. Phys., 48, 1410.
10. Crank, J., and Park, G.S. (1968), "Diffusion in Polymers," Academic Press, New York.
11. Debye, P. (1946), "The Intrinsic Viscosity of Polymer Solutions," J. Chem. Phys., 14, 636.
12. Delgado, L. (1976), "Degradation of Poly(vinylchloride) Due to Electron Beam Bombardment," Ph.D. Thesis, University of Minnesota, Minneapolis, Minnesota.
13. Duda, J.L., and Vrentas, J.S. (1966), "Establishment of Position of Initial Interface in Free Diffusion Experiments," I&EC Fund., 5, 434.

14. Duda, J.L., Vrentas, J.S., and Jarzebski, C.M. (1976), "A Deborah Number for Diffusion in Polymer-Solvent Systems," *AIChE J.*, 21, 894.
15. Duda, J.L., and Vrentas, J.S. (1978), "Diffusion in Polymer-Solvent Systems. III. Construction of Deborah Number Diagrams," submitted for publication.
16. Edwards, S.F., and Grant, J.W.V. (1973), "The Effects of Entanglements on Diffusion in a Polymer Melt," *J. Phys.*, A6, 1169.
17. Ertl, H., Ghai, R.K., and Dullien, F.A.L. (1973), "Liquid Diffusion of Non-Electrolytes, I," *AIChE J.*, 19, 881.
18. Ferry, J.D. (1970), "Viscoelastic Properties of Polymers," Wiley, New York.
19. Fick, A. (1855), "Über Diffusion," *Ann. Physik u. Chem.*, 170 (Bande 94), 59.
20. Fox, T.G. (1956), "Influence of Diluent and of Copolymer Composition on the Glass Temperature of a Polymer System," *Am. Phys. Soc. Bull.*, 1, 123.
21. Frenkel, I. (1926), "Über die Wärmebewegung in festen und flüssigen Körpern (Thermal Agitation in Solids and Liquids)," *Z. Phys.*, 35, 652.
22. de Gennes, P.G. (1971), "Reptation of a Polymer Chain in the Presence of Fixed Obstacles," *J. Chem. Phys.*, 55, 572.
23. de Gennes, P.G. (1976), "Dynamics of Entangled Polymer Solutions. II. Inclusion of Hydrodynamic Interactions," *Macromolecules*, 9, 594.
24. Graessley, W.W. (1973), "The Entanglement Concept in Polymer Rheology," *Adv. Polym. Sci.*, 16, 1.
25. Hawkins, W.L. (1972), "Polymer Stabilization," Wiley-Interscience, New York.
26. Holt, D.B., Muir, M.D., Grant, P.R., and Boswarva, I.M. (1974), "Quantitative Scanning Electron Microscopy," Academic Press, New York.
27. Johnson, P.A., and Babb, A.L. (1956), "Liquid Diffusion of Non-Electrolytes," *Chem. Rev.*, 56, 387.

28. Jost, W. (1952), "Diffusion in Solids, Liquids, and Gases," Academic Press, New York.
29. Joy, D.C., and Maher, D.M. (1977), "Sensitivity Limits for Thin Specimen X-Ray Analysis," IITRI/SEM, 1, 325.
30. Klein, J., and Briscoe, B.J. (1976), "Diffusion of Large Molecules in Polymers: A Measuring Technique Based on Microdensitometry in the Infra-Red," Polymer, 17, 481.
31. Klein, J. (1977), "Diffusion of Long Molecules Through Solid Polyethylene. I. Topological Constraints," J. Poly. Sci., Poly. Phys. Ed., 15, 2057.
32. Klein, J., and Briscoe, B.J. (1977), "Diffusion of Long Molecules Through Solid Polyethylene. II. Measurements and Results," J. Poly. Sci., Poly. Phys. Ed., 15, 2065.
33. Knoll, M. (1935), "Static Potential and Secondary Emission of Bodies under Electron Irradiation," Z. Tech. Phys., 11, 467.
34. Koleske, J.V., and Lundberg, R.D. (1969), "Lactone Polymers. I. Glass Transition of Poly( $\epsilon$ -caprolactone) by Means of Compatible Polymer Mixtures," J. Poly. Sci. A-2, 7, 795.
35. Krause, S. (1972), "Polymer Compatibility," J. Macromol. Sci.--Revs. Macromol. Chem., C7, 251.
36. Lee, C.F. (1971), "On the Solution of Some Diffusion Equations with Concentration Dependent Diffusion Coefficients," J. Inst. Math. Applic., 8, 251.
37. Lifshin, E., Morris, W.G., and Bolon, R.B. (1969), "The Scanning Electron Microscope and Its Applications in Metallurgy," J. Metals, 21(12), 43.
38. Machin, D., and Rogers, C.E. (1972), "Free Volume Theories for Penetrant Diffusion in Polymers," Makromol. Chem., 155, 269.
39. Matano, C. (1933), "On the Relation Between the Diffusion Coefficients and Concentration of Solid Metals (Nickel-Copper System)," Trans. Jap. J. Phys., 8, 109.
40. Maurice, F., Sequin, R., and Henroc, J. (1965), in "International Symposium on X-Ray Optics and Microanalysis," Castaing et al., eds., Orsay, France, 57.

41. Ong, C.-J.J. (1973), "Crystallization of Polyblends: Blends of Poly( $\epsilon$ -caprolactone) and Poly(vinyl chloride)," Ph.D. Thesis, University of Massachusetts, Amherst, Massachusetts.
42. Paul, D.R. (1967), "Measurement of Diffusion Coefficients for Concentrated Binary Polymer Solutions," I&EC Fund., 6(2), 217.
43. Pearson, J.A.R. (1976), "The Fusion of Continuum and Molecular Ideas in the Rheology of Technologically Important Polymers," VIIth Int'l. Cong. Rheol.
44. Porter, R.S., and Johnson, J.F. (1966), "The Entanglement Concept in Polymer Systems," Chem. Rev., 66, 1.
45. Prest, W.M., Jr. (1970), "Viscoelastic Properties of Blends of Entangled Polymers," J. Poly. Sci. A-2, 8, 1897.
46. Reed, S.J.B. (1965), in "X-Ray Optics and Microanalysis," Orsay, France, 339.
47. Roberts, G.E., and White, E.F.T. (1973), "Relaxation Processes in Amorphous Polymers," in "The Physics of Glassy Polymers," R.N. Haward, ed., Wiley, New York.
48. Russ, J.C. (1972), "Elemental X-Ray Analysis of Materials: EXAM Methods," EDAX Lab. Div., NC.
49. Russell, T., and Stein, R.S. (1978), unpublished data.
50. Shoemaker, D.P., and Garland, C.W. (1967), "Experiments in Physical Chemistry," McGraw-Hill, New York.
51. Sillescu, H. (1977), "Matrix Diffusion Technique for Slow Translational Motion of Macromolecules in Polymers," Makromol. Chem., 178, 2759.
52. Stewart, A.D.G., and Snelling, M.A. (1965), "A New Scanning Electron Microscope," pp. 55-56 in Elec. Microsc. Proc., Prague, 1964, M. Titlebach, ed.
53. Stokes, R.H. (1952), "One-Dimensional Diffusion with the Diffusion Coefficient a Linear Function of Concentration," Trans. Far. Soc., 48, 887.
54. Voyutskii, S.S. (1963), "Autohesion and Adhesion of Polymers," Interscience, New York.



55. Voyutskii, S.S., Kamenskii, A.N., and Fodimann, N.M. (1965), "Electron Microscope Study of Mutual Diffusion in Polymeric Systems," *Vysokomol. Soed.*, 7, 696.
56. Voyutskii, S.S., Kamenskii, A.N., and Fodimann, N.M. (1966), "Direkter Nachweis von Selbst--und Gegen-diffusion beim Zustandekommen Von Adhäsionbindung zwischen den Polymeren," *Koll. Zeit.*, 215, 36.
57. Voyutskii, S.S. (1973), "Some Comments on the Series of Papers 'Interfacial Contact and Bonding in Adhesion'," *J. Adhesion*, 3, 69.
58. Wagner, C., and Schottky, W. (1931), "Theorie der geordneten Mischphasen (Theory of Ordered Mixed Phases)," *Z. Physik. Chem., Abt. B*, 11, 163.
59. Wake, W.C. (1969), "Elastomeric Adhesives," in "Treatise on Adhesion and Adhesives," Vol. 2, R.L. Patrick, ed., Marcel Dekker, New York.
60. Warner, F., Stein, R.S., Khambatta, F., and Russell, T. (1976), "Low Angle X-Ray Studies of Polymer Blends," *J. Poly. Sci.*, B14, 1391.
61. Wells, O.C. (1974), "Scanning Electron Microscopy," McGraw-Hill, New York.
62. Wilkins, J.E., Jr. (1963), "Diffusion in an Infinite or Semi-Infinite Medium Whose Diffusion Coefficient Depends Linearly on the Concentration," *J. Soc. Indust. Appl. Math.*, 11(3), 632.
63. Woldseth, R. (1973), "All You Ever Wanted to Know About XES," Kerex Corp., Illinois.

A P P E N D I X    A  
 REGRESSION ANALYSIS

The data were fit to the solution of the diffusion equation, Equation 27, to find the diffusion coefficient, D, by using a non-linear least squares algorithm as follows.

Definitions:

$Y_j$  =  $j^{\text{th}}$  observed value

$B_i$  = unknown material constant

$B_i^{\circ}$  = initial guess of  $B_i$

$X_{ji}$  = input data for  $j^{\text{th}}$  observation, summation on  $i$   
 implied

$f_j = f_j(B_i^{\circ}, X_{ji})$  = known equation to be evaluated  
 for the  $B_i$ 's using the data  $X_{ji}$ .

Procedure:  $y_i$  is expanded about the initial guesses  $B_i^{\circ}$  in a Taylor series of  $i$  variables of the known function  $f_j$ . Only first order terms are used and an approximate expression for  $y_j$ , called  $\tilde{y}_j$ , is obtained.

$$y_j = \tilde{y}_j = f_j(B_i^{\circ}, X_{ji}) + \left. \frac{\partial f_j}{\partial B_1} \right|_{B_i^{\circ}} (B_1 - B_1^{\circ}) + \left. \frac{\partial f_j}{\partial B_2} \right|_{B_i^{\circ}} (B_2 - B_2^{\circ}) + \dots$$

or

$$\tilde{y}_j = f_j + \sum_i \left. \frac{\partial f_i}{\partial B_i} \right|_{B_i^0} (B_i - B_i^0)$$

or

$$\tilde{y}_j = f_j + \sum_i P_{ij} \Delta B_i \quad (36)$$

where

$$P_{ij} \equiv \left. \frac{\partial f_i}{\partial B_i} \right|_{B_i^0}, \quad \Delta B_i = B_i - B_i^0$$

The error,  $E$ , between this approximate expression and the exact expression is given by the sum of the squares of the differences between  $y_j$  and  $\tilde{y}_j$ :

$$E = \sum_j (y_j - \tilde{y}_j)^2 \quad (37)$$

Using Equation 36, we obtain

$$E = \sum_j [y_j - (f_j + \sum_i P_{ij} \Delta B_i)]^2 \quad (38)$$

To minimize the error, the partial derivatives of  $E$  with respect to the  $\Delta B_i$ 's are set to zero to form a system of equations:



$$\frac{\partial E}{\partial \Delta B_1} = -2 \sum_i P_{1j} [Y_j - (f_j + \sum_i P_{ij} \Delta B_i)] = 0 \quad (39)$$

$$\frac{\partial E}{\partial \Delta B_2} = -2 \sum_j P_{2j} [Y_j - (f_j + \sum_i P_{ij} \Delta B_i)] = 0$$

etc. These equations yield the following:

$$\sum_j P_{1j} (\sum_i P_{ij} \Delta B_i) = \sum_j Y_j P_{1j} - \sum_j f_j P_{1j} \quad (40)$$

$$\sum_j P_{2j} (\sum_i P_{ij} \Delta B_i) = \sum_j Y_j P_{2j} - \sum_j f_j P_{2j}$$

etc. Expanding the left-hand side of the first equation in (40) reveals that:

$$\begin{aligned} \sum_j P_{1j} (P_{1j} \Delta B_1 + P_{2j} \Delta B_2 + P_{3j} \Delta B_3 + \dots) = \\ \Delta B_1 (\sum_j P_{1j} P_{1j}) + \Delta B_2 (\sum_j P_{1j} P_{2j}) + \Delta B_3 (\sum_j P_{1j} P_{3j}) + \dots \quad (41) \end{aligned}$$

The unknowns are the  $\Delta B_i$  and the coefficients of the matrix are the  $P_{ij}$  products. This can be expressed as the matrix equation:

$$[P]\{\Delta B\} = \{Y\} \quad (42)$$

and is solved by inversion of the  $[P]$  matrix to obtain:

$$\{\Delta B\} = [P]^{-1}\{Y\} \quad (43)$$

If the function  $f_j$  is linear in  $\Delta B_i$ , then Equation 43

gives the exact solution. If not, as in the case of the diffusion equation, the partial derivative  $[P]$  and, hence,  $[P]^{-1}$  will depend on the  $\Delta B_i$ 's, and in the usual trial-and-error methods for computing least squares estimates,  $\{\Delta B\}$  is re-evaluated at each iteration, using the maximum neighborhood, until one of several convergence criteria are met.

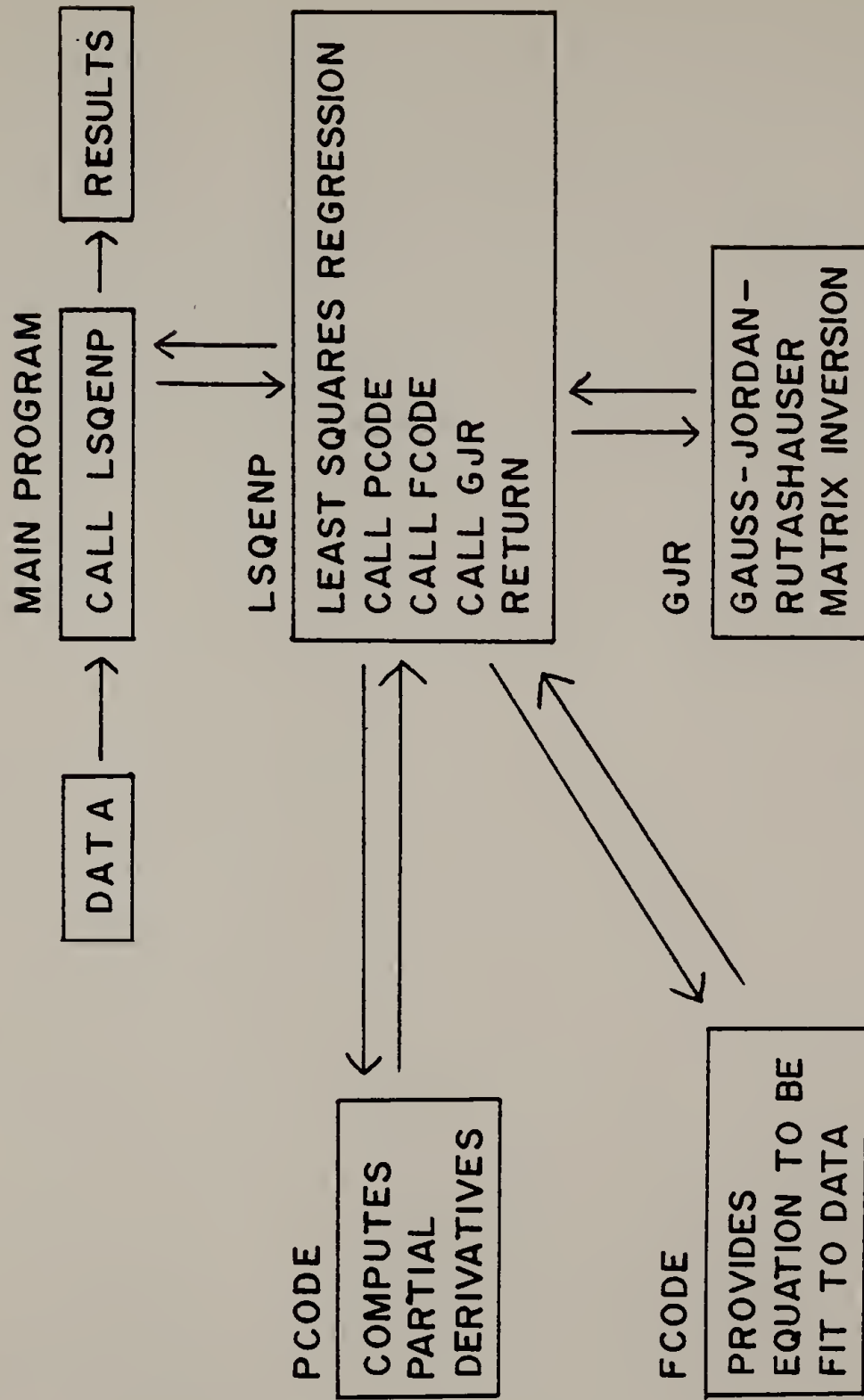
For this problem, the solution to the diffusion equation yields

$$c(x) = 1/2 \left[ 1 - \operatorname{erf} \left( \frac{x - x_0}{2\sqrt{Dt}} \right) \right] \quad (44)$$

$c(x)$  is the observed value,  $y_j$ ,  $(x-x_0)/2\sqrt{Dt}$  is the data,  $X_{ji}$ , and  $D$  is the only known, hence  $B_1$ . The problem is reduced to analysis of a one-dimensional matrix (a scalar), still not trivial due to the existence of the highly non-linear error function.

A copy of the program may be obtained from the author. A flow chart is shown in Figure 34. Documentation of the non-linear regression code was obtained from D.F. Vronay, Aerojet General Corp., P.O. Box 13400, Sacramento, CA 95813.

Figure 34. Flow chart of non-linear regression analysis.



A P P E N D I X B  
PROPAGATION OF ERROR

A standard propagation of error routine was carried out to estimate the error in the calculated value of the diffusion coefficient (Shoemaker and Garland, 1967). A sample calculation of this value,  $\lambda(D)$ , follows.

$$\lambda \left( \frac{C - C_0}{C_1 - C_0} \right) = \lambda(C_{\text{red}}) = \lambda[\frac{1}{2}(1 + \text{erf } \eta)]$$

where  $\eta = (x-x_0)/\sqrt{4Dt}$ . The error in D is calculated by differentiating the solution to the diffusion equation with respect to all variables:  $x, x_0, t, C, C_1, C_0, D$ .

$$\lambda(C_{\text{red}}) = \frac{\partial C_{\text{red}}}{\partial C} \lambda(C) + \frac{\partial C_{\text{red}}}{\partial C_1} \lambda(C_1) + \frac{\partial C_{\text{red}}}{\partial C_0} \lambda(C_0)$$

$$\begin{aligned} \lambda[\frac{1}{2}(1 + \text{erf } \eta)] &= \lambda(\text{erf } \eta) = \frac{\partial}{\partial t}(\text{erf } \eta)\lambda(t) + \frac{\partial}{\partial x}(\text{erf } \eta)\lambda(x) \\ &+ \frac{\partial}{\partial x_0}(\text{erf } \eta)\lambda(x_0) \\ &+ \frac{\partial}{\partial D}(\text{erf } \eta)\lambda(D) \end{aligned}$$

As is normal, absolute values are used in the calculation.

$$\lambda(C_{\text{red}}) = \frac{1}{C_1 - C_0} \left[ \lambda(C) + \frac{C - C_0}{C_1 - C_0} \lambda(C_1) + \frac{C - C_1}{C_1 - C_0} \lambda(C_0) \right]$$

$$\lambda(\text{erf } \eta) = \frac{2}{\sqrt{\pi}} e^{-\eta^2} \left[ \frac{1}{4Dt} \left( \lambda(x) - \lambda(x_0) \right) - \frac{1}{2} \left( \frac{x - x_0}{\sqrt{4Dt}} \right) \left( \frac{\lambda(t)}{t} + \frac{\lambda(D)}{D} \right) \right]$$

For a particular data set:

$$C = 350 \text{ counts} \qquad \lambda(C) = 35$$

$$C_1 = 1100 \text{ counts} \qquad \lambda(C_1) = 110$$

$$C_0 = 100 \text{ counts} \qquad \lambda(C_0) = 10$$

$$t = 1.28 \times 10^6 \text{ sec} \qquad \lambda(t) = 5 \times 10^3$$

$$x = 4.00 \times 10^{-4} \text{ cm} \qquad \lambda(x) = 0.02$$

$$x_0 = 29.56 \times 10^{-4} \text{ cm} \qquad \lambda(x_0) = 1.25$$

$$D = 6.54 \times 10^{-12} \text{ cm}^2/\text{sec}$$

An error estimate of the individual x-ray count measurements was made by taking four measurements of  $C_1$  and  $C_0$  for each data set. The standard deviation was consistently 10% throughout all samples, so this was used as the error in  $C$  as well. The error in time of diffusion is quite small. The error in  $x$  is estimated from the error in the vernier calipers used to measure the distances between concentration measurements. Error in position of the electron beam on the surface (on the order of  $10 \text{ \AA}$ ) is negligible. The values of  $x_0$ ,  $D$ , and  $\lambda(x_0)$  are computed from the regression analysis routine. The regression analysis also calculates the error

in D (~10%) but does not account for all variables. Using the values given above:

$$\lambda(C_{\text{red}}) = 0.07$$

$$0.07 = \frac{2}{\sqrt{\pi}} \exp(-.9961) \left[ \frac{1.245}{57.87} + \frac{25.56}{115.74} \left( \frac{5 \times 10^3}{1.28 \times 10^6} + \frac{\lambda(D)}{D} \right) \right]$$

Therefore,

$$\frac{\lambda(D)}{D} = 0.18$$

A reasonable estimate, then, of the error in the diffusion coefficient is  $\pm 25\%$ .





